Mechanistic Insights into Regulation of Vesicular SOCS3 Secretion by Alveolar Macrophages: Interplay Between Cell Stress and Metabolic Remodeling

by

Mikel D. Haggadone

A dissertation submitted in partial fulfillment
of the requirements for the degree of
Doctor of Philosophy
(Immunology)
in the University of Michigan
2021

Doctoral Committee:

Professor Marc Peters-Golden, Chair
Professor Jeffrey Curtis
Associate Professor Costas Lyssiotis
Professor Bethany Moore
Professor Mary O'Riordan
Professor Joel Swanson

Mikel D. Haggadone

haggamd@umich.edu

ORCID iD: 0000-0002-7001-9132

Dedication

To anyone who has known the weight of mental illness.

Acknowledgments

This dissertation is the product of love and guidance provided to me by many amazing people. First, I want to express sincere gratitude to my mentor and friend, Dr. Marc Peters-Golden. Marc took me on as a graduate student during a particularly challenging period of my life, and he has been there through the many trials and tribulations of this doctoral work. Marc gave me the space to fail, learn, and grow. He embraced my ideas and – above all – he believed in them. He believed in me. Nothing I say here will do justice to the love and acceptance that I have felt from Marc, especially when at my worst. But the inability to articulate these thoughts and feelings is exactly why I will always hold the last six years close to my heart. Every graduate student deserves a mentor who truly sees and embraces them as they are, as Marc has done for me. I will leave the University of Michigan a better scientist and more fulfilled human being, which would not have been possible without Marc's mentorship.

I would also like to thank my dissertation committee: Drs. Mary O'Riordan, Beth Moore, Jeff Curtis, Joel Swanson, and Costas Lyssiotis. Our committee meetings together have proved invaluable for improving the quality of my work. Beyond this, each committee member has taken the time to affirm and empower me as a scientist, instilling belief when I needed it most. I want to especially thank Beth who, as Director of the Graduate Program in Immunology, moved mountains so that I could return to the University of Michigan – my home – to complete this doctoral research. I would not be here today without her advocacy and support. I also want to thank Costas for all his help and guidance in furthering my research on alveolar macrophage metabolism. Completion of the work included in Chapter 3 would not have been possible without his collaboration.

The Peters-Golden lab has also been an irreplaceable source of constructive criticism and encouragement. Presenting at Wednesday morning lab meetings was when I learned and grew the most during graduate school. I want to especially thank Jennifer Speth and Raghu Penke for all their selflessness in helping me to complete experiments throughout the last year of my PhD. I also want to highlight Teresa Murphy for her invaluable work as our Lab Manager, and for helping me to smile when doing so felt impossible.

I feel incredibly privileged to have done my PhD as part of such an amazing graduate community. Our Directors, past and present, have included Drs. Beth Moore, Malini Raghavan, Durga Singer, and Gary Huffnagle, and each has shown commitment to my growth and well-being as a student. I am also so appreciative of our remarkable Program Administrator, Zarinah Aquil, who consistently has gone above and beyond the call of duty to make our time in graduate school as rich as is possible. Many bad days have been made better by Zarinah's tenderness.

Furthermore, I would not be where I am today without the sacrifice of my parents, David Haggadone and Linda Winters, and stepparents, Sharon Haggadone and Jim Winters. Through life's challenges, they have always been there with unconditional love and support. I feel particularly fortunate to have been granted the most wonderful mother and father anyone could ever ask for. They are my inspiration, my friends, and my greatest supporters, and none of this would have been possible without them. I love you with all my heart, Mom and Dad.

I also want to express sincere gratitude to the many friends and mentors who have all enriched my life in unique and formative ways. My lifelong best friend, Nick Anderson, and his family have been an irreplaceable part of my life almost since the day I was born. To them I owe so much. I am also thankful to have had the best graduate school friends, Eli Olson, Jazib Uddin, Emily Yarosz, Ashley Munie, and Dawit Mengistu, who were there for me during the most difficult

days of my PhD. Nights spent with Eli and Jazib at The Ravens Club and/or Vinology helped to create memories that I will never forget. I also want to thank the trail and long-distance running community for giving me the opportunity to be part of such a beautiful sport. Tommy Byrne and Bigger Than The Trail have made my running about something bigger, the pursuit of a world where mental health care is made accessible to everyone. Additionally, I want to thank my coach, David Roche, for always bringing me back to the simplicity of love. Without him, completing this PhD would have been far less meaningful.

And finally, to Audrey, my partner, my adventure buddy, my best friend: I have spent the entirety of this PhD questioning what would come of its many failures and missteps. There are infinite possible answers to this question manifesting in every parallel universe, and yet the one I've been given here is the most meaningful: all along, they were simply putting in motion an improbable journey toward finding you. I love you more than any string of words could ever tell, and I really hope you know that.

Table of Contents

List of Figures

Abstract

Extracellular vesicles (EVs) serve as important vectors for intercellular communication by delivering a myriad of packaged cargo molecules (i.e., proteins, lipids, and nucleic acids) from a source cell to a recipient cell. In the lung, alveolar macrophages (AMs) tonically secrete EVs containing suppressor of cytokine signaling 3 (SOCS3) protein. Uptake of SOCS3-containing EVs by alveolar epithelial cells is critical for restraint of cytokine-induced Janus kinase-signal transducer and activator of transcription 3 signaling to promote homeostasis in the distal lung. Changes in vesicular cargo secretion – including but not limited to SOCS3 – have been described in response to various microenvironmental cues, but the cellular and molecular mechanisms that control these changes remain poorly understood. Furthermore, use of quantitative methods to assess alterations in EV cargo packaging remain limited. In this dissertation, we address these gaps in knowledge by studying two perturbations relevant to the lung alveolar microenvironment: oxidative stress and metabolic remodeling.

Firstly, we used cigarette smoke (CS) as a clinically relevant model of oxidative stress to test the effect of reactive oxygen species (ROS) on vesicular SOCS3 release by AMs. Treatment of primary and immortalized AMs with an aqueous extract of CS (CSE) potentiated the secretion of SOCS3 in a ROS-dependent manner. Use of nanoparticle tracking analysis alongside a newly developed carboxyfluorescein succinimidyl ester-based cargo packaging assay demonstrated that CSE augmented AM vesicular SOCS3 release by enhancing both EV biogenesis and the amount of SOCS3 packaged into EVs. Furthermore, use of a 20S proteasome activity assay along with conventional proteasome inhibitors strongly suggested that ROS stimulated SOCS3 secretion via

inactivation of the proteasome. These data demonstrate that microenvironmental oxidants tune proteasome activity to modulate vesicular SOCS3 secretion by AMs.

Secondly, as AMs exhibit remarkably low levels of glycolysis at baseline – a metabolic phenotype that supports their homeostatic function – we sought to investigate the effect of glycolytic flux on the release of SOCS3. Primary AMs were treated with the growth and activating factor granulocyte-macrophage colony-stimulating factor (GM-CSF), which promoted increases in glucose metabolism. Consequently, GM-CSF diminished SOCS3 secretion in a glycolysis-dependent manner. Furthermore, inhibition of vesicular SOCS3 release by GM-CSF relied on pyruvate transport into the mitochondria, export of mitochondrial citrate to the cytosol, and the subsequent conversion of cytosolic citrate to acetyl-CoA by ATP citrate lyase (ACLY). Therefore, our data demonstrate that ACLY links increases in glycolysis to diminished release of SOCS3 by metabolically remodeled AMs.

In tandem, our results show that ROS enhance, whereas glycolytic flux inhibits, AM secretion of vesicular SOCS3. These findings significantly advance our understanding of the cellular determinants of vesicular cargo packaging. Although we anticipate these mechanisms to be important for influencing the cargo content of EVs secreted in virtually all tissues, they may be especially meaningful in the lung alveolar milieu characterized by high oxygen tension and low levels of glucose. Future studies are needed to elucidate the molecular chaperones and/or motifs present within SOCS3 that control its vesicular sorting into AM-derived EVs.

Chapter 1 – Introduction

Portions of this chapter have been published:

Haggadone MD, Peters-Golden M. Microenvironmental Influences on Extracellular Vesicle-Mediated Communication in the Lung. *Trends Mol. Med*. (2018) 24(11):963-975. PubMed PMID: 30244822.

Scope of the Dissertation

This dissertation comprises two mechanistic studies that address how alveolar macrophages (AMs) tune the cargo content of their secreted extracellular vesicles (EVs). My work is specifically contextualized through the lens of two important microenvironmental perturbations: cell stress and metabolic remodeling. Chapter 1 will introduce the unique demands of the lung microenvironment. I will provide an overview of the phenotype, ontogeny, and function of macrophages present within the steady-state lung with a specific emphasis on AMs. I will also discuss how AMs interact with their niche to maintain pulmonary immune homeostasis. In so doing, I will introduce the biology of EVs and highlight the role of vesicular transfer of homeostatic cargoes from AMs to lung epithelial cells (ECs). This discussion will specifically emphasize the role of vesicular secretion of suppressor of cytokine signaling (SOCS) proteins. Lastly, I will cover the two contextually relevant perturbations central to the experimental work presented herein: oxidative stress and metabolic remodeling. Chapter 2 will focus on regulation of AM release of vesicular SOCS3 by reactive oxygen species (ROS). In particular, I will illuminate a mechanism of enhanced SOCS3 secretion involving oxidative inactivation of the proteasome. Chapter 3 will demonstrate how glycolytic remodeling in AMs compromises the release of vesicular SOCS3 in a manner dependent on increases in acetyl-CoA. Finally, in Chapter 4, I will

discuss the contribution of this work to our broader understanding of EV biology and immune regulation within the lung microenvironment.

Lung Alveolar Biology

The respiratory system carries out the vital physiologic function of gas exchange between the blood and external environment. It is multi-compartmental, comprised of the nose, oropharynx, larynx, trachea, bronchi, bronchioles, and pulmonary alveoli. Semi-rigid conducting airway tubes – supported by cartilage, smooth muscle, and extracellular matrix – bifurcate, branch, and taper leading to the alveoli, terminal sacs where oxygen is transported into the capillary network, thus entering the arterial system. Remarkably, with over 300 million alveoli, the human lung dedicates approximately the surface area of a tennis court to gas exchange. Despite continuous exposure to toxins, allergens, and pathogens, this system is protected by a robust innate and adaptive immune system, which, in turn, must be appropriately restrained to ensure pulmonary homeostasis. Indeed, immunologic quiescence is a key feature of the lung microenvironment, and the research included herein focuses on inflammatory restraint conferred via homeostatic intercellular communication in the alveolar space.

The lung alveolus is comprised of epithelial cells that interface with the air, endothelial cells that interface with the capillaries, and mesenchymal cells found in the lung interstitium, the space between the epithelia and endothelia. These cell types exhibit substantial diversity at the single-cell level (1-3). The alveolar epithelium consists of two primary lineages: the alveolar epithelial type 1 (AT1) and type 2 (AT2) cells. Most of the alveolar surface area (~95%) is covered by AT1 cells, whereas AT2 cells are responsible for generating pulmonary surfactant. This substance is critical for reducing alveolar surface tension to prevent the lungs from collapsing with every breath. Furthermore, AT1 and AT2 cells are specified early on during development, but AT2

cells have stem-cell-like properties allowing them to both self-renew and regenerate AT1 cells after injury (4). Additionally, the alveolar compartment is rich in immune cells including AMs and interstitial macrophages (IMs). These macrophage populations are adapted to the quiescent microenvironment of the lung, and yet exhibit sufficient plasticity to mount inflammatory responses in the context of injury/insult. In particular, AMs, the predominant lung-resident immune cells, act as first lines of defense against microorganisms or particles reaching the lower airways. Below, the ontogeny, phenotype, and function of these pulmonary macrophages will be discussed.

Pulmonary Macrophages: Ontogeny and Phenotype

Ontogeny and Phenotype of AMs

Macrophages are present in all mammalian organs with phenotypes specifically tuned to fulfill the needs of that particular tissue. As such, they exhibit remarkable diversity and functional specialization, which is regulated by instructive signals provided from the local niche (5). In mice, macrophage progenitors seed tissues in three developmental waves from the yolk sac, fetal liver, and bone marrow (6,7). AMs are the best studied pulmonary macrophage subset, as they are readily retrieved from the alveoli by lavage, from which they can be easily purified by adherence. Ontogenically, AMs originate from fetal monocytes that populate the lung after birth and differentiate into mature cells due to local production of granulocyte-macrophage colony-stimulating factor (GM-CSF) by AT2 cells, which is responsible for induction of the critical transcription factors peroxisome proliferator-activated receptor ɣ (PPARɣ) (8) and PU.1 (9). In addition to PPARɣ and PU.1, other transcription factors, such as Bach2 and CCAAT/enhancer binding protein β, and autocrine production of transforming growth factor β (TGFβ), are known to be important for AM development and homeostasis (10-12). Unlike other tissue-resident

macrophages, however, AMs develop and persist independent of macrophage colony-stimulating factor (M-CSF) signaling (13).

At steady state, AMs are largely of embryonic origin; the original pool of seeded AMs proliferates locally and maintains independent of any substantial contribution from recruited adult monocytes (14-17). Although these foundational observations were made in mice, there is evidence in human lung transplant recipients that the donor-derived AM pool is remarkably stable (18,19). However, lung injury has been shown to result in the depletion of AMs and recruitment of circulating monocytes to the alveolar space (20-22). Depending on the degree of injury, AMs are restored either by local proliferation or the differentiation of recruited cells into macrophages (23). The latter scenario results in an AM pool of mixed origin (embryonic and monocytic) where – according to the "niche competition model" – the extent to which monocyte-derived macrophages occupy the alveolar niche is determined by the magnitude of resident AM depletion (24). Taken together, these findings suggest that in the absence of insult, AMs are embryonically derived and long-lived, but can be replaced by circulating monocytes that replenish a depleted AM pool resulting from lung perturbation.

Phenotypically, AMs express some canonical macrophage markers (e.g., MerTK, CD206, and F4/80), but are distinct from other tissue macrophages in that they express low levels of the integrin CD11b and fractalkine receptor CX3CR1 (16,25-27). Instead, bona fide AMs express high levels of the sialic acid-binding lectin Siglec F and the integrin CD11c (16,25-27). Furthermore, as will be discussed below, AMs are functionally unique and highly adapted to the quiescent microenvironment of the lung.

Ontogeny and Phenotype of IMs

Whereas AMs are abundant and resident in the lumen of the lung, IMs are less populous and reside in the interstitial space between the epithelium and capillaries. As such, these cells can be considered as a second line of defense against microbes that have circumvented removal by AMs and made their way into the interstitium. Experimentally, IM isolation requires tissue digestion and selection making them more difficult to study than AMs. Phenotypically, IMs are distinct from AMs in that they ubiquitously express canonical macrophage markers including CD11b and CX3CR1 and lack expression of CD11c and Siglec F (25,28). Furthermore, IMs express higher levels of the M-CSF receptor (i.e., *Csfr1*), but lower levels of the GM-CSF receptor (i.e., *Csfr2a* and *Csfr2b*) (25), demonstrating differential dependence on these two growth factors by AMs and IMs.

Ontogenically, in contrast to AMs, IMs are present in the lung before birth (29), but are later replaced by an influx of blood monocytes at steady state (25,28-30). Accordingly, transplantation studies have demonstrated that IMs have a much higher turnover rate than do AMs (31). These findings indicate that the initial contribution of yolk sac macrophages to the IM pool is higher than for AMs. However, whereas fetal monocyte-derived AMs stably persist in the lung over time, IMs are progressively diluted, first by fetal monocytes and then by monocytes recruited from the bone marrow. Lastly, two major populations of IMs have been identified: LYVE-1^{low}MHC-II^{high} cells that are present adjacent to neurons and specialize in antigen presentation, and LYVE-1^{high}MHC-II^{low} perivascular cells specialized in wound healing and tissue repair (30). The ontogeny, localization, and phenotype of these pulmonary macrophages are summarized in **Figure 1-1**.

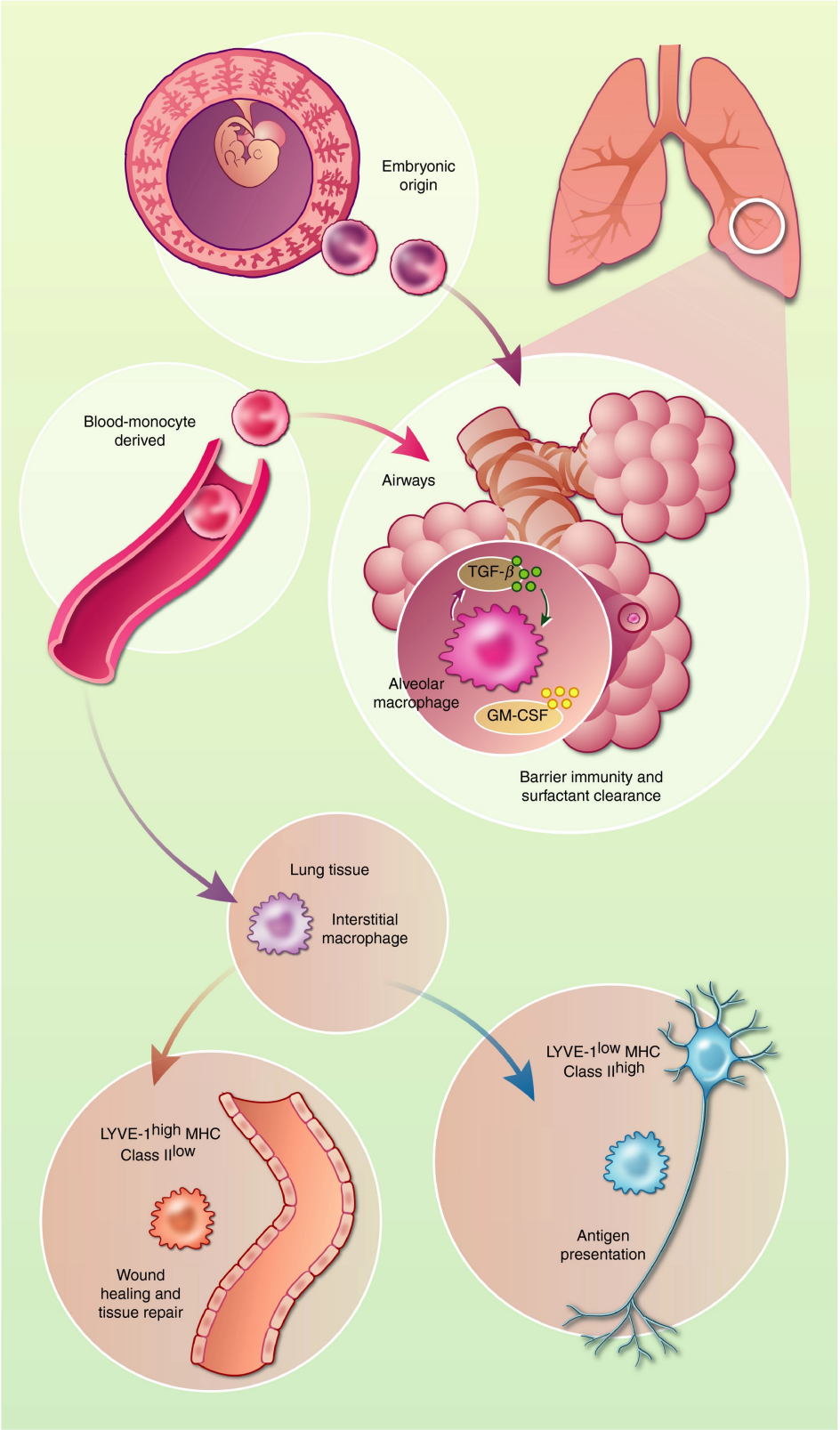

Figure 1-1: Ontogeny, localization, and phenotype of pulmonary macrophages

From (Evren et al., 2019).

Functional Tuning of AMs by the Alveolar Niche

AMs are developmentally and functionally tuned according to the unique characteristics and demands of the alveolar space in which they reside – including high oxygen tension, an abundance of pulmonary surfactant, and the need for inflammatory restraint to ensure efficient gas exchange. For example, AMs deficient in their ability to sense oxygen caused by deletion of the von Hippel-Lindau tumor suppressor protein, a negative regulator of the hypoxia-inducible factor (HIF) transcription factors, fail to terminally differentiate, self-renew, and exert their homeostatic functions (32). This elegantly demonstrates how AMs develop in coordination with the constraints imposed upon them by their environment. Likewise, AMs are critical for recycling the pulmonary surfactant generated by AT2 cells, as GM-CSF knockout mice containing functionally impaired AMs accumulate surfactant lipids and proteins in the alveoli (33). Thus, there is a bidirectional relationship between AMs and their niche: the niche provides trophic factors (e.g., GM-CSF) to support AMs, which reciprocally support the niche by promoting their homeostatic functions.

Immunologically, AMs have also long been recognized as cellular determinants of inflammatory quiescence within the airways and alveolar space (34). A variety of mechanisms have been implicated in their quiescent phenotype. Lipid metabolism promoted by PPARγ expression in AMs is known to be important for airway immunosedation (35). TGFβ secretion, which as mentioned previously is critical for AM homeostasis, is also appreciated for its role in suppressing the release of inflammatory mediators by AMs (36). Consequently, AMs are poor antigen presenting cells (37-39), and they render antigen-specific T cells unresponsive due to minimal expression of co-stimulatory molecules (e.g., CD86) (40). AMs additionally suppress T cell responses through the production of TGFβ, inhibitory prostaglandins (41), and retinoic acid (42). In particular, release of immunosuppressive factors by AMs is augmented through their

phagocytosis of apoptotic cells, thus highlighting the anti-inflammatory role of AMs during the resolution phase of inflammation (43-45).

This tolerogenic phenotype of AMs also reflects contributions of both contact-dependent and -independent signals provided by neighboring respiratory ECs. For example, CD200 expression on the luminal aspect of AT2 cells ligates CD200R on AMs to prevent their expansion and activation (46). Additionally, interleukin (IL)-10 production by the epithelium inhibits AM inflammatory responses (47). The same is true for the secretion of surfactant proteins by AT2 cells (48), which are known to bind to signal-regulatory protein-α on AMs to suppress their phagocytic activity (49). In turn, AMs also regulate the lung epithelium. As will be discussed in more detail below, elaboration of homeostatic EVs by AMs limits inflammatory signaling in neighboring ECs (50,51). Furthermore, in a contact-dependent manner, AMs relay immunosuppressive signals to ECs in the form of calcium waves through gap junction-like connections (52). Together, these findings underscore the regulatory phenotype of AMs resident in a microenvironment requiring their quiescence.

It is also evident, however, that AMs participate in the inflammatory response and in the pathogenesis of various disease states, such as respiratory tract infections, chronic obstructive lung disease, asthma, and lung fibrosis (53). The long-held paradigm is that AMs are highly plastic cells that promote inflammation by recruiting neutrophils and other leukocytes. However, recent evidence calls into question resident AM plasticity and the circumstances under which these cells exhibit changed reactivity. For example, influenza virus infection has little effect on the transcriptional profile or functional phenotype of resident AMs; rather it results in the recruitment of pro-inflammatory AMs that persist in the lung (54). Similar observations have been made in the context of lung fibrosis. While recruited AMs drive fibrotic disease, transcriptionally distinct

resident AMs remain phenotypically unchanged and play no role in promoting fibrogenesis (55). Likewise, resident AMs suppress, whereas recruited monocyte-derived AMs promote, allergic inflammation (56). These studies suggest that – in some scenarios – resident AMs are uninfluenced by the inflammatory milieu, thus retaining their homeostatic properties endowed by the steady-state alveolar niche. On the contrary, transcriptomic analyses of resident and recruited AMs during acute lung injury (ALI) have demonstrated that both populations contribute to peak inflammation, albeit in transcriptionally and kinetically distinct ways (57). Furthermore, resident AMs have been shown in some experimental settings (i.e., *Pseudomonas aeruginosa* vaccine administration and adenoviral infection) to undergo long-term pro-inflammatory changes, a phenomenon referred to as "trained immunity" (58,59). It is currently unclear why some scenarios favor the development of pro-inflammatory AMs via inflammatory monocyte recruitment while others favor inflammatory changes within the resident AM compartment. Consequently, there still exists some ambiguity regarding the plasticity of AMs and their participation in the inflammatory response; however, it appears likely that context plays an important determinative role.

In conclusion, AMs are heavily influenced by, and adapted to, the quiescent compartment in which they reside. Their functions are tuned to fulfill the needs of the alveolar niche, and their quiescent phenotype is ideally suited to protect the physiologic imperative for gas exchange at this crucial anatomic interface despite the continual barrage of potentially inflammatory insults. While recent evidence suggests that terminal differentiation limits their plasticity, AMs are also appreciated for their role in launching and mediating inflammatory responses. However, the extent to which resident versus recruited AMs contribute to inflammation in the lung has yet to be fully contextually elucidated.

Janus Kinase (JAK)-Signal Transducer and Activator of Transcription (STAT) Signaling

The JAK-STAT pathway signals in response to more than 50 immunomodulatory cytokines and growth factors. Requiring only three components (i.e., membrane receptor, coupled kinase, and activated transcription factor), it is a simple system for transmitting signals from the cell surface to the nucleus where transcription of target genes occurs. This axis is comprised of four JAK proteins (JAK1-3 and TYK2) and seven STAT proteins (STAT1-4, STAT5A, STAT5B, and STAT6).

Each cytokine that uses JAK-STAT signaling binds to a specific receptor on the surface of the cell, which results in receptor oligomerization. As these receptors contain intracellular domains constitutively associated with members of the JAK family of kinases, ligand-receptor binding brings JAKs in close proximity to facilitate their auto-activation by transphosphorylation (60-65). Upon activation, JAKs phosphorylate the cytokine receptor tails, which creates docking sites for the recruitment of STAT transcription factors (66). STATs are then phosphorylated by JAKs (67,68) allowing for their dimerization and translocation to the nucleus where they promote transcription of target genes, the vast majority of which are pro-inflammatory in nature. However, as is typical for such intensely pro-inflammatory signaling pathways, there are built-in negative feedback mechanisms to ensure that signaling is switched off when appropriate. Accordingly, JAK-STAT signaling results in the expression of a family of Src homology 2 (SH2)-containing proteins called SOCS that negatively regulate these signaling axes; there are eight SOCS proteins: SOCS1-7 and cytokine-inducible SH2-containing protein (69,70). A general rule is that a cytokine binds to a specific receptor that activates specific JAK(s) and STAT(s), which are negatively regulated by a particular SOCS protein; however, there are exceptions to this rule owing to a

substantial degree of promiscuity among STAT and SOCS isoforms. JAK-STAT signaling and negative regulation by SOCS is summarized in **Figure 1-2**.

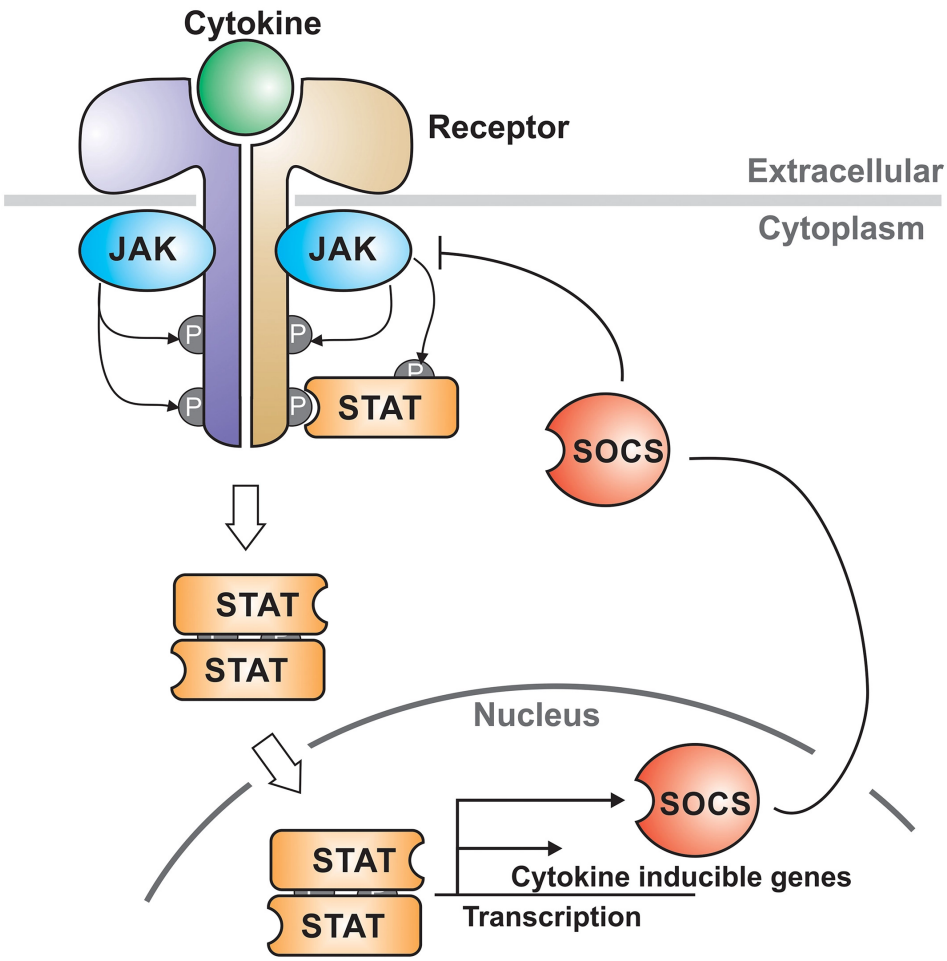

Figure 1-2: JAK-STAT signaling and negative regulation by SOCS

From (Morris et al., 2018).

This dissertation focuses on SOCS3, the prototypic negative regulator of STAT3 signaling. Activation of STAT3 occurs downstream of receptor binding to numerous cytokines and growth factors, including those utilizing the IL-6 signal-transducing receptor chain gp130 (e.g., IL-6 and IL-11), protein tyrosine kinase receptors (e.g., epidermal growth factor), and homodimeric cytokine receptors (e.g., granulocyte colony-stimulating factor) (71-74). STAT3 signaling has

been implicated in a number of lung inflammatory contexts, for example, asthma (75), ALI (76), pulmonary fibrosis (77), and lung cancer (78). During inflammation, SOCS3 is expressed in the lung epithelium to a lesser degree than it is in leukocytes (79). Furthermore, in the normal lung, SOCS3 expression in alveolar epithelial cells (AECs) is markedly lower than it is in AMs (80). This low endogenous expression and the importance of SOCS3 for restraining inflammation in the terminal air space highlight the utility of AECs acquiring this regulatory protein from another cell source. As will be described below, this occurs through an unconventional means of transcellular SOCS3 delivery from AMs to AECs.

Biology of EVs: Roles in Lung Homeostasis and Inflammation

Classification

EVs are membrane-delimited structures that are secreted into the extracellular milieu by a source cell and that transmit molecular information capable of influencing recipient cells. This information consists of a variety of cargoes within EVs, including proteins, various forms of RNA (e.g., mRNA and miRNA), and lipids. Although they comprise a spectrum of sizes and biochemically defined subtypes, EVs are traditionally divided into two major classes, exosomes (Exos) and microvesicles (MVs), reflecting their divergent mechanisms of biogenesis (summarized in **Figure 1-3**) (81). Exos are the smallest type of vesicles, ranging from approximately 30 to 100 nm in diameter. They are derived from intraluminal vesicles (ILVs) that form as a result of the inward budding of endosomal membranes during maturation of multivesicular endosomes (MVEs). Upon exocytosis of MVEs, ILVs are released into the extracellular environment, where they are called Exos. Consistent with their intracellular origin, Exos are enriched in proteins normally associated with endosomes and endosomal sorting pathways (82). Conversely, MVs are vesicles that arise at the cell surface due to outward budding

of the plasma membrane (PM) and subsequent shedding. MVs are typically larger than Exos (50 - 1,000 nm in diameter), although some size overlap does exist. In keeping with their origin, they are enriched in PM-embedded and cytosolic cargoes (83). Recent advances in knowledge about EVs call into question the utility of traditional classification schemes that categorically differentiate between Exos and MVs. As noted above, overlaps in size exist. In addition, cargo molecules long considered as markers of one subset have been identified in the other (e.g., endosomal proteins in PM-derived MVs) (82,83). Finally, no major functional differences between Exos and MVs are recognized, as both are capable of being internalized by and hence transmitting cargo to recipient cells (84).

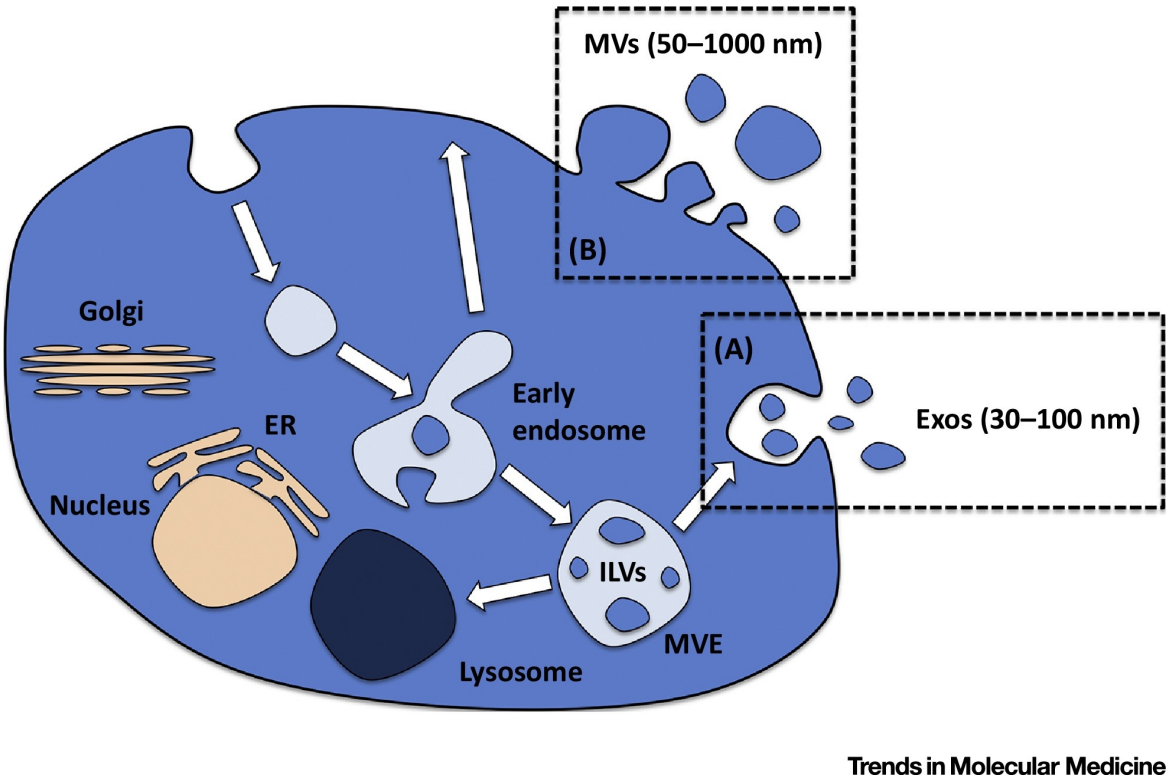

Figure 1-3: Divergent mechanisms of MV and Exo biogenesis

(**A**) Exos are derived from ILVs that form during maturation of MVEs. While some MVEs are destined for degradation in the lysosome, those that fuse with the PM exocytose ILVs, giving rise to Exos. (**B**) Conversely, MVs are generated via outward budding of the PM and release into the extracellular milieu. From (Haggadone and Peters-Golden, 2018).

EV Control of Lung Homeostasis

While studies of lung EVs have largely focused on their composition and biologic activity in the context of inflammation, emerging evidence demonstrates that they are critically involved in lung homeostasis as well, reflecting crosstalk between AMs and ECs. This is exemplified by the finding that SOCS proteins in EVs served as vectors of communication between AMs and ECs (51). Exos (100,000 x *g* pellet fraction of conditioned medium [CM]) released by resting AMs contained SOCS1, while their MVs (17,000 x *g* pellet fraction of CM) contained SOCS3; both were internalized by, and suppressed cytokine-induced JAK-STAT signaling in, AECs. The transcellular acquisition of this regulatory cargo was a critical brake on AEC production of the STAT-dependent gene product monocyte chemoattractant protein-1 (MCP-1), one of the key chemokines responsible for recruitment of monocytes to the lung during inflammation. Moreover, constitutive AM secretion of SOCS3 *in vitro* and *in vivo* was subject to bidirectional modulation by various microenvironmental factors, being inhibited by cigarette smoke (CS) but potentiated by immunosuppressive mediators IL-10 and prostaglandin E_2 (PGE_2). Therefore, it is possible that loss of this previously unrecognized endogenous brake may favor smoking-related inflammation. It could be further envisioned that a similar defect in SOCS3 secretion also serves to facilitate development of other chronic inflammatory disorders of the lung. Accordingly, loss of SOCS3 secretion has been shown to occur during, and exacerbate the pathophysiology of, allergic inflammation (85) and lung cancer (86).

Furthermore, because AECs themselves expressed negligible levels of endogenous SOCS3 and are thus dependent on AMs for its acquisition, whether AECs may have the capacity to tune AM provision of this vesicular cargo during acute exposure to inflammatory stimuli was explored. Indeed, lipopolysaccharide (LPS) or microbial challenge *in vitro* and *in vivo* heightened the

capacity of AECs to "request" SOCS3 from AMs, an effect that was mediated by increases in AEC elaboration of PGE_2 (87). These observations support a model in which AMs and AECs engage in intricate bidirectional crosstalk to utilize EV-encapsulated SOCS3 protein to restrain inflammation and facilitate homeostasis even in the face of acute environmental insults. Interestingly, neither abundant expression of SOCS3 nor the ability to package it within secreted EVs is shared by all mononuclear phagocytic cells, as neither peritoneal macrophages nor peripheral blood monocytes do so (51); the microenvironmental cues responsible for endowing AMs with this dual capacity remain to be determined. We postulate that this symbiotic relationship between AMs and AECs reflects their co-evolution in a challenging site with a mandate to restrain inflammation.

More recent work has also demonstrated the ability of AMs to direct, via elaboration of insulin-like growth factor 1 (IGF-1), enhanced uptake of MVs by ECs in a model of allergic inflammation (50). This dampened house dust mite (HDM)-induced airway inflammation, further highlighting the importance of vesicular communication between AMs and lung ECs for promoting lung homeostasis (summarized in **Figure 1-4**). It is assumed that AM-derived vesicular cargoes other than SOCS3 contribute to restraint of AEC inflammatory signaling pathways. Moreover, it is likely that AECs simultaneously secrete EVs that restrain AM function. A better understanding of the cargo composition of EVs secreted not only during inflammation but also at baseline and during inflammation resolution is necessary to further our knowledge of the homeostatic roles that EVs play within the alveolar compartment.

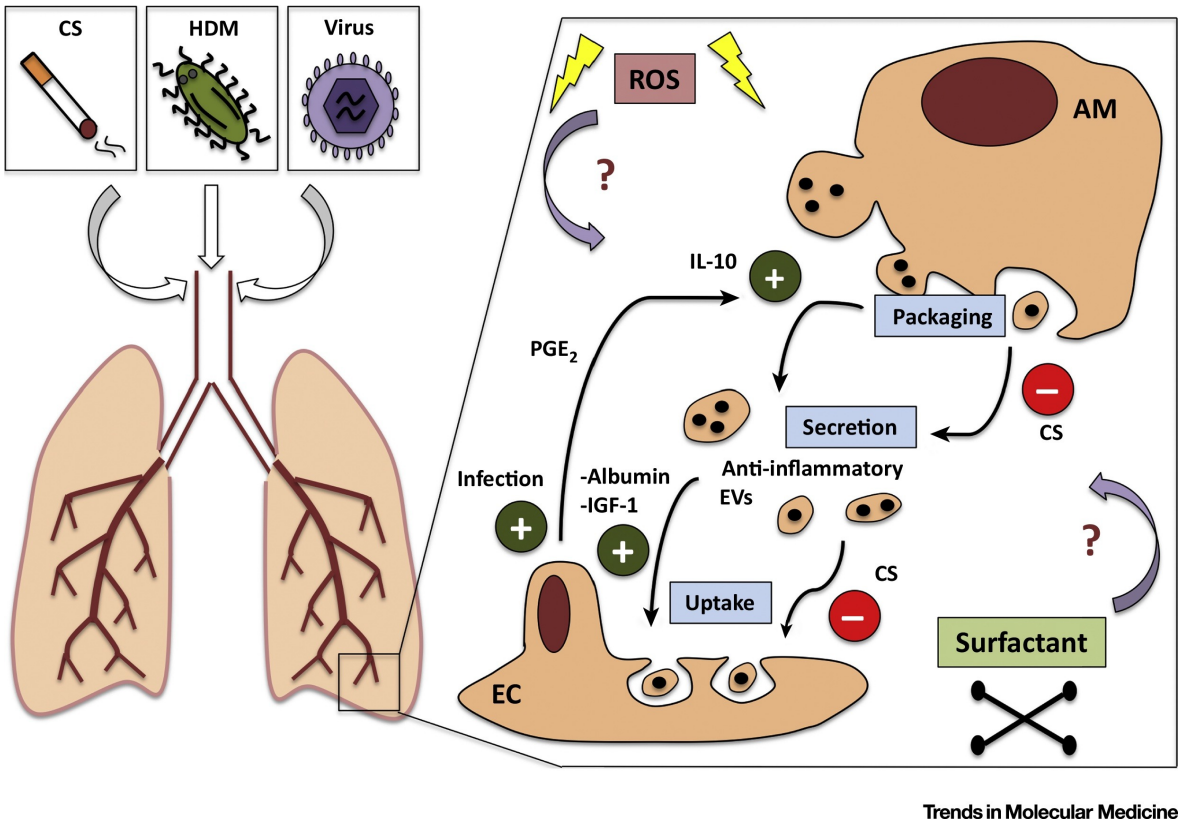

Figure 1-4: EV-mediated maintenance of homeostasis in the lung microenvironment

The airways and alveoli of the lung are continuously exposed to noxious environmental stimuli (left), such as environmental toxins (e.g., CS), allergens (e.g., HDM), and pathogens (e.g., respiratory viruses). Maintenance of homeostasis at these mucosal surfaces therefore requires intricate crosstalk between the predominant lung-resident immune cell, the AM, and the major cellular constituent of the respiratory surface, the respiratory EC (right). Packaging of anti-inflammatory cargo molecules such as SOCS proteins within EVs and their transmission from AMs to respiratory ECs is a recognized mechanism for restraining inflammation in the lung. The secretion and acquisition of vesicular information are regulated, however, at many steps. For example, AM packaging of vesicular SOCS3 is modulated by endogenous and exogenous factors; SOCS3 release is suppressed by exposure to CS but is enhanced by exposure to IL-10 and EC-derived PGE_2. Exposure of ECs to respiratory pathogens or LPS increases their synthesis of PGE_2, thereby serving as a signal to "instruct" AMs to enhance their packaging of homeostatic SOCS3 cargo. Furthermore, uptake of EVs by respiratory ECs is subject to external regulation; EV uptake is inhibited by CS but is enhanced by extracellular albumin and IGF-1. IGF-1 secretion itself is augmented upon exposure to HDM, and resulting increases in EV uptake by ECs serve to attenuate HDM-induced inflammation. This vesicular crosstalk between AMs and respiratory ECs takes place in the unique lung microenvironment that is characterized by high levels of ROS and pulmonary surfactant. The impact of ROS and surfactant proteins on AM-EC vesicular communication, however, remains incompletely understood. From (Haggadone and Peters-Golden, 2018).

Lung EVs in Inflammation

In addition to EVs serving as homeostatic vectors of communication between AMs and AECs, they are also influenced by, and participate in, pro-inflammatory crosstalk between these two cell types. ROS are a prominent constituent of the inflammatory milieu, and significant

attention has been directed at understanding the effects of oxidative stress on EV production and cargo composition. Given its uniquely high oxygen tension, this influence is especially relevant in the lung. Hyperoxic exposure was reported to increase the number of lung EVs, with their predominant source being ECs (88). Addition of such EC-derived EVs to AMs promoted AM production of the inflammatory chemokine macrophage inflammatory protein-2 that was, in turn, dependent on the caspase-3 content of the EVs. In parallel, intrapulmonary administration of these hyperoxia-derived EVs *in vivo* promoted macrophage and neutrophil influx into the lung. Further work has suggested a predominant effect of oxidative stress on the miRNA profile of EVs secreted by lung ECs (89). Two hyperoxia-induced EC miRNA cargoes, miR-221 and miR-320a, were sufficient for promoting macrophage activation. Finally, comparable pro-inflammatory effects of lung EC-derived EVs on AM function have been described in the context of allergic inflammation (90), respiratory syncytial virus infection (91), acid-induced lung injury (92), cystic fibrosis (93), and acute respiratory distress syndrome (94).

While less well studied, perturbation of macrophages has also been shown to cause elaboration of pathogenic EVs that promote EC activation. For example, exposure to CS elicited rapid shedding of EVs from human mononuclear cells that, when added to AECs, caused upregulation of the inflammatory chemokines IL-8 and MCP-1 (95). In addition, treatment of AMs with LPS *in vitro* and intratracheal administration of LPS *in vivo* generated tumor necrosis factor-containing EVs that promoted lung EC activation, as reflected by upregulation of intracellular adhesion molecule-1 (96). It is evident, then, that transmission of EV-dependent information is a dynamic process that is subject to modulation by a variety of physiologic perturbations affecting both source and recipient cells, and that it can ultimately promote inflammation or homeostasis. EV-mediated information flow requires several distinct steps: EV biogenesis by source cells, cargo

packaging within EVs, uptake of EVs by recipient cells, and accessibility of EV-contained cargo for utilization. Each of these steps could be influenced by local factors in the microenvironment. The remainder of this section focuses on these topics.

Mechanisms of Biogenesis

The mechanisms of EV formation have been best studied for Exos. ILV budding and cargo sorting into MVEs is largely dependent on various constituents of the endosomal sorting complex required for transport (ESCRT) family of proteins, which consist of four different complexes: ESCRT-0, -1, -II, -III, and an associated ATPase complex vacuolar protein sorting-associated protein 4 (97). RNAi screening experiments have identified the specific contributions of each ESCRT family member to both Exo biogenesis and cargo packaging (98). However, generation of Exos can also occur independent of ESCRTs. For example, tetraspanins have long been known to participate in ESCRT-independent biogenesis (99), as CD9, CD82, tetraspanin 8, and CD63 all promote Exo secretion (100-102). Furthermore, lipids such as ceramide generated by neutral sphingomyelinase 2 that promote membrane curvature are also known to play a role in the generation of Exos (103).

The mechanisms of biogenesis of MVs are less well characterized, but also involve activity of ESCRT proteins (104). One means of ESCRT recruitment to the PM involves the adaptor protein arrestin domain-containing protein 1 (ARRDC1) (105). Polyubiquitination of ARRDC1 results in the enhanced generation of a subtype of MVs termed ARRDC1-mediated microvesicles (ARMMs), which contain ESCRT subunits (105). Small GTPase proteins, such as ARF1, ARF6, and RhoA can also facilitate MV budding from the PM (106-108). Finally, similar to Exos, generation of ceramide by acid sphingomyelinase also promotes MV secretion (109,110).

Cargo Packaging

Packaging of specific proteins into Exos has been attributed to a variety of post-translational modifications (PTMs) (111), with ESCRT-dependent sorting of ubiquitin-tagged cargoes being one of the most recognized (112,113). Phosphorylation and farnesylation are other PTMs that also regulate Exo cargo sorting (114,115). Additionally, similar to their role in promoting Exo biogenesis, ceramide and tetraspanins can determine Exo cargo composition independent of ESCRTs (100,103,116). Much less is known, however, about the signals and machinery involved in packaging of nucleic acid cargoes such as RNA. Sumoylated heterogeneous nuclear ribonucleoprotein A2B1 was identified as a chaperone capable of binding particular *cis*-acting motifs within miRNAs to facilitate their entry into Exos (117). This miRNA-sorting function was also ascribed to synaptotagmin-binding cytoplasmic RNA-binding protein (118,119). Interestingly, studies of mRNA secretion in Exos have revealed enrichment of particular 3' untranslated region sequences, which implies that specific nucleotide sequences serve as "zipcodes" to direct packaging within Exos (120). A similar mechanism was described for mRNA sorting into MVs; this mechanism, however, involved an interaction between 3' untranslated region zipcode sequences in mRNAs and MV-packaged miRNAs (121). The importance of ribonucleoprotein chaperones and miRNA-mRNA complexes in packaging of these RNA cargoes requires further research.

Very little is known about how proteins, in particular those residing in the cytosol, are selectively targeted for inclusion into MVs that bud from the PM. A body of early work suggested that higher-order protein oligomerization and various *cis*-acting signals that anchor proteins to the PM were sufficient for protein packaging into EVs (122-124). These included PTMs resulting in PM targeting (e.g., prenylation, palmitoylation, and myristoylation tags) and domains mediating binding to phosphatidylinositol 4,5-bisphopshate and phosphatidylinositol (3,4,5)-trisphosphate

on the internal face of the PM. However, as the proteins in these studies were genetically engineered to encode these elements, the biologic relevance of these determinants for MV packaging of endogenous proteins remains uncertain. In addition to its role in MV biogenesis, a recent body of research has highlighted a novel role for ARRDC1 in cargo packaging. Through its polyubiquitination and interactions with E3 ligases, ARRDC1 can serve as an adaptor for vesicular inclusion of proteins such as neurogenic locus notch homolog protein 2 (125) and the divalent metal transporter 1 into ARMMs (126). Collectively, these observations suggest that EV packaging of proteins likely involves the combined effects of PM targeting of proteins through *cis*-acting signals and targeted delivery of proteins via dedicated adaptors. Accordingly, a secretory autophagy pathway was recently described involving membrane targeting of microtubule-associated protein 1A/1B-light chain 3 and its concomitant loading of protein and RNA cargoes into EVs (127). Despite these advances, however, the precise mechanistic determinants of cargo packaging within various types of EVs, both at baseline and in response to microenvironmental cues, remain poorly understood.

Mechanisms and Modulation of EV Uptake and Cargo Delivery

Transmission of vesicular information requires either activation of cell-surface receptors on, or internalization of EVs by, recipient cells. Among the reported mechanisms of EV uptake, receptor-dependent and -independent forms of endocytosis predominate, although direct membrane fusion, phagocytosis, and micropinocytosis of EVs have also been reported (128). Unlike their divergent modes of biogenesis, however, there are no clear distinct internalization pathways for Exos versus MVs. It was reported that AM-derived MVs were rapidly internalized by AECs via a receptor-independent (i.e., fluid-phase) form of endocytosis that depended on the GTPase dynamin and actin polymerization (129). In addition, uptake was subject to bidirectional

modulation by endogenous and exogenous perturbations. For example, uptake was enhanced by extracellular albumin, whose accumulation in the alveolar space is a typical consequence of the disruption of endothelial and epithelial integrity seen during inflammatory ALI. In this scenario, augmented internalization of AM-derived anti-inflammatory cargoes such as SOCS3 would be expected to facilitate homeostasis. Conversely, MV uptake was inhibited by CS, owing to oxidative disruption of actin polymerization (129). This illustrates the potential for disruption of AM-AEC homeostatic communication and the potentiation of inflammation by noxious environmental stimuli. Furthermore, as discussed previously, signals such as IGF-1 that are derived from AMs can enhance EV uptake by AECs to dampen their inflammatory response and favor homeostasis in the lung (50).

While modulation and mechanisms of EV uptake by AMs have not been carefully explored, investigation of other macrophage subtypes suggests that EV uptake pathways for AMs might differ from AECs. In particular, receptor-dependent mechanisms of EV uptake by macrophages have been implicated. For example, endocytosis of reticulocyte-derived EVs was demonstrated for primary peritoneal and J774 macrophages, a process suggested to depend on direct interaction between EV-packaged galectin-5 and glycoproteins present on the macrophage PM (130). In addition, phagocytic mechanisms of EV uptake for RAW-264.7 macrophages (131) and macropinocytic mechanisms for microglia (132), which were attributed to direct binding to phosphatidylserine present on the surface of EVs, have been described. Although confirmation requires dedicated investigation, it seems likely that the mechanisms of EV internalization described for other macrophage populations are shared, at least in part, by AMs.

One final step in cell-cell communication via EVs that merits mechanistic understanding is how internalized EV cargoes such as SOCS3 are liberated and delivered to the appropriate

intracellular compartment of recipient cells. Direct membrane fusion would easily enable direct cytosolic delivery of vesicular contents, and some studies have suggested this as a route of cargo acquisition (133,134). However, as mentioned above, EV internalization occurs mainly via endocytic mechanisms, and the predominant destination for EV constituents appears to be the lysosome (135), with a small fraction being routed to the recycling endosome (136). Although direct escape from endosomal-to-cytosolic compartments has been proposed as a model for cargo delivery, recent work suggests that this mechanism is not functionally operative (137,138). Rather, what appears to occur is trafficking of EVs into endosomes that scan, and allow for functional delivery of cargoes into, the endoplasmic reticulum (ER) before eventual delivery of EVs to (and degradation in) the lysosome (139). While targeting to the ER would account for the efficacy of delivery of miRNA and siRNA via EVs, the relevance of this sorting circuitry for transmission of protein content remains unclear. In particular, no current models would explain how an intravesicular protein surrounded by both EV and endosomal membranes reaches the cytosol to exert its biologic function (e.g., as must occur for SOCS proteins to inhibit the kinase activity of JAK) rapidly. Only when we better understand the fundamental mechanisms determining EV cargo packaging, secretion, internalization, and availability can we envision strategies to maximize the transmissibility of protective cargoes and/or limit the transmissibility of pathogenic cargoes *in vivo*.

ROS Generation and Regulation of Protein Degradation

ROS comprise a group of reactive molecules and free radicals derived from molecular oxygen that assume diverse roles within and outside of the cell. Once thought to exclusively promote the oxidation and accumulation of damaged lipids, proteins, and nucleic acids, it is now appreciated that ROS also have beneficial effects on cellular function (140). There are two major

sources and a variety of minor sources of ROS within the cell. NAPDH oxidases (NOX proteins) represent one major source in the cytosol, particularly in phagocytes which generate large amounts of ROS during their participation in host defense (141). ROS are also a byproduct of aerobic metabolism involving electron transport and the generation of a proton gradient to produce ATP, making mitochondria the other major source of cellular ROS (142). Additional organelles and enzyme complexes involved in ROS generation include the endoplasmic reticulum, peroxisomes, xanthine oxidase, nitric oxide synthase, cyclooxygenases, lipoxygenases, and cytochrome P450 enzymes (140).

In eukaryotic cells, the ubiquitin-proteasome and autophagy-lysosome systems are the two major pathways that control protein degradation, both of which are regulated by ROS. The 26S proteasome is a multimeric complex comprised of a 20S core particle (CP) and 19S regulatory particle (RP) that selectively hydrolyze protein substrates tagged for degradation by ubiquitination (143). Specifically, the 19S RP binds polyubiquitinated substrates and uses ATP to unfold and translocate them into the 20S CP, which contains enzymatic activity necessary for protein degradation. Alternatively, the 20S CP may associate with other regulatory proteins for ubiquitin/ATP-independent protein degradation (144). Both ubiquitin-dependent (145) and -independent (146-148) mechanisms are known to be important for the removal of oxidized proteins, and the proteasome plays an important role in maintaining cell viability in response to oxidative stress (147). ROS are known, however, to bidirectionally regulate proteasome activity in a kinetically determinative manner. Acutely, oxidative stress causes dissociation of the 26S proteasome (148), attenuation of ubiquitin conjugation (149), reduced 19S RP ATPase activity (150), and a loss of 20S CP catalytic activity (151,152). Conversely, recovery from oxidative stress (i.e., the post-treatment period) is associated with increases in proteasome activity (149,152,153)

to remove oxidized proteins within the cell. Therefore, ROS play a key role in tuning the activity of this pathway central to cellular proteostasis, and the research included in this dissertation will focus on proteasome inhibition during exposure of AMs to ROS. In addition to regulating the ubiquitin-proteasome system, ROS are also known to regulate protein degradation controlled by autophagy, the process through which cytoplasmic macromolecules and organelles are delivered to the lysosome for degradation (154). ROS augment autophagic flux through regulation of transcription, protein activity, and organellar degradation (155). Accordingly, oxidative stress is implicated in the selective removal of mitochondria through mitophagy (156). In addition, like the ubiquitin-proteasome system, degradation of oxidized proteins through chaperone-mediated autophagy, which is induced by ROS, promotes cell viability during oxidative stress (157). Therefore, oxidative stress exerts substantial control over protein degradation within the cell through control over proteasome activity and autophagic flux, and both of these processes are important for removal of oxidized proteins to maintain cellular integrity.

Macrophage Immunometabolism

In addition to providing the energy necessary to support immune cell activity, metabolic adaptations are also central to changes in immune cell function through control over transcriptional and post-transcriptional events. Macrophages have long been recognized to undergo metabolic switches in response to activation (158). In particular, pro-inflammatory macrophages (conventionally referred to as M1 macrophages), which are activated by diverse stimuli (e.g., LPS and interferon ɣ [IFNɣ]), depend on aerobic glycolysis and the pentose phosphate pathway (PPP) to meet their ATP requirements, while anti-inflammatory macrophages (conventionally referred to as M2 macrophages) activated by stimuli such as IL-4 generate energy through enhanced fatty acid oxidation and oxidative metabolism (159-161).

The key transcription factor involved in the commitment toward aerobic glycolysis in pro-inflammatory macrophages is HIF-1α, which induces expression of both glycolytic genes (e.g., glucose transporter 1 [*Glut1*] and hexokinase 2 [*Hk2*]) and inflammatory genes (e.g., IL-1β) (162). HIF-1α activation occurs downstream of many signals and signaling pathways, including Krebs cycle-derived succinate (160), mitochondrial ROS (163), Toll-like receptor/nuclear factor κ-light-chain enhancer of B-cell signaling (164), and AKT/mammalian target of rapamycin signaling (165). In turn, glycolytic remodeling is critical for various macrophage effector functions including ROS production, phagocytosis, and the release of pro-inflammatory cytokines (159,166). Glycolysis also supplies the PPP, which generates intermediates such as ribose for nucleotides, amino acids for protein synthesis, and NADPH used for fatty acid synthesis and the generation of ROS by NOX (167). Production of nitric oxide (NO) through metabolism of arginine by inducible nitric oxide synthase (iNOS) is another hallmark of pro-inflammatory macrophages (168). Finally, generation of ROS caused by dysfunctional oxidative phosphorylation (169,170) and reverse electron transport (RET) at complex I (163) is characteristic of macrophages with "broken" mitochondrial metabolism.

In addition to generating ROS as a consequence of these mitochondrial alterations, glycolytically reprogrammed macrophages are also characterized by a Krebs cycle that is interrupted at key points, which allows the intermediate metabolites citrate, succinate, and itaconate to escape the mitochondria and exert their regulatory functions. In particular, citrate production links mitochondrial and cytosolic metabolism. Under normal conditions, citrate is produced by condensation of oxaloacetate and acetyl-CoA, which is then converted to α-ketoglutarate (αKG) by isocitrate dehydrogenase (IDH). In pro-inflammatory macrophages, however, IDH expression is suppressed (161) concomitant with transcriptional upregulation of

mitochondrial citrate carrier (CIC) (171), which exports citrate from the mitochondria into the cytosol. Once in the cytosol, citrate is enzymatically converted to acetyl-CoA by ATP citrate lyase (ACLY) – whose expression is also elevated in pro-inflammatory macrophages (172) – where it serves as a substrate for the production of numerous regulatory molecules. For example, through the activity of ACLY and its conversion to acetyl-CoA, citrate drives protein and histone acetylation (173). Citrate-derived acetyl-CoA also serves as a substrate for fatty acid and lipid synthesis through activity of acetyl-CoA carboxylase (174). Furthermore, cytosolic citrate generates NO, ROS, and prostaglandins to promote macrophage inflammatory responses (171,172). Therefore, citrate is a key metabolite involved in the functional programming of glycolytic macrophages.

Itaconate is also abundant within pro-inflammatory macrophages (175) due to upregulation of, and its generation by, immune-responsive gene 1 (IRG1) (176). Itaconate has well-characterized bactericidal properties (177,178), and yet, despite accumulating in pro-inflammatory macrophages, it also exhibits anti-inflammatory properties by limiting ROS production, inflammasome activation, and pro-inflammatory cytokine release (179). Itaconate additionally elaborates its anti-inflammatory effects through stabilization of nuclear factor erythroid 2-related factor 2 to induce the expression of immunosuppressive and anti-oxidant genes (180). Nonetheless, itaconate is also linked to succinate accumulation due to its inhibition of succinate dehydrogenase (SDH). As mentioned previously, succinate assumes a key signaling role in stabilizing the transcription factor HIF-1α (160). Furthermore, high levels of cytosolic succinate promote post-translational lysine succinylation, a modification that changes protein charge, structure, and function (181,182). For example, succinylation of the enzyme pyruvate kinase M2 (PKM2) stimulates its translocation to the nucleus, interaction with HIF-1α, and induction of IL-1β

expression (183). Finally, succinate can also be released from the cell and act extracellularly by binding to its receptor SUCNR1/GPR91 to potentiate inflammation (184).

In stark contrast to pro-inflammatory macrophages, however, anti-inflammatory macrophages have an intact Krebs cycle and enhanced mitochondrial metabolism to support their phenotype and function (185). The role of glycolysis in fueling this metabolic phenotype has remained controversial with more recent studies suggesting that it is dispensable as long as oxidative phosphorylation remains intact (186). Rather, anti-inflammatory macrophages appear to be more metabolically flexible, using glutamine as fuel when glucose is limited (186) while also relying on fatty acid metabolism supported by STAT6, PPARɣ (187), and PPARɣ coactivator (188). And while citrate, succinate, and itaconate accumulation is characteristic of a "broken" Krebs cycle in pro-inflammatory macrophages, production of αKG orchestrates anti-inflammatory macrophage activation through metabolic and epigenetic reprogramming (189). Therefore, pro-inflammatory and anti-inflammatory macrophages exhibit substantial metabolic differences (summarized in **Figure 1-5**) that are essential to programming their respective functions.

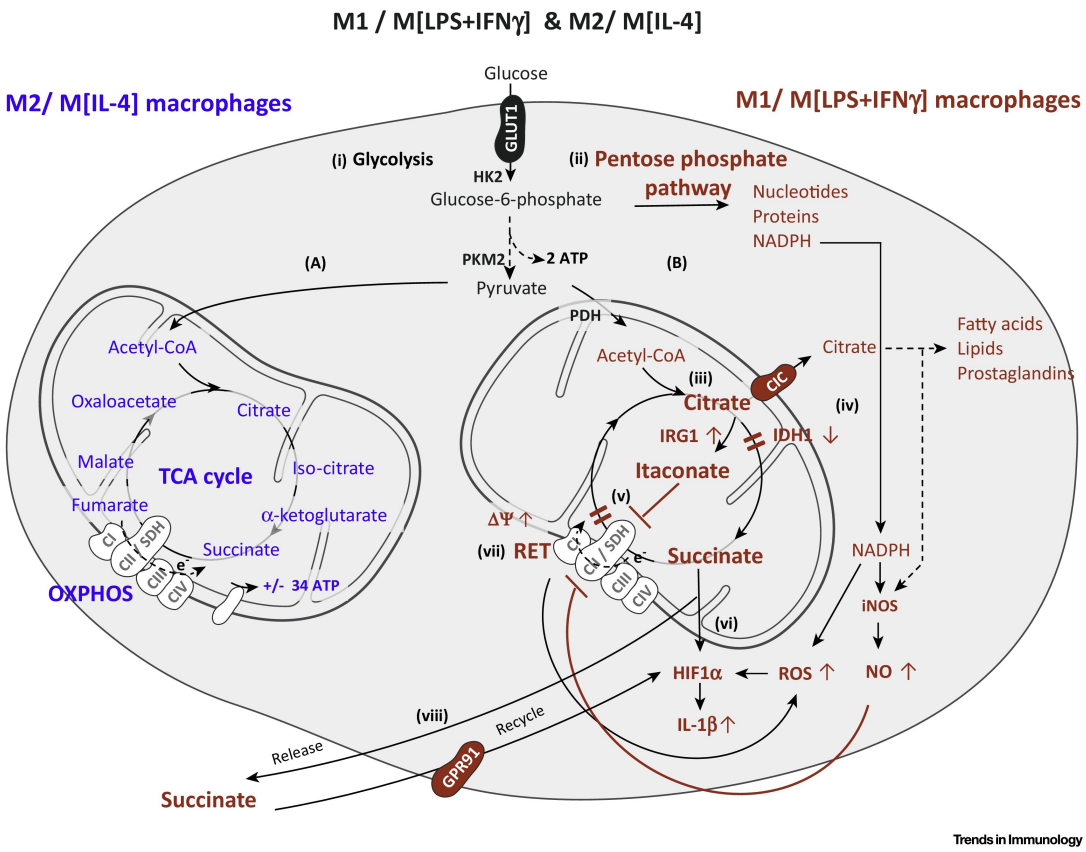

Figure 1-5: Metabolism of pro-inflammatory and anti-inflammatory macrophages

Anti-inflammatory (i.e., M2) macrophages canonically activated by IL-4 and pro-inflammatory (i.e., M1) macrophages canonically activated by LPS and IFNγ exhibit distinct metabolic phenotypes that support their respective functions. (**A**) Anti-inflammatory macrophages are characterized by an intact Krebs (i.e., tricarboxylic acid [TCA]) cycle and enhanced oxidative phosphorylation, whereas (**B**) pro-inflammatory macrophages exhibit specific Krebs cycle "breakpoints" leading to dysfunctional mitochondrial metabolism. While (**i**) glycolysis (involving activity of GLUT1, HK2, and PKM2) can support, but is not essential for, the metabolic phenotype of anti-inflammatory macrophages, it is critical for driving the phenotype and function of pro-inflammatory macrophages. In pro-inflammatory macrophages, glycolysis supplies the PPP (**ii**), which generates substrates for nucleotide and protein synthesis while also producing NADPH required for the generation of ROS, synthesis of fatty acids, and iNOS-generated NO. Due to their "broken" Krebs cycle, pro-inflammatory macrophages also accumulate the metabolic intermediates citrate, itaconate, and succinate. (**iii**) Citrate accumulates due to downregulation of IDH leading to its cytosolic transport through the CIC where it (**iv**) serves as a substrate for fatty acid synthesis. (**v**) Itaconate is generated from citrate due to upregulation of IRG1, and it inhibits SDH to cause accumulation of succinate. (**vi**) Together with ROS generated by RET (**vii**), succinate stabilizes HIF-1α to promote increased expression of IL-1β. (**viii**) Furthermore, succinate can be released from macrophages to potentiate inflammation by binding to its receptor SUCNR1/GPR91. From (Van den Bossche et al., 2017).

Metabolism of AMs

Given their residence in a lipid-rich, glucose-limited, and immunologically quiescent microenvironment, it is unsurprising that AMs exhibit a metabolic phenotype most closely

associated with anti-inflammatory macrophages. Transcriptional analyses comparing AMs to IMs (190) or recruited macrophages (57) has revealed that AMs exhibit a gene signature consistent with upregulation of PPAR signaling, Krebs cycle flux, fatty acid metabolism, and oxidative phosphorylation. Consistent with these findings, AMs exhibit remarkably low levels of glycolysis at steady state (191), a metabolic phenotype programmed by the lung microenvironment (192). In particular, restraint of HIF-1α signaling appears to be important for glycolytic attenuation in these cells (193,194). However, this metabolic program is to some extent plastic, as AM glycolytic activity is increased in the context of lung fibrosis (195) and infection (59,196). Despite this knowledge, however, there is a major gap in our understanding of the functional importance of glycolytic restraint in AMs, though some evidence suggests that it is critical for the elaboration of their homeostatic properties (192). Therefore, in conclusion, although investigation of AM metabolism is still in its early stages, the extant body of literature suggests that these cells rely heavily on fatty acid metabolism and oxidative phosphorylation for energy production and functional programming, while glycolysis is substantially restrained.

Conclusion

The lung perhaps best exemplifies an anatomic site where the inflammatory consequences of the continuous demand for innate immune defense must be restrained to minimize dysregulated inflammation and maintain homeostasis. As such, the predominant immune cell resident to the lung, the AM, is functionally tuned by its niche to assume an immunosedated phenotype. Reciprocally, AMs interact with the alveolar epithelium to restrain a myriad of inflammatory signaling pathways, including but not limited to JAK-STAT. Restraint of epithelial JAK-STAT signaling occurs via the transcellular delivery of AM-derived SOCS proteins, which are packaged within EVs and acquired by surrounding AECs via an endocytic uptake mechanism. This vesicular

homeostatic communication network is tuned by endogenous and exogenous factors through modulation of SOCS protein secretion by AMs and uptake of SOCS-containing EVs by AECs.

There is a significant gap in our understanding of how EV cargo packaging is regulated at the cellular and molecular level. This is particularly true for cytosolic proteins released in EVs that bud from the PM. In addition, how cargo sorting is altered in response to microenvironmental changes remains poorly understood – not only within the lung, but in virtually all tissues. It is contextually advantageous to address these concepts in the lung alveolar space that is continuously challenged by exposure to inhaled noxious stimuli. Therefore, the research included herein focuses on dynamic alterations in the vesicular secretion of SOCS3 by AMs, specifically in the context of two relevant perturbations within the lung: oxidative stress and metabolic remodeling.

Chapter 2 of this dissertation describes exposure of AMs to CS as a clinically relevant model of oxidative stress for investigating the effect of ROS on vesicular SOCS3 release. This work addresses two important facets of EV biology. First, Chapter 2 reveals a novel mechanism of proteasomal control over SOCS3 packaging, and it demonstrates how changes in microenvironmental oxidants dynamically tune proteasome activity to regulate SOCS3 secretion by AMs. Furthermore, this chapter semi-quantitatively addresses specificity in changes to SOCS3 sorting caused by ROS, the first study to do so in a robust and unbiased manner. Then, Chapter 3 of this dissertation addresses the fundamental and yet understudied question of how cellular metabolism influences vesicular cargo secretion. In particular, given the unique metabolic phenotype of AMs characterized by glycolytic restraint, this work centers around the influence of glycolytic flux on vesicular SOCS3 release through control over the cytosolic generation of acetyl-CoA. Collectively, these studies significantly advance our understanding of EV biology and open new avenues of inquiry into the fundamental mechanisms of vesicular cargo secretion.

Chapter 2 – Oxidative Inactivation of the Proteasome Augments Alveolar Macrophage Secretion of Vesicular SOCS3

This chapter has been published:

Haggadone MD, Mancuso P, Peters-Golden M. Oxidative Inactivation of the Proteasome Augments Alveolar Macrophage Secretion of Vesicular SOCS3. *Cells* (2020) 9(7):1589. PubMed PMID: 32630102.

Abstract

Extracellular vesicles (EVs) contain a diverse array of molecular cargoes that alter cellular phenotype and function following internalization by recipient cells. In the lung, alveolar macrophages (AMs) secrete EVs containing suppressor of cytokine signaling 3 (SOCS3), a cytosolic protein that promotes homeostasis via vesicular transfer to neighboring alveolar epithelial cells. Although changes in the secretion of EV molecules – including but not limited to SOCS3 – have been described in response to microenvironmental stimuli, the cellular and molecular machinery that control alterations in vesicular cargo packaging remain poorly understood. Furthermore, the use of quantitative methods to assess the sorting of cytosolic cargo molecules into EVs is lacking. Here, we utilized cigarette smoke extract (CSE) exposure of AMs as an *in vitro* model of oxidative stress to address these gaps in knowledge. We demonstrate that the accumulation of reactive oxygen species (ROS) in AMs was sufficient to augment vesicular SOCS3 release in this model. Using nanoparticle tracking analysis in tandem with a new carboxyfluorescein succinimidyl ester-based intracellular protein packaging assay, we show that the stimulatory effects of CSE were at least in part attributable to elevated amounts of SOCS3 packaged per EV secreted by AMs. Furthermore, the use of a 20S proteasome activity assay alongside treatment of AMs with conventional proteasome inhibitors strongly suggest that ROS

stimulated SOCS3 release via inactivation of the proteasome. These data demonstrate that tuning of AM proteasome function by microenvironmental oxidants is a critical determinant of the packaging and secretion of cytosolic SOCS3 protein within EVs.

Introduction

Tissue homeostasis is maintained by the dynamic regulation of information transfer amongst cells. In addition to the contributions of direct cell-cell contact and the release of soluble mediators, the importance of extracellular vesicles (EVs) as vectors for the local and systemic transfer of diverse molecular cargoes between cells has become increasingly appreciated (197,198). Classically, EVs have been classified into exosomes (Exos) and microvesicles (MVs) based on differences in mode of biogenesis, size, and the presence of specific molecular cargoes. However, substantial overlap in size and molecular characteristics is now recognized to limit the ability to categorically differentiate these two classes of EVs when using traditional isolation methods (82,83).

Under normal conditions, the pulmonary alveolar space is characterized by uniquely high oxygen tension. Furthermore, reactive oxygen species (ROS) – whose generation is amplified during inflammatory responses to inhaled pathogens, antigens, and xenobiotics – are well known to promote pro-inflammatory signaling pathways including the interleukin (IL)-6/signal transducer and activator of transcription 3 (STAT3) axis (199,200). EVs produced by lung cells in response to pro-inflammatory stimuli have been shown to contribute to a variety of pathologic responses (88,89,96). On the other hand, our previous finding that resident alveolar macrophages (AMs) – the main immune cell in the distal lung – at steady-state tonically secrete EVs containing suppressor of cytokine signaling 3 (SOCS3) (51) exemplifies an opposing paradigm. Upon uptake of these EVs by neighboring alveolar epithelial cells (AECs) (129), the transcellular acquisition of

vesicular SOCS3 serves as a critical restraint on cytokine-induced Janus kinase (JAK)-STAT3 signaling therein, which helps to maintain homeostasis in the distal lung (51,86,87). We and others have demonstrated that secretion of vesicular constituents is a dynamically regulated phenomenon. For example, intrapulmonary administration of IL-10 augments, whereas lipopolysaccharide inhibits the secretion of SOCS3 in EVs by AMs (51). Nevertheless, the specific cellular and molecular machinery that controls the packaging of cargoes of cytosolic origin into EVs represents a major gap in our understanding of EV biology. Furthermore, quantitative interrogation into how vesicular cargo packaging changes in response to exogenous and endogenous stimuli is currently lacking.

Catalytic inactivation of the proteasome by ROS is known to result in the accumulation of oxidized and polyubiquitinated proteins (150,151). Proteasome inhibitors have emerged as an effective approach for anti-cancer therapy (201,202), and their efficacy has been attributed, at least in part, to modulation of the content and function of cancer cell-derived EVs that results in inhibition of processes such as angiogenesis (203). Despite this knowledge, the influence of microenvironmental regulation of the proteasome on the packaging and secretion of EV cargoes has never been explored. Here, we demonstrate proteasomal control over vesicular secretion of SOCS3 by AMs and its dynamic alteration by a clinically relevant source of oxidative stress, cigarette smoke extract (CSE). We show that ROS augment AM release of SOCS3 in EVs by inactivating the proteasome. Furthermore, we describe a novel, semi-quantitative intracellular protein packaging assay that reveals specificity in the stimulatory effects of ROS and proteasome inhibition on the incorporation of SOCS3 into EVs. These studies advance both the mechanistic understanding of microenvironmental regulation of packaging and secretion of a vesicular cargo protein and the methodologic means for its evaluation.

Methods

Preparation of CSE

CSE was prepared by bubbling the smoke from 5 research cigarettes (Lot #3R4F, University of Kentucky Research Institute, Lexington, KY, USA) through 50 mL of RPMI 1640 culture medium (Thermo Fisher Scientific, Waltham, MA, USA) using a glass impinger (Ace Glass, Vineland, NJ, USA). CSE was then filtered through a 40-μm cell strainer (BD) and 1 mL aliquots of CSE were stored at -80°C (204).

Isolation and Culture of Primary and Immortalized AMs

Primary AMs were collected from lung lavage fluid of pathogen-free female Wistar rats (Charles River Laboratories, Wilmington, MA, USA), as described (205). Animals were maintained at the University of Michigan Unit for Laboratory Animal Medicine, and studies were approved by the Institutional Animal Care and Use Committee. MH-S cells, an immortalized murine AM cell line (ATCC, Manassas, VA, USA), passaged 1:10 every 3-4 days, were grown in polystyrene flasks in RPMI 1640 culture medium supplemented with 10% FBS and penicillin/streptomycin. For treatment with oxidants and proteasome inhibitors, primary AMs and MH-S cells were plated in serum-free RPMI 1640 culture medium (1 - 1.5 x 10^6 cells/mL) in 6-well, polystyrene plates. Cells were adhered for at least 1 h and then washed prior to treatment to remove EVs and other secreted products released during adherence to plastic. Cells were treated with CSE or H_2O_2 (Fisher Scientific, Hampton, NH, USA) at the indicated concentrations for 1 h, washed, and then incubated in serum-free medium for the durations specified. For proteasome inhibition experiments, MH-S cells were treated with bortezomib or MG132 (both from MilliporeSigma, Burlington, MA, USA) at the indicated concentrations and for specified durations in serum-free medium. For experiments using antioxidants, cells were treated for 1 h with 50 μM

of the broad-spectrum antioxidant *N*-acetyl-L-cysteine (NAC, Sigma-Aldrich, St. Louis, MO, USA) prior to stimulation with CSE. NAC was also present in the culture medium post-CSE stimulation to quench the production of endogenous ROS by cells.

EV Isolation

Conditioned medium (CM) from cells pulsed for 1 h with CSE or H_2O_2, or continuously treated with MG132 or bortezomib, was collected after 20 h culture. CM was sequentially centrifuged at 500 x *g* for 10 min and 2,500 x *g* for 12 min to remove dead cells, cell debris, and apoptotic bodies. EVs were then isolated using two approaches (206). (1) For rapid concentration of all EVs, CM was centrifuged at 4,000 x *g* for 20 min in 100-kDa centrifugal filter units (MilliporeSigma), and the resulting >100-kDa fraction was used to analyze secretion of EVs, SOCS3, and vacuolar protein sorting-associated protein 4a (VPS4a). (2) For fractionation of EVs by ultracentrifugation, CM was spun at 17,000 x *g* for 160 min to pellet "large EVs (lEVs)," from which the supernatant (non-lEV fraction) was then spun at 100,000 x *g* for 90 min to pellet "small EVs (sEVs)" (51). The resulting lEV and sEV fractions were used for analysis of SOCS3 secretion.

Western Blot

For probing of cell lysates, protein concentrations were determined by DC protein assay (Bio-Rad, Hercules, CA, USA), and aliquots containing 10 μg protein were used for analysis. For probing of CM vesicular concentrate samples, entire >100-kDa, lEV, or sEV fractions were collected from cells treated in culture and used to detect SOCS3. All samples were separated by SDS-PAGE using 12.5% gels and transferred to nitrocellulose membranes using Trans-Blot Turbo Mini Nitrocellulose Transfer Packs (Bio-Rad). Membranes were blocked for 1 h with 4% BSA and incubated overnight with commercially available monoclonal antibodies directed against SOCS3 (mouse, SO1) (Abcam, Cambridge, GBR), VPS4a (rabbit, EPR14545[B]) (Abcam), or

GAPDH (rabbit, 14C10) (Cell Signaling Technology, Danvers, MA, USA). After washing and incubation with peroxidase-conjugated anti-mouse or anti-rabbit secondary antibodies, the film was developed using ECL detection (GE Healthcare, Chicago, IL, USA). Exposure times for each experiment were selected to optimize a wide linear dynamic range, ensuring detection of a control vesicular SOCS3 band while limiting – to the best of our abilities – saturation of enhanced vesicular SOCS3 bands resulting from treatment of AMs with ROS or proteasome inhibitors. Developed films were then scanned using a desktop scanner at a dots per inch of 300 or greater. The optical density (OD) for SOCS3 bands was quantified using NIH ImageJ software (Version 1.51, Bethesda, MD, USA) as an area under the profile curve. As consistently as possible, background noise was corrected for by enclosing each peak at the same distance from its baseline. When present as a double-banded signal in vesicular fraction (>100-kDa) samples, both SOCS3 bands were enclosed for OD quantification. Densitometry was expressed relative to the control values for each experiment.

LDH Assay

Toxicity of primary AMs and MH-S cells was calculated using CyQUANT LDH Cytotoxcity Assay (Thermo Fisher Scientific). After centrifugation of CM to remove dead cells, cell debris, and apoptotic bodies, 50 μL aliquots were collected to measure extracellular LDH release. To determine maximal measurable cytotoxicity, lysis buffer was added to cells for 20 h in parallel to the protocol described above for treatment of cells with CSE, H_2O_2, or bortezomib.

ROS Assay

Oxidative stress in MH-S cells was determined using the well-established DCFDA/H2DCFDA Cellular ROS Assay Kit (Abcam) (207). As previously described (208), cell-permeant DCFDA (also known as DCFH-DA) was added to cells where it became hydrolyzed by

intracellular esterases to form non-fluorescent DCFH. In the presence of ROS, DCFH was oxidized to the fluorescent compound DCF, thus allowing for indiscriminate measurement of total ROS by quantifying fluorescence using a microplate reader.

To measure oxidants directly delivered to cells by CSE, adherent MH-S cells (2.5×10^4) were labeled with DCFDA and then stimulated with CSE in 96-well, polystyrene plates. Fluorescence intensity (i.e., ROS) was determined after treatment for 1 h. To measure endogenous oxidants generated by cells in response to incubation with CSE, adherent MH-S cells were treated with CSE for 1 h, washed, and subsequently labeled with DCFDA. Fluorescence intensity was then determined 4 h post-treatment. To correct for background fluorescence contributed by particulates contained in CSE, fluorescence intensity from unlabeled MH-S cells was subtracted from values obtained for DCFDA-labeled cells treated with CSE in parallel. All data were expressed relative to control values for each experiment.

Nanoparticle Tracking Analysis (NTA)

The concentration and size distribution of EVs secreted by MH-S cells was determined using NanoSight NS300 (Malvern Panalytical, Malvern, GBR). Entire vesicular fraction (>100-kDa) samples collected from CM were diluted to yield 10 - 80 particles per frame and injected via continuous infusion (flow rate ~15). Particles were analyzed over a 60 s capture period, and at least 3 capture periods were generated for each sample per experiment. Results indicating low concentration (<10 particles per frame) and/or high vibration were omitted. Injection with at least 1 mL PBS was used to wash tubing in between samples.

Carboxyfluorescein Succinimidyl Ester (CFSE)-Based Vesicular SOCS3 Packaging Assay

To fluorescently label intracellular proteins in MH-S, cells were incubated in serum-free culture medium with 10 μM CFSE (Sigma-Aldrich) for 15 min at 37°C. Excess CFSE was

quenched by adding equal volumes of serum-containing culture medium, and cells were pelleted at 500 x *g* for 10 min, adhered, and treated as stated above in 6-well, polystyrene plates. EVs were collected by 100-kDa filtration and vesicular CFSE (>100-kDa) fluorescence was quantified for each experimental condition. SOCS3 was also probed by Western blot of >100-kDa vesicular fraction samples collected from unlabeled cells treated in parallel. Specific packaging of SOCS3 as compared to all intracellular proteins was then semi-quantitatively determined by dividing the densitometry value for vesicular SOCS3 (relative to control) by the raw CFSE fluorescence value quantified for parallel samples (vesicular SOCS3/vesicular CFSE).

Quantification of MVs by Flow Cytometry

Flow cytometry was performed using a BD Biosciences (Franklin Lakes, NJ, USA) LSRFortessa. After centrifugation of CM as described above to remove dead cells, cell debris, and apoptotic bodies, 150 μL aliquots were incubated with 5 μL annexin V-FITC (BioLegend, San Diego, CA, USA) for 20 min in the dark at room temperature. Using 1 μm beads of known concentration (Thermo Fisher Scientific), MVs were determined as annexin V^+ particles having a diameter <1 μm, and MV concentration in CM was calculated by determining the fraction of beads analyzed. Data were generated using FlowJo software (Version 10.5.0, BD Biosciences). To measure vesicular SOCS3 packaging by flow cytometry (vesicular SOCS3/MVs), the densitometric value for >100-kDa SOCS3 (relative to control) was divided by the number of MVs quantified (% of control) in an aliquot collected from the same sample prior to 100-kDa centrifugal filtration.

20S Proteasome Activity Assay

Measurement of 20S proteasome activity (relative to control) in MH-S cell lysates was determined using a 20S Proteasome Assay Kit (Cayman Chemical, Ann Arbor, MI, USA).

Adherent cells (5 x 10^5) were treated in 12-well, polystyrene plates and lysates were collected after 20 h culture. Fluorescence resulting from SUC-LLVY-AMC substrate proteolysis was used to calculate the catalytic activity of the proteasome in cells following treatment with CSE, H_2O_2, or bortezomib.

Data Collection and Analysis

Results were from at least 3 independent experiments containing single samples per condition unless specified otherwise in the figure legend. Pooled data were expressed as mean ± SEM and analyzed using the Prism 5.0 statistical program from GraphPad software. Significance was determined using a one-way ANOVA or paired student's *t*-test, as appropriate, and was inferred at a $p < 0.05$. Significant values were labeled with varying numbers of asterisks (*), and corresponding *p* values were defined in the figure legends.

Results

CSE Enhances SOCS3 Secretion by Primary AMs in a ROS-Dependent Manner

Given the imperative to restrain inflammation in the oxygen-rich microenvironment of the lung, we hypothesized that AMs would respond to oxidative stress by increasing the release of vesicular SOCS3. To explore this possibility, we used the well-established *in vitro* experimental tool of CSE, an aqueous extract of the common environmental toxin, cigarette smoke, which was known to both contain a myriad of exogenous oxidants (209-211) and to stimulate endogenous cellular production of ROS (212-217). We exposed primary rat AMs to increasing doses of CSE for 1 h. Following treatment, AMs were washed and incubated for 20 h to allow for the elaboration of detectable levels of SOCS3-containing EVs into CM, as measured by Western blot. Treatment of primary AMs with CSE led to an increase in vesicular SOCS3 release, which was marked at a 7.5% dose (**Figure 2-1A**). This dose of CSE was within the range commonly employed in *in vitro*

macrophage studies (95,218,219) and did not cause significant cytotoxicity in our experimental system (**Figure 2-2**). Additionally, CSE caused no significant change in the amount of intracellular SOCS3 present in AMs, though it was associated with some decrease in lysate GAPDH (**Figure 2-1B**). Given that decreased intracellular levels of GAPDH did not extend to SOCS3, along with our data showing minimal cytotoxicity in AMs, we speculated that this effect was attributable to either robust non-vesicular GAPDH release into CM, as had been previously described (83), and/or transcriptional/translational shutdown caused by oxidative stress. Together, these data suggested that CSE stimulated the release of intracellular SOCS3 from primary AMs, rather than by augmenting the intracellular pool of SOCS3 available for secretion.

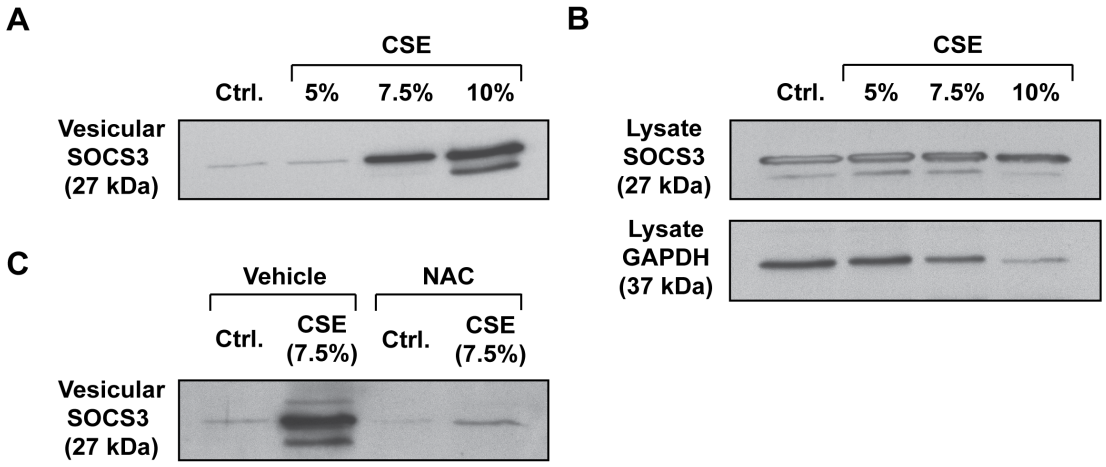

Figure 2-1: CSE stimulates the secretion of vesicular SOCS3 by primary AMs in a ROS-dependent manner

(**A**-**C**) Adherent AMs collected by lung lavage were treated with specified concentrations of CSE for 1 h. Following CSE treatment, AMs were washed and incubated for 20 h. (**A**) EVs in CM were concentrated by 100-kDa centrifugal filtration and vesicular SOCS3 secretion was determined via Western blot of the total vesicular fraction (>100-kDa) samples. Data are from 1 experiment representative of 3 independent experiments. (**B**) Following CSE stimulation (1 h) and incubation of AMs for 20 h, lysates were collected and subjected to Western blot for determination of SOCS3 expression, with GAPDH as a loading control. Data are from 1 experiment representative of 3 independent experiments. (**C**) Prior to CSE (7.5%) stimulation of AMs, NAC (50 μM) was added to AMs and maintained for the subsequent 20 h incubation. SOCS3 in the EV fraction of CM was analyzed by Western blot. Data are from 1 experiment representative of 3 independent experiments. Ctrl. = control.

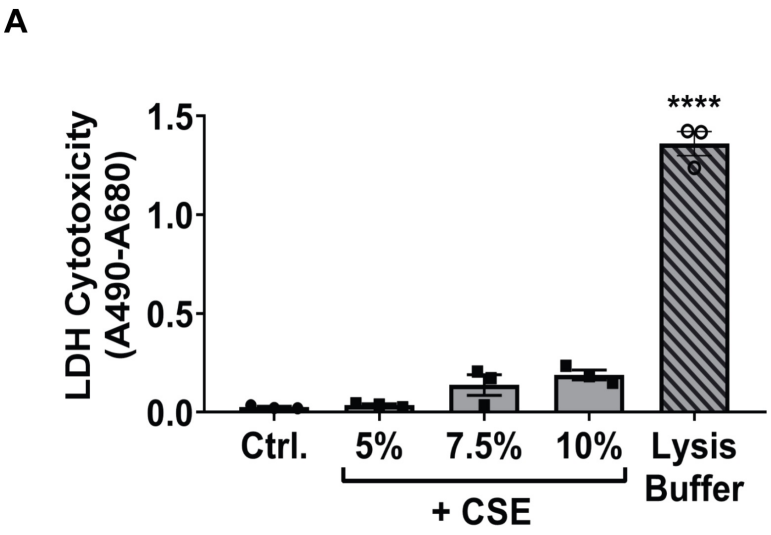

Figure 2-2: CSE does not cause toxicity in primary AMs

(**A**) Adherent AMs collected by lung lavage were treated with specified concentrations of CSE for 1 h. Following CSE stimulation, AMs were washed and incubated for 20 h. CM aliquots were obtained for measurement of extracellular LDH, and maximal measurable LDH release was determined by incubating AMs with lysis buffer for 20 h. Data (mean ± SEM) are representative of 3 independent experiments with each condition analyzed in technical duplicates. Significance was determined by one-way ANOVA. Ctrl. = control. ****, $p < 0.0001$ *versus* control. "Circles" indicate data points for Ctrl. samples, "squares" indicate data points for CSE samples, and "open circles" indicate data points for lysis buffer samples.

To determine whether the increased secretion of SOCS3 was a consequence of the oxidant stress posed by CSE, we treated primary AMs with the general antioxidant NAC prior to CSE stimulation. NAC completely abrogated the stimulatory effects of CSE on vesicular SOCS3 secretion (**Figure 2-1C**). These data indicated that CSE potentiates SOCS3 secretion by primary AMs in a ROS-dependent manner.

Endogenous and Exogenous ROS Stimulate SOCS3 Release by Immortalized AMs

Given the relatively low yield of primary AMs that can be obtained by lung lavage, and that large numbers of AMs are required to detect a tonically secreted SOCS3 signal, we turned to MH-S cells – an immortalized line of cells derived by SV40 treatment of primary mouse AMs – to more thoroughly interrogate the mechanisms underlying ROS enhancement of vesicular SOCS3 secretion. To first determine whether immortalized AMs were appropriate for modeling the

stimulatory effect of CSE on SOCS3 release observed in primary cells, we treated MH-S cells with increasing doses of CSE. Similar to the response observed for primary rat AMs, CSE elevated MH-S vesicular SOCS3 secretion in a threshold manner, an effect that became significant at a 3% dose (**Figure 2-3A**) and was unaccompanied by detectable levels of cytotoxicity (**Figure 2-4A**). The increment in SOCS3 secretion exhibited by MH-S cells at 3% CSE was comparable to that displayed by primary AMs at 7.5%. Given the data in **Figure 2-1C** demonstrating a role for ROS, we speculated that this greater resistance to (i.e., a higher dose required for) the stimulatory effects of CSE on SOCS3 secretion in primary than immortalized AMs reflects their heightened antioxidant defenses acquired during residence in the oxygen-rich alveolar milieu.

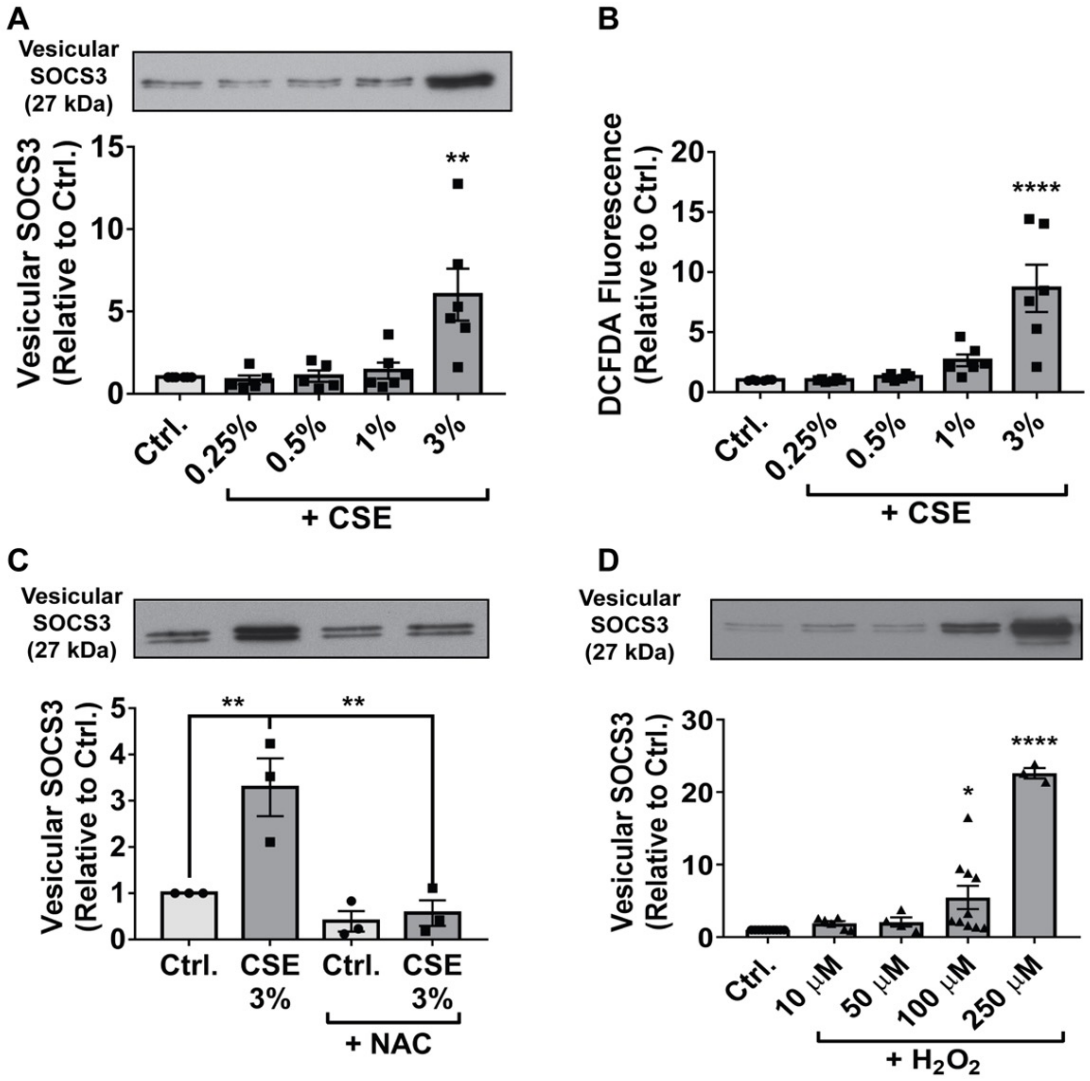

Figure 2-3: ROS augment vesicular SOCS3 secretion by immortalized AMs

(**A**) Adherent MH-S cells were treated for 1 h with indicated concentrations of CSE. Following CSE stimulation, cells were washed and incubated for 20 h. EVs were concentrated by 100-kDa centrifugal filtration, and SOCS3 secretion was determined by Western blot of total vesicular fraction (>100-kDa) samples. Densitometry data (mean ± SEM) are from >3 independent experiments, and significance analyzed by one-way ANOVA. (**B**) Adherent MH-S cells were treated with specified concentrations of CSE for 1 h, washed, and labeled with DCFDA. Fluorescence intensity was measured after 4 h culture. Duplicate samples were analyzed for each condition, and data (mean ± SEM) are from 3 independent experiments. Significance was analyzed by one-way ANOVA. (**C**) Prior to CSE (3%) treatment of MH-S cells, NAC (50 μM) was added for 1 h and maintained for the subsequent 20 h incubation. SOCS3 secretion was analyzed by Western blot of vesicular fraction samples. Densitometry data (mean ± SEM) are from 3 independent experiments, and significance analyzed by one-way ANOVA. (**D**) Adherent MH-S cells were treated with specified concentrations of H_2O_2 for 1 h. Following treatment, cells were washed and cultured for 20 h. Vesicular fraction samples were harvested and probed for SOCS3 by Western blot. Densitometry data (mean ± SEM) are from >3 independent experiments, and significance analyzed by one-way ANOVA. Ctrl. = control. *, ** and ****, $p < 0.05$, $p < 0.01$ and $p < 0.0001$, respectively *versus* control. "Circles" indicate data points for Ctrl. samples, "squares" indicate data points for CSE samples, and "triangles" indicate data points for H_2O_2 samples.

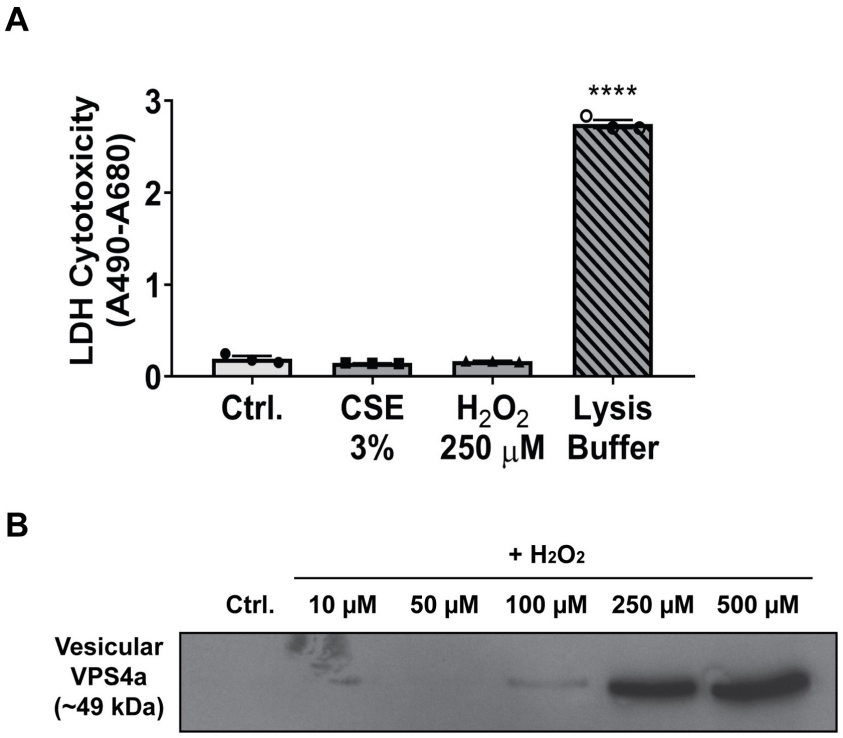

Figure 2-4: ROS do not cause toxicity in MH-S cells but promote release of vesicular VPS4a

(**A**) Adherent MH-S cells were treated with CSE (3%) or H_2O_2 (250 μM) for 1 h. Following treatment, cells were washed and incubated for 20 h. CM aliquots were obtained for measurement of extracellular LDH, and maximal measurable LDH release was determined by incubating cells with lysis buffer for 20 h. Data (mean ± SEM) are representative of 3 independent experiments with each condition analyzed in technical duplicates. Significance was determined by one-way ANOVA. *(***B**) Adherent MH-S cells were treated with specified concentrations of H_2O_2 for 1 h. Following treatment, cells were washed and cultured for 20 h. Vesicular fraction samples were harvested and probed for VPS4a by Western blot. Data are from 1 experiment representative of 3 independent experiments. Ctrl. = control. ****, $p < 0.0001$ *versus* control. "Circles" indicate data points for Ctrl. samples, "squares" indicate data points for CSE samples, "triangles" indicate data points for H_2O_2 samples, and "open circles" indicate data points for lysis buffer samples.

To further investigate the oxidative stress response in MH-S cells, we first measured ROS levels following CSE treatment. Stimulation with CSE led to increases in MH-S cell ROS that paralleled those for SOCS3 secretion (**Figure 2-3B**). Furthermore, as with primary AMs, pre-treatment of MH-S cells with NAC completely abrogated the stimulatory effects of CSE on SOCS3 secretion (**Figure 2-3C**).

Accumulation of ROS in CSE-treated MH-S cells was not observed before 4 h following the addition of CSE (data not shown), suggesting that measured ROS were generated from

endogenous cellular sources, rather than reflecting those delivered directly by the CSE itself. Although CSE has been reported to promote mitochondrial ROS production (212,213), pre-treatment of MH-S cells with the mitochondria-specific anti-oxidant MitoTEMPO (10 μM) had no effect on SOCS3 secretion in response to CSE (data not shown). Finally, to interrogate whether exogenous sources of ROS exerted the same effect as endogenous ROS on SOCS3 release, we treated MH-S cells for 1 h with increasing doses of the important oxidant species H_2O_2. In a similar manner to CSE, H_2O_2 treatment led to dose-dependent increases in SOCS3 secretion by MH-S cells (**Figure 2-3D**) without causing significant increases in cytotoxicity (**Figure 2-4A**). In parallel, H_2O_2 also enhanced >100-kDa release of VPS4a (**Figure 2-4B**), an ATPase whose vesicular recruitment is required for endosomal sorting complexes required for transport (ESCRT)-dependent EV biogenesis (220), thus indicating active release of EVs. A similar but modest and inconsistent effect on vesicular VPS4a secretion was observed following the treatment of MH-S cells with CSE (data not shown). Taken together, these data demonstrate that both endogenous and exogenous sources of ROS significantly potentiate the active secretion of vesicular SOCS3 by MH-S cells.

CSE Augments MH-S Cell Secretion of SOCS3 by Stimulating Production of, and Packaging of SOCS3 into, EVs

We reasoned that the stimulatory effect of ROS on the secretion of vesicular SOCS3 could be caused by three mechanisms, either acting alone or in combination: 1) Increasing the intracellular pool of SOCS3 available for secretion in EVs; 2) enhancing the total number of EVs released; and/or 3) specifically augmenting the packaging of SOCS3 per released EV. To determine whether CSE increased intracellular expression of SOCS3, we measured protein levels in MH-S cell lysates by Western blot 20 h after exposure. As demonstrated for primary AMs

(**Figure 2-1B**), CSE had no effect on SOCS3 expression in MH-S cells (**Figure 2-5A**). These results suggested that the stimulatory effects of ROS on SOCS3 secretion were independent of increased intracellular content, and instead reflect increased EV production and/or vesicular SOCS3 packaging.

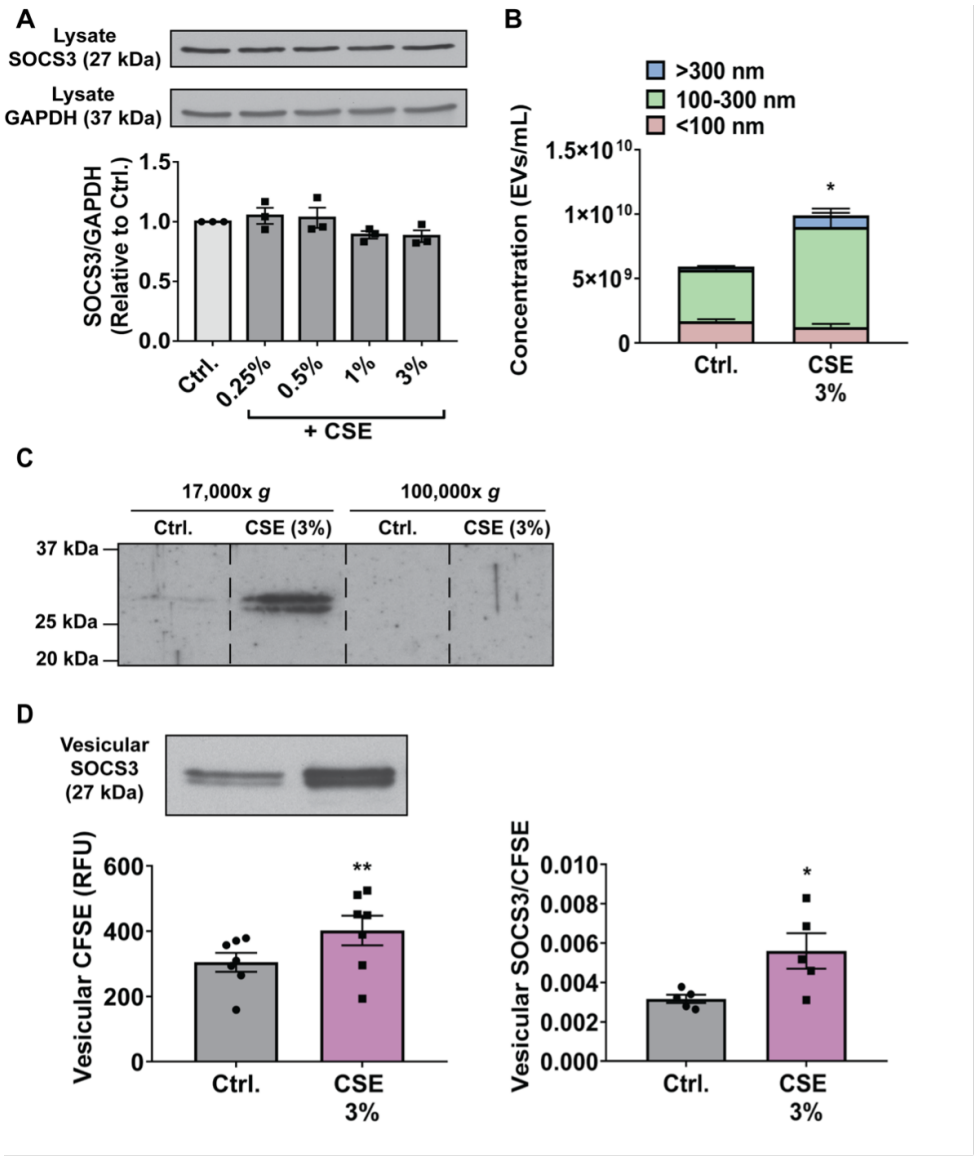

Figure 2-5: CSE potentiates MH-S cell production of EVs and packaging of vesicular SOCS3

(A-**B**) Adherent MH-S cells were treated (1 h) with specified concentrations of CSE, washed, and cultured for 20 h. (**A**) Lysates were collected and SOCS3 expression was assessed by Western blot, with GAPDH as a loading control. Densitometry data (mean ± SEM) are from ≥3 independent experiments, and significance analyzed by one-way ANOVA. (**B**) EVs were collected by 100-kDa centrifugal filtration, diluted in PBS, and quantified by NTA. Data are from 3 independent experiments in which ≥3 capture periods (60 s) were analyzed for each sample. Significance was determined using a paired sample *t*-test. (**C**) EVs were isolated by sequential ultracentrifugation of CM at 17,000 x *g* and 100,000 x *g* to pellet lEVs and sEVs, respectively, and probed for SOCS3 via Western blot. Dashed lines indicate splicing of discontinuous lanes from the same blot. Data are from 1 experiment representative of 3 independent experiments. (**D**) Prior to treatment (1 h) with CSE, MH-S cells were labeled with CFSE. Unlabeled cells were also treated with CSE in parallel for measuring secretion of vesicular SOCS3 into CM. Following treatment, wash, and culture of cells for 20 h, CM was collected, and vesicular fraction samples were either probed for SOCS3 via Western blot (*left panel, top*) or CFSE fluorescence determined (*left panel, bottom*). SOCS3 packaging was then measured, as described in "Methods" (*right panel*). Data (mean ± SEM) are from >3 independent experiments, and significance was determined using paired sample *t*-test. Ctrl. = control. * and **, $p < 0.05$ and $p < 0.01$, respectively *versus* control. "Circles" indicate data points for Ctrl. samples and "squares" indicate data points for CSE samples.

As oxidative stress has been previously demonstrated to enhance generation of total EVs (89,221-223), we quantified EVs in MH-S cell CM using NTA. In accordance with these prior reports, elaboration of EVs from MH-S cells treated with CSE was increased (**Figure 2-5B** and **Figure 2-6**). Increases in EV numbers were localized to those ≥100 nm in diameter, which was consistent with the size range reported for lEVs (82,83). To determine whether the stimulatory effect of CSE on SOCS3 secretion paralleled this effect on EV production, we performed differential ultracentrifugation using well-defined sedimentation rates (82,83) to isolate a 17,000 x *g* lEV pellet and 100,000 x *g* sEV pellet. As previously reported (51), basal SOCS3 secretion by MH-S cells was detected in lEVs but not sEVs (**Figure 2-5C**). Additionally, and consistent with our NTA data, CSE promoted robust increases in SOCS3 packaging in a lEV fraction but not sEV fraction (**Figure 2-5C**). These differential centrifugation data both confirmed the localization of SOCS3 in CM to EVs and further demonstrated that CSE potentiates vesicular release of SOCS3 specifically in lEVs.

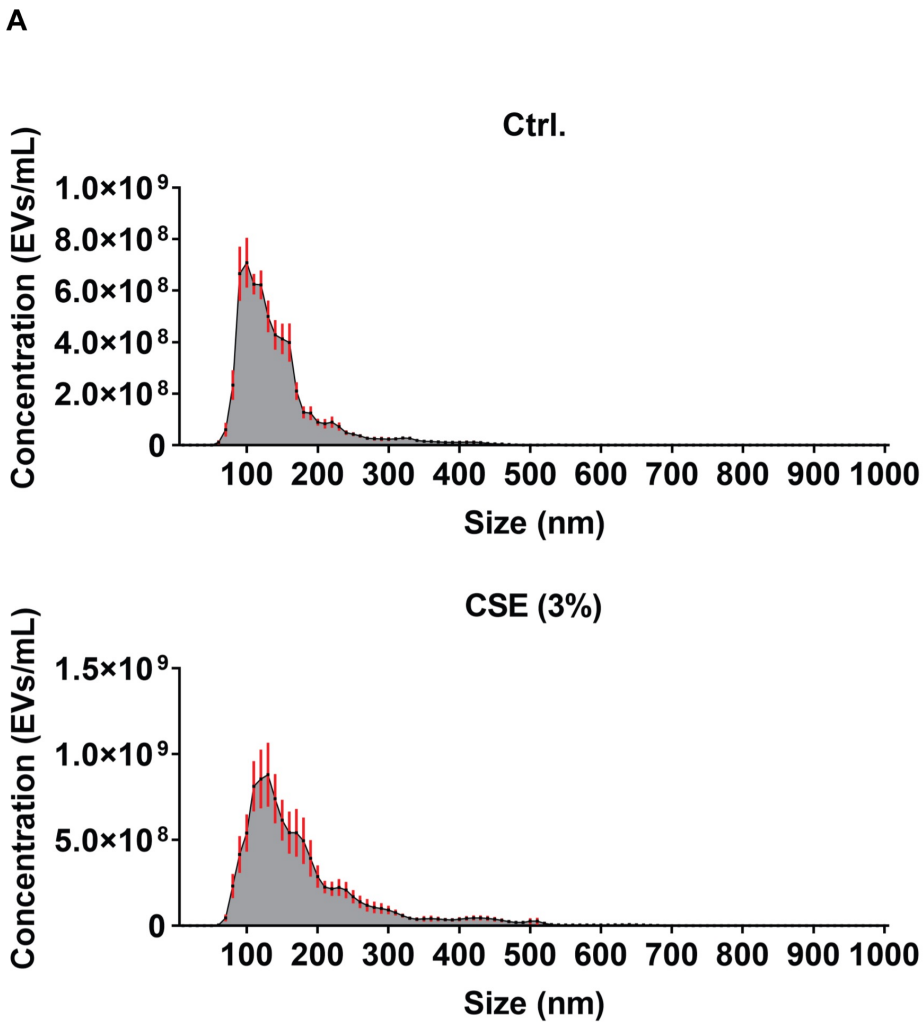

Figure 2-6: Histograms of NTA data collected for MH-S cells stimulated with CSE

(**A**) Adherent MH-S cells were treated (1 h) with CSE, washed, and cultured for 20 h. EVs were collected by 100-kDa centrifugal filtration, diluted in PBS, and quantified by NTA. Data (mean ± SEM) are from 3 independent experiments in which ≥3 capture periods (60 s) were analyzed for each sample. Ctrl. = control.

The incremental increase in EV production (**Figure 2-5B**) was quantitatively insufficient to account for the relatively greater fold change in vesicular SOCS3 secretion caused by CSE (**Figure 2-3A**). These results suggested that, in addition to enhancing EV biogenesis – thus leading to non-specific increases in SOCS3 release – ROS may also augment the amount of SOCS3 specifically packaged per EV. As SOCS3 is a cytosolic protein, we developed a novel assay to semi-quantitatively assess the effects of CSE on vesicular release of SOCS3 relative to the total

amount of all intracellular proteins packaged into MH-S cell-derived EVs. Specifically, we labeled MH-S cells with CFSE and quantified the relative fluorescence in a vesicular fraction following treatment with CSE as a measure of overall intracellular protein content in EVs. Consistent with the increased EV generation determined by NTA, treatment with CSE caused significant increases in the total amount of intracellular proteins (i.e., CFSE fluorescence) present in a vesicular fraction (**Figure 2-5D**). However, determination of the relative ratio of vesicular SOCS3 to vesicular intracellular protein content in parallel samples of CM from the same cultures revealed that CSE disproportionally augmented the release of SOCS3 in EVs (**Figure 2-5D**). These data suggested that some proportion of the oxidant-induced increment in intracellular protein packaging into MH-S-derived EVs was specific to SOCS3. To our knowledge, this semi-quantitative assay provided the most specific and unbiased interrogation of intracellular protein packaging yet reported. That CSE specifically enhanced SOCS3 packaging within EVs was further supported by employing an alternative but arguably less specific assay that determined the relative ratio of vesicular SOCS3 to the total amount of annexin V^+ MVs (the subset of EVs previously reported (51) to preferentially encapsulate SOCS3) present in MH-S cell CM, as determined by Western blot and flow cytometry, respectively (**Figure 2-7**). In tandem, these data suggest that, in addition to increasing the total amount of EVs produced by MH-S cells, ROS also specifically augment the amount of SOCS3 packaged into secreted EVs.

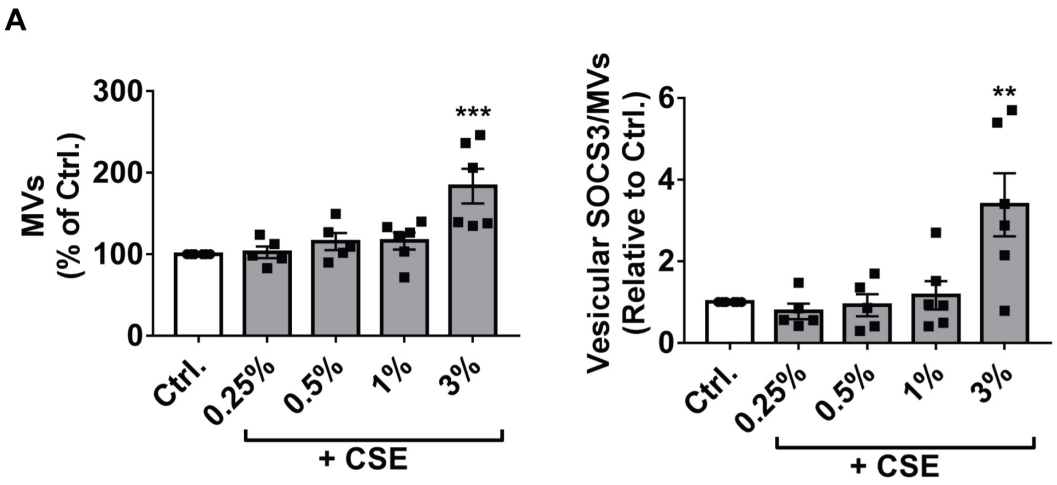

Figure 2-7: Flow cytometric analysis of CSE effects on MV production and vesicular SOCS3 packaging by MH-S cells

(**A**) Adherent MH-S cells were treated for 1 h with indicated concentrations of CSE, washed, and cultured for 20 h. Aliquots were obtained from CM for quantification of MVs by flow cytometry (*left panels*). EVs were then concentrated in remaining CM samples by 100-kDa centrifugal filtration for probing of secreted vesicular (>100-kDa) SOCS3. SOCS3 packaging was then determined, as described in "Methods" (*right panel*). Data (mean ± SEM) are from ≥3 independent experiments, and significance analyzed by one-way ANOVA. Ctrl. = control. ** and ***, $p < 0.01$ and $p < 0.001$, respectively *versus* control. "Circles" indicate data points for Ctrl. samples and "squares" indicate data points for CSE samples.

Inhibition of the 20S Proteasome Mimics the Stimulatory Effects of ROS on Vesicular SOCS3 Secretion by MH-S Cells

Cargo sorting and biogenesis of plasma membrane (PM)-derived EVs are known to rely, at least in part, on the recruitment of adaptor proteins such as arrestin domain-containing protein 1 (ARRDC1) to the cell surface (105,125,126,224). Furthermore, polyubiquitination of ARRDC1 is known to augment the production of PM-derived EVs (105). The association observed between altered proteasome activity and SOCS3 secretion led us to hypothesize that ROS might stimulate SOCS3 packaging in MH-S cells by inhibiting the proteasome, thus potentially increasing the amount of polyubiquitinated ARRDC1 available to facilitate enhanced cargo sorting and EV biogenesis.

We first sought to confirm that ROS at the concentrations we employed inhibit catalytic activity of the 20S proteasome in MH-S cells. In accordance with prior observations in other cell types (148,225,226), treatment with H_2O_2 led to a dose-dependent reduction in 20S proteasome activity (**Figure 2-8A**); notably, the doses of H_2O_2 required for substantial inhibition of the 20S proteasome (100 μM and 250 μM) were those that most prominently increased vesicular release of SOCS3 by MH-S cells (**Figure 2-3D**). CSE also inactivated the 20S proteasome (**Figure 2-8A**), but only at the dose (3%) at which it augmented secretion of vesicular SOCS3 (**Figure 2-3A**). Pre-treatment of MH-S cells with NAC completely abrogated the inhibitory effect of CSE on 20S proteasome activity (**Figure 2-8B**), thus demonstrating that the ability of CSE to inhibit the 20S proteasome is ROS-dependent, just as is its ability to stimulate vesicular SOCS3 release. Analyzing all our experimental data with CSE and H_2O_2, there was a strong quantitative correlation between the degree of proteasome inhibition within MH-S cells and the amount of SOCS3 secretion within EVs elicited by ROS (**Figure 2-8C**).

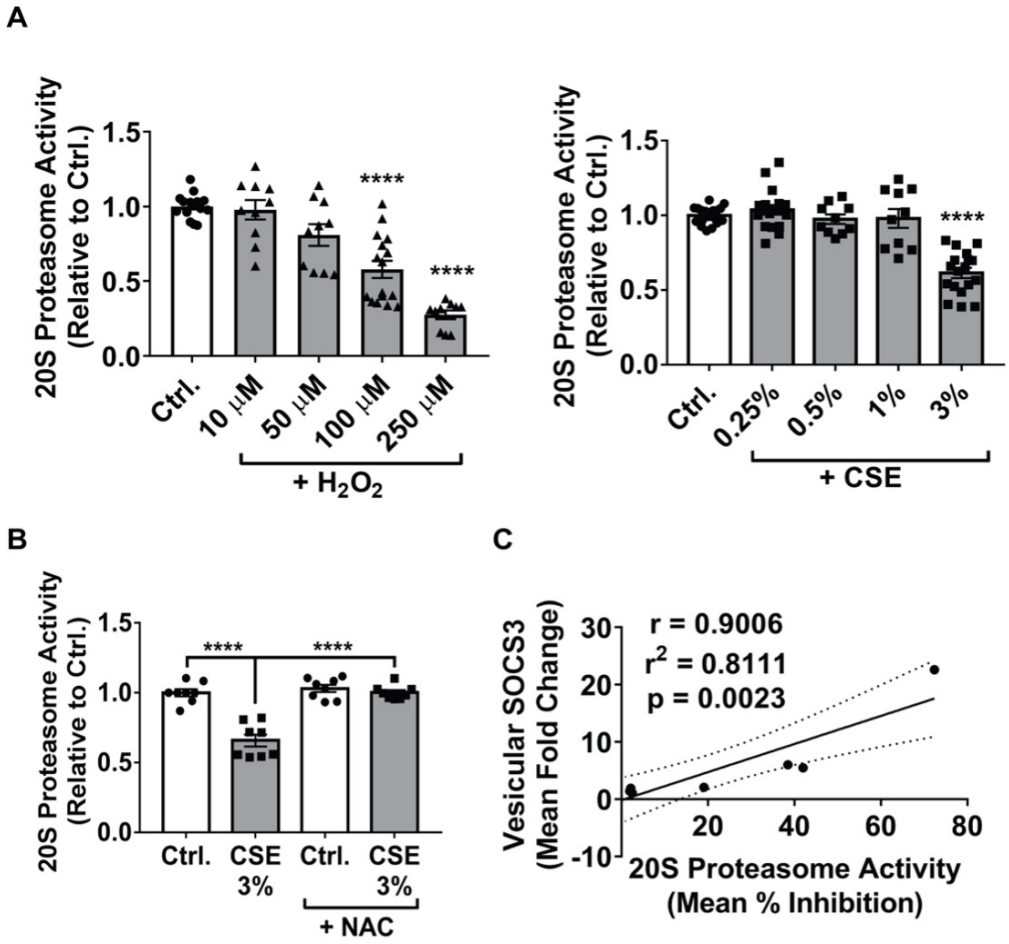

Figure 2-8: Oxidative inactivation of the proteasome in MH-S cells correlates with enhanced release of vesicular SOCS3

(**A**-**B**) Adherent MH-S cells were treated with indicated concentrations of H_2O_2 or CSE for 1 h, washed, and cultured for 20 h. Lysates were collected and proteasome activity was determined. Duplicate samples were analyzed for each condition, and data (mean ± SEM) are from >3 independent experiments. Significance was determined by one-way ANOVA. (**B**) Prior to CSE (3%) stimulation of MH-S cells, NAC (50 μM) was added to cells for 1 h and maintained for the subsequent 20 h incubation. Duplicate samples were analyzed for each condition, and data (mean ± SEM) are from >3 independent experiments. Significance was determined by one-way ANOVA. (**C**) Vesicular SOCS3 secretion data collected for every dose of CSE and H_2O_2 specified in **Figure 2-3A** and **Figure 2-3D** were correlated with 20S proteasome activity data collected for parallel CSE and H_2O_2 treatments, as specified in **Figure 2-8A**. Results are depicted on an XY plot with the correlation coefficient (r and r^2) and *p*-value (two-tailed) stated. Ctrl. = control. ****, $p < 0.0001$ *versus* control. In (**A**-**B**) "circles" indicate data points for Ctrl. samples, "triangles" indicate data points for H_2O_2 samples, and "squares" indicate data points for CSE samples.

Although these data established a strong association between oxidant enhancement of SOCS3 secretion in EVs and inhibition of 20S proteasome activity in MH-S cells, we sought to definitively demonstrate a causal role for the proteasome in controlling vesicular SOCS3 secretion. To do so, we treated MH-S cells with two known proteasome inhibitors, MG132 and bortezomib,

hypothesizing that proteasome inactivation by pharmacologic agents would mimic the proteasome-inhibitory and SOCS3 secretion-stimulatory effects of ROS. Indeed, MG132 substantially augmented levels of SOCS3 released by MH-S cells (**Figure 2-9A**). Likewise, bortezomib, a highly potent inhibitor of 20S proteasome activity (**Figure 2-10A**) (227), also augmented vesicular SOCS3 release by MH-S cells (**Figure 2-9B**), albeit at 10-fold lower concentrations than MG132; this effect was independent of any apparent cellular cytotoxicity (**Figure 2-10B**) and involved parallel increases in the release of vesicular VPS4a (**Figure 2-10C**). Taken together, these results are suggestive of a model in which at baseline, the proteasome acts as an endogenous brake on MH-S cell secretion of SOCS3, which can be disrupted by ROS to actively potentiate SOCS3 release in EVs.

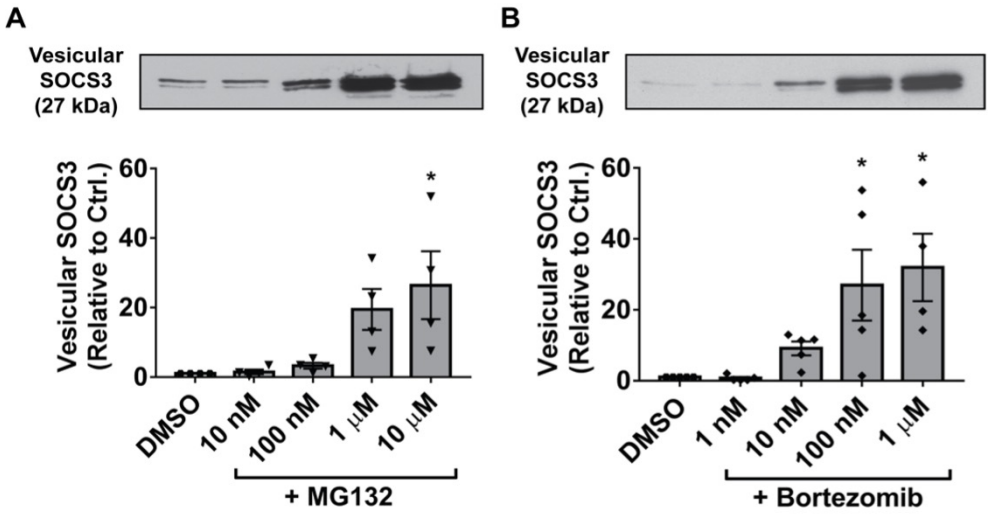

Figure 2-9: Inhibition of the proteasome stimulates MH-S cell secretion of vesicular SOCS3

(**A**-**B**) Adherent MH-S cells were treated with specified concentrations of MG132 or bortezomib for 20 h. EVs were harvested by 100-kDa centrifugal filtration and SOCS3 secretion was determined by Western blot of total vesicular fraction (>100-kDa) samples. Densitometry data (mean ± SEM) are from >3 independent experiments, and significance analyzed by one-way ANOVA. DMSO = DMSO control. *, $p < 0.05$ *versus* DMSO control. "Hexagons" indicate data points for DMSO samples, "inverted triangles" indicate data points for MG132 samples, and "diamonds" indicate data points for bortezomib samples.

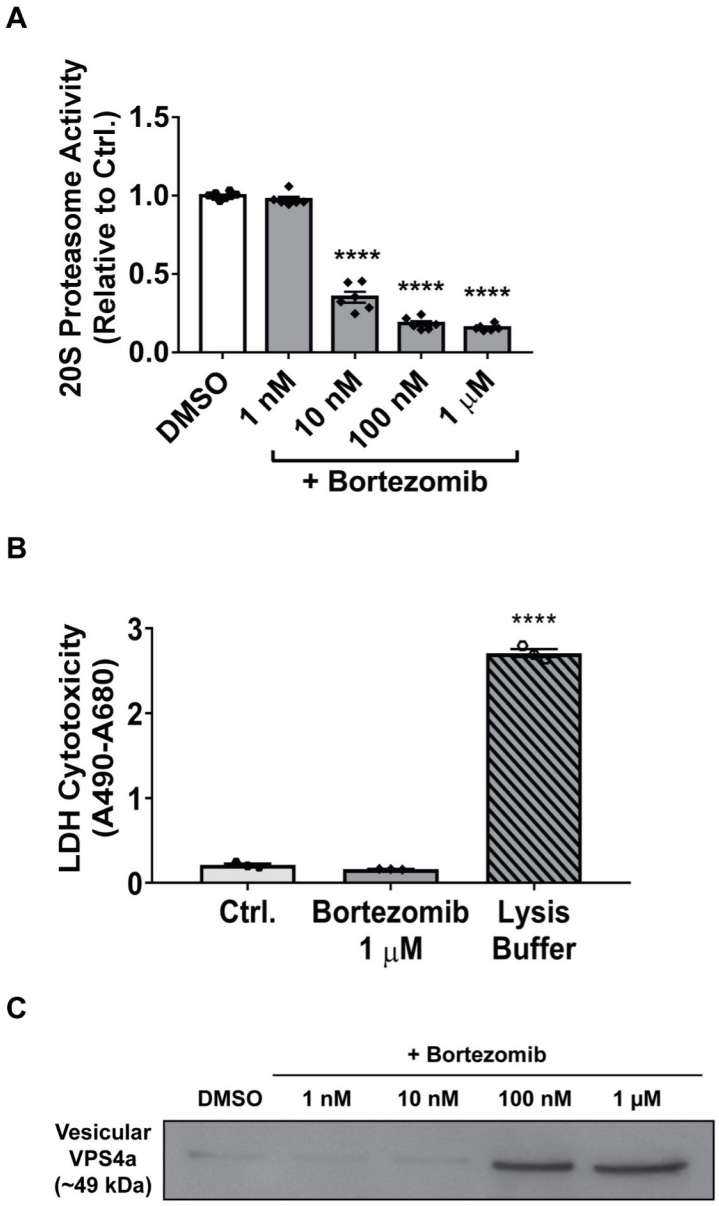

Figure 2-10: Bortezomib dose-dependently inhibits the proteasome and augments release of vesicular VPS4a without causing toxicity in MH-S cells

(**A**-**B**) Adherent MH-S cells were treated with the specified concentrations of bortezomib for 20 h. (**A**) Lysates were collected and proteasome activity was determined. Duplicate samples were analyzed for each condition, and data (mean ± SEM) are from 3 independent experiments. Significance was determined by one-way ANOVA. (**B**) CM aliquots were obtained for measurement of extracellular LDH, and maximal measurable LDH release was determined by incubating cells with lysis buffer for 20 h. Data (mean ± SEM) are representative of 3 independent experiments with each condition analyzed in technical duplicates, and significance determined by one-way ANOVA. (**C**) Adherent MH-S cells were treated with specified concentrations of bortezomib for 20 h. Vesicular fraction samples were harvested and probed for VPS4a by western blot. Data are from 1 experiment representative of 2 independent experiments. DMSO = DMSO control. ****, $p < 0.0001$ *versus* DMSO control. "Hexagons" indicate data points for DMSO samples, "diamonds" indicate data points for bortezomib samples, and "open circles" indicate data points for lysis buffer samples.

Proteasome Inactivation in MH-S Cells Augments SOCS3 Secretion by Stimulating Production of, and Packaging of SOCS3 into, EVs

As with CSE exposure, we next sought to determine whether the stimulatory effect of proteasome inhibitors on SOCS3 secretion by MH-S cells reflected increases in intracellular SOCS3 expression, production of EVs, and/or vesicular packaging of SOCS3. As our data suggested that oxidative inactivation of the proteasome was responsible for the increases in SOCS3 secretion promoted by CSE (**Figure 2-8** and **Figure 2-9**), we hypothesized that proteasome inhibitors similarly acted by increasing both EV production and SOCS3 packaging. Indeed, treatment of MH-S cells with either MG132 or bortezomib failed to significantly alter intracellular SOCS3 expression (**Figure 2-11A**). Although bortezomib at a dose of 1 μM caused increased production of EVs with diameters <100 nm and ≥100 nm (**Figure 2-11B** and **Figure 2-12**), its stimulatory effect on SOCS3 secretion was, as with that of CSE, localized to a 17,000 x *g* lEV pellet but not a 100,000 x *g* sEV pellet (**Figure 2-11C**). Furthermore, we noted that the <two-fold change in EV production was insufficient to account for the ~30-fold increase in vesicular SOCS3 secretion caused by bortezomib (**Figure 2-9B**). To semi-quantitatively determine if bortezomib, like ROS, promoted increases in vesicular SOCS3 packaging, we employed the CFSE-based SOCS3 packaging assay to show that bortezomib disproportionally augmented release of SOCS3 in EVs relative to other intracellular proteins (**Figure 2-11D**). Such an effect on packaging was also supported by determining the relative ratio of vesicular SOCS3 to the total amount of annexin V^+ MVs present in MH-S cell CM (**Figure 2-13**). Therefore, taken together, our data demonstrate that proteasome inhibitors act in the same manner as CSE to both elevate production of EVs and to specifically augment the amount of SOCS3 packaged into secreted EVs.

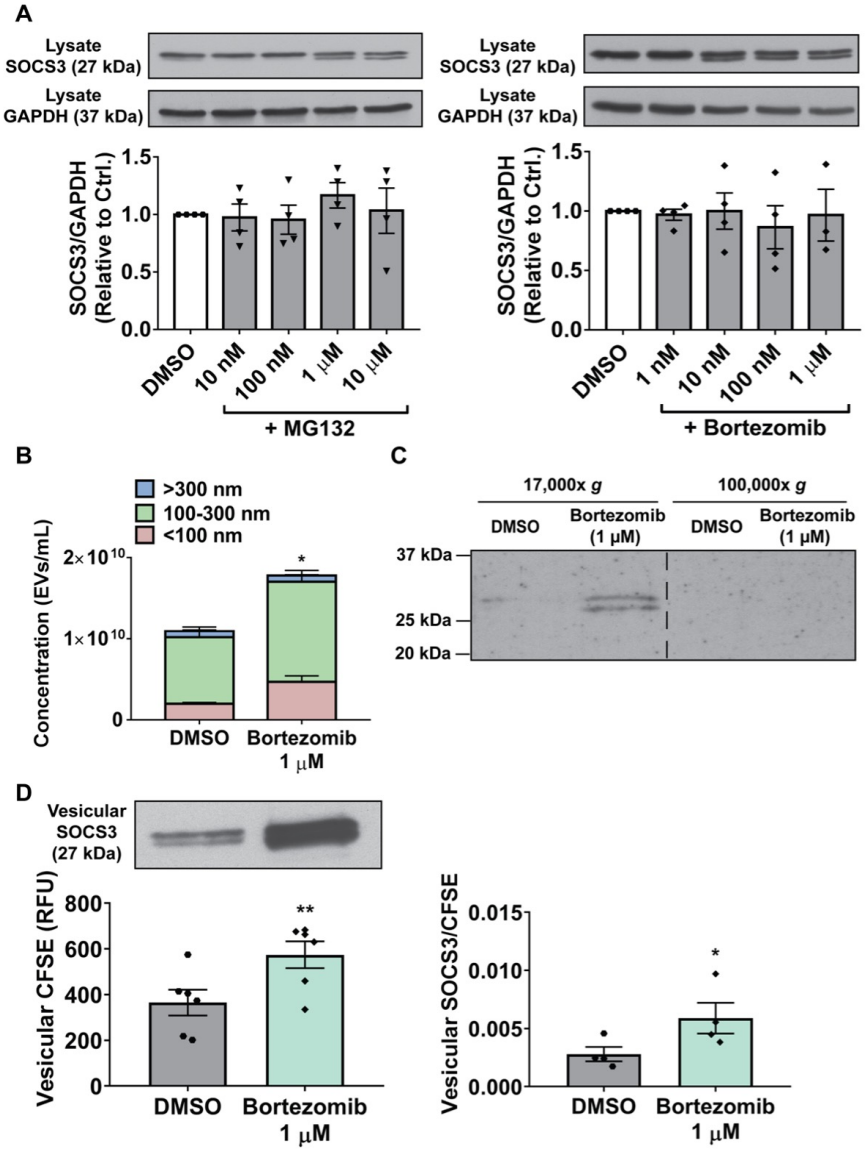

Figure 2-11: Inactivation of the proteasome potentiates MH-S cell production of EVs and packaging of vesicular SOCS3

(**A**-**B**) Adherent MH-S cells were treated for 20 h with specified concentrations of MG132 or bortezomib. (**A**) Lysates were collected and SOCS3 expression was assessed by Western blot, with GAPDH as a loading control. Densitometry data (mean ± SEM) are from ≥3 independent experiments, and significance analyzed by one-way ANOVA. (**B**) EVs were collected by 100-kDa centrifugal filtration, diluted in PBS, and quantified by NTA. Data (mean ± SEM) are from >3 independent experiments in which ≥3 capture periods (60 s) were analyzed for each sample. Significance was determined using paired sample *t*-test. (**C**) EVs were isolated by sequential ultracentrifugation of CM at 17,000 x *g* and 100,000 x *g* to pellet lEVs and sEVs, respectively, and probed for SOCS3 via Western blot. Dashed line indicates splicing of discontinuous lanes from the same blot. Data are from 1 experiment representative of 3 independent experiments. (**D**) Prior to stimulation with bortezomib, MH-S cells were labeled with CFSE. Unlabeled cells were also treated with bortezomib in parallel for measuring secretion of vesicular SOCS3. Following treatment, wash, and culture of cells for 20 h, vesicular fraction samples were concentrated via 100-kDa centrifugal filtration and either probed for SOCS3 via Western blot (*left panel, top*) or CFSE fluorescence (*left panel, bottom*). SOCS3 packaging was then measured, as described in "Methods" (*right panel*). Data (mean ± SEM) are from >3 independent experiments, and significance analyzed using paired sample *t*-test. DMSO = DMSO control. * and **, $p < 0.05$ and $p < 0.01$, respectively *versus* DMSO control. "Hexagons" indicate data points for DMSO samples, "inverted triangles" indicate data points for MG132 samples, and "diamonds" indicate data points for bortezomib samples.

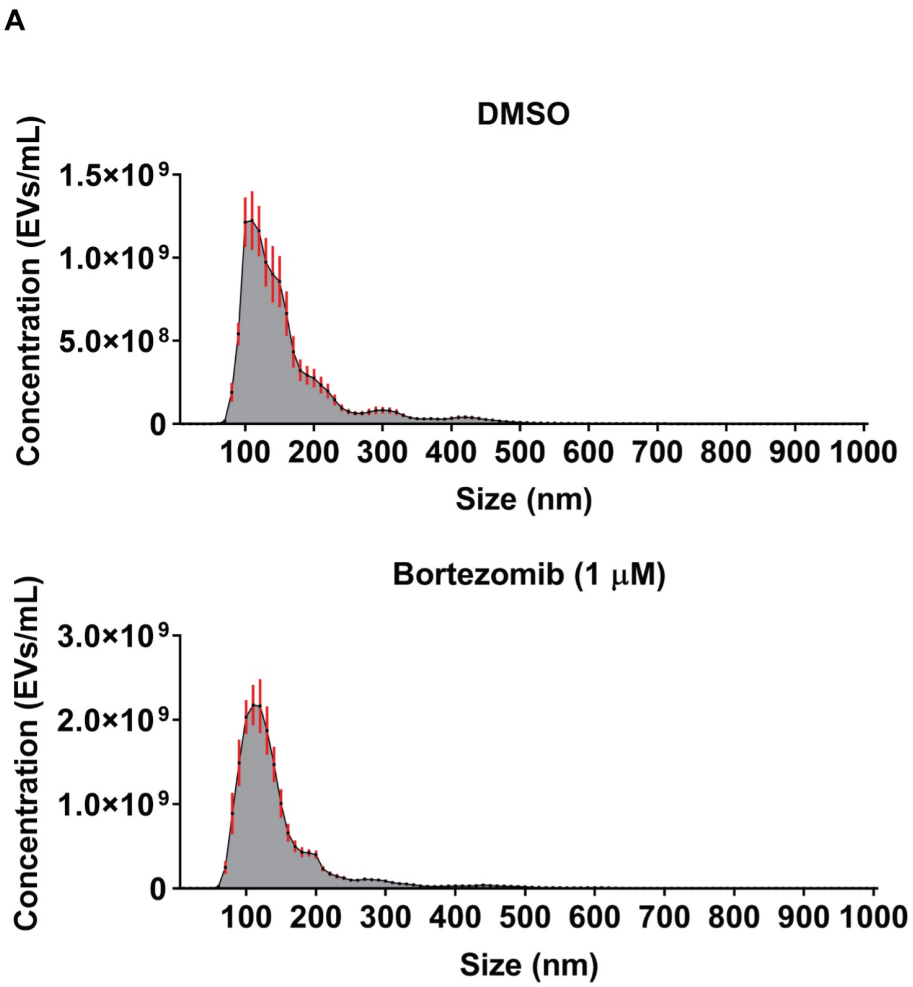

Figure 2-12: Histograms of NTA data collected for MH-S cells treated with bortezomib

(**A**) Adherent MH-S cells were treated (20 h) with bortezomib (1 μM). EVs were collected by 100-kDa centrifugal filtration, diluted in PBS, and quantified by NTA. Data (mean ± SEM) are from >3 independent experiments in which ≥3 capture periods (60 s) were analyzed for each sample. DMSO = DMSO control.

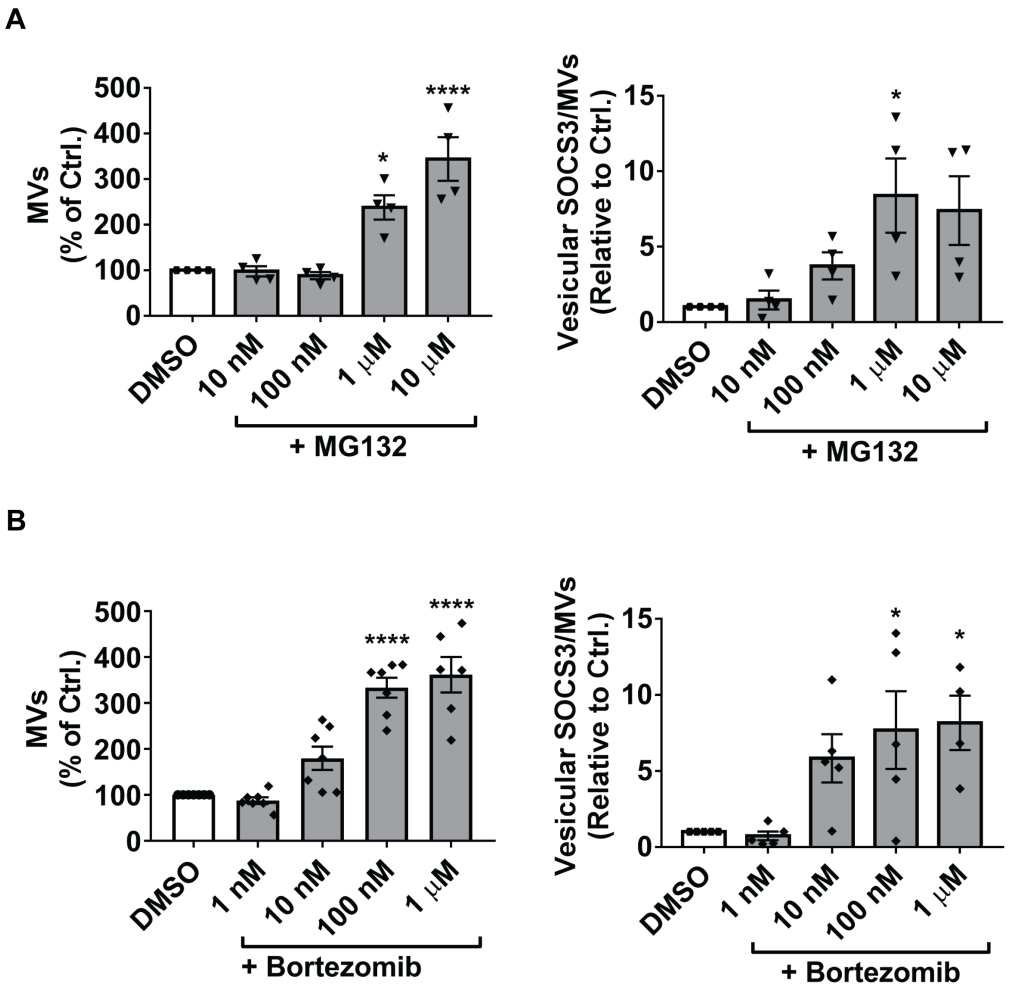

Figure 2-13: Flow cytometric analysis of proteasome inhibitor effects on MV production and vesicular SOCS3 packaging by MH-S cells

(**A**-**B**) Adherent MH-S cells were treated for 20 h with indicated concentrations of MG132 or bortezomib. Aliquots were obtained from CM for quantification of MVs by flow cytometry (*left panels*). EVs were then concentrated in remaining CM samples by 100-kDa centrifugal filtration for probing of secreted vesicular (>100-kDa) SOCS3. SOCS3 packaging was then measured, as described in "Methods" (*right panel*). Data (mean ± SEM) are from ≥3 independent experiments, and significance analyzed by one-way ANOVA. DMSO = DMSO control. * and ****, $p < 0.05$ and $p < 0.0001$, respectively *versus* DMSO control. "Hexagons" indicate data points for DMSO samples, "inverted triangles" indicate data points for MG132 samples, and "diamonds" indicate data points for bortezomib samples.

Discussion

Using CSE treatment as a clinically relevant *in vitro* model for oxidative stress within the alveolar microenvironment, we demonstrate that ROS augment vesicular SOCS3 release by primary and immortalized AMs (i.e., MH-S cells), a phenomenon attributable at least in part to

catalytic inactivation of the 20S proteasome. These results are the first to suggest that proteasomal control over secretion of EVs and vesicular cargoes is subject to dynamic regulation by microenvironmental stimuli. Further, our findings expand on the limited body of literature illuminating the critical importance of proteasome activity for dictating extracellular elaboration of vesicular content (203). Although we anticipate that this interplay between microenvironmental signals, proteasome function, and EV number/composition extends to other tissue contexts, the importance of oxidative stress as a determinant of these processes may be especially meaningful in the oxidant-rich environment of the distal lung. Although the incremental increases in MH-S cell vesicular SOCS3 secretion caused by ROS and proteasome inhibitors are quantitatively modest, our previous findings predict that changes of this magnitude are sufficient to significantly dampen STAT3 signaling in AECs. We therefore anticipate that augmented SOCS3 release by AMs assumes an important role for inflammatory restraint in the hyperoxic alveolar milieu.

We also sought to mechanistically determine whether the alterations in SOCS3 release by MH-S cells subjected to oxidant stress and proteasome inhibition involved changes in intracellular SOCS3 expression, EV secretion, and/or specific packaging of SOCS3 into EVs. To our knowledge, no previous study has applied such semi-quantitative methods to interrogate the mechanistic basis for regulated packaging of a vesicular cargo. We developed a novel CFSE-based packaging assay to semi-quantitatively assess SOCS3 release relative to other EV-packaged intracellular proteins, all of which would be expected to be labeled to a comparable extent by CFSE. We consider this unbiased and global readout of intracellular protein secretion to be superior to analyses based on measuring the secretion of a single such protein (e.g., β-actin) (228), which is likely to be subject to its own dynamic regulation by endogenous/exogenous stimuli. Using this assay, we found that the stimulatory effects of CSE and bortezomib on SOCS3 release

were at least in part a reflection of its greater specific packaging within MH-S cell-derived EVs. However, we cannot fully discount the possibility that passive incorporation of cytosolic content into budding EVs contributed to observed increases in SOCS3 secretion. Future studies should couple packaging assays with biochemical characterization of a vesicular fraction to additionally confirm absence of non-vesicular cytosolic constituents in the context of an exogenous stimulus. Nevertheless, our findings advance semi-quantitative assessment of intracellular protein packaging and highlight the need to develop analogous modalities for measuring the sorting of vesicular cargoes originating in other cellular compartments.

We acknowledge three methodologic concerns that limit our overall stated conclusions. The first of these is our use of Western blot to semi-quantitatively assess changes in vesicular SOCS3 release. Despite our best efforts to correct for background and optimize a linear dynamic range for each experiment, it is nonetheless likely that the densitometry value measured for vesicular SOCS3 by Western blot is not a perfect linear correlate to its absolute concentration. Therefore, although the semi-quantitative effects of ROS and proteasome inhibitors on SOCS3 packaging and secretion were strikingly consistent across experiments, the exact magnitude of these effects remain unclear. It will be important for follow-up studies to employ more precise methodologies that enable the measurement of absolute changes in EV content to fully appreciate the influence of microenvironmental factors on regulated cargo sorting. Second is the limitation of using 100-kDa filtration for measuring vesicular SOCS3 and vesicular CFSE fluorescence given the myriad non-EV mechanisms that could contribute to the release of cytosolic content into CM. Cytotoxicity assays revealed no accumulation of extracellular LDH following treatment of MH-S cells with CSE or bortezomib, thus arguing against a meaningful contribution of cell lysis to the amount of SOCS3 and CFSE measured in the >100-kDa concentrate. Additionally, given our

foundational report describing an unconventional, temperature-dependent mechanism of SOCS3 secretion specifically confined to annexin V^+ lEVs pelleted at 17,000 x *g*, here we used ultracentrifugation to confirm localization of SOCS3 in CM to lEVs and verify that changes in SOCS3 release detected by 100-kDa size-exclusion paralleled those observed in a 17,000 x *g* pellet (51). Data showing comparable changes in SOCS3 secretion using these two approaches support our conclusion that the effects of oxidative stress and proteasome inhibition on SOCS3 release are specific to a vesicular fraction. As further evidence that ROS and proteasome inhibitors actively potentiate SOCS3 secretion within EVs rather than via some passive, non-specific mechanism, we observed increased vesicular (i.e., >100-kDa) secretion of VPS4a by MH-S cells treated with ROS and bortezomib. As vesicular recruitment of VPS4a is required for EV biogenesis (220), our results – which paralleled the effect of these treatments on SOCS3 release by MH-S cells – strongly suggest that oxidative stress/proteasome inactivation specifically and actively promote EV cargo sorting, biogenesis, and release. Additionally, we observed near parallel increases in EV number and vesicular CFSE fluorescence caused by CSE and bortezomib using our novel packaging assay. These data argue in favor of EVs as being the predominant contributor to CFSE fluorescence detected in a >100-kDa concentrate and support our conclusion of enhanced vesicular SOCS3 sorting relative to the total intracellular protein pool. Lastly, we acknowledge the limitation of defining EV fractions according to sedimentation velocity without providing physical or biochemical verification of EV size, purity, or enrichment of known molecular markers. Importantly, we observed parallel increases in the secretion of ≥100 nm EVs (by NTA) and packaging of SOCS3 in a 17,000 x *g* pellet following treatment of MH-S cells with CSE and bortezomib. Importantly, these treatments had minimal or no effect on secretion of <100 nm EVs and packaging of SOCS3 in a 100,000 x *g* pellet. Therefore, our results strongly argue in favor of

the conclusion that ROS and proteasome inhibitors achieve their stimulatory effects on SOCS3 secretion by specifically augmenting packaging in lEVs. However, it will be important for future studies to demonstrate parallel enrichment of known markers – for example, α-actinin-4 in lEVs and CD81 in sEVs (82,83) – to corroborate specificity in EV cargo sorting.

ROS effects on miRNA and mRNA content of EVs have been previously described (89,223,229,230), though data on ROS regulation of vesicular protein sorting remains limited (231). To our knowledge, oxidative stress has not been demonstrated to specifically alter the packaging of a protein resident to the cytosol. The extant body of literature reporting ROS effects on EVs is limited to studies of the effect of exogenous H_2O_2. Our data additionally demonstrated that the generation of endogenous ROS via treatment of MH-S cells with CSE was sufficient for augmenting SOCS3 release. CSE is known to promote the production of intracellular ROS primarily through its actions on nicotinamide adenine dinucleotide phosphate (NADPH) oxidase and mitochondrial activity (212-217). Our results suggested that the effects of CSE on stimulated SOCS3 release by MH-S cells did not involve mitochondrial ROS generation. Therefore, we suspect that the activation of NADPH oxidase complexes by CSE caused elevated levels of ROS and corresponding increases in SOCS3 secretion by AMs. However, the involvement of other enzymatic (e.g., lipoxygenase, xanthine oxidase, etc.) and organellar (e.g., endoplasmic reticulum) sources of ROS following exposure to CSE (232-236) is possible. It will be informative in future studies to determine whether all sources of intracellular ROS act similarly to alter mechanisms of EV biogenesis and/or cargo packaging, or whether there is specificity in modulatory actions for ROS generated by particular enzymes and/or in particular subcellular compartments.

Despite the critical importance of protein turnover for maintaining cellular homeostasis and the recognition that proteasome components are packaged in EVs (237-240), investigation into

the functional crosstalk between proteasome activity and EVs is limited. Bortezomib was first reported to suppress the production of EVs by T-lymphocytes activated to undergo apoptosis by UVB irradiation (237). These results suggested that the proteasome promotes the secretion of EVs in the presence of an exogenous stimulus. However, a recent report using resting multiple myeloma cells demonstrated a stimulatory role for bortezomib on production of EVs (203). These data highlight differences in the directionality of proteasome regulation of EV biogenesis, depending on whether an activating stimulus is present. Our study using MH-S cells supports a model in which – at steady state – the proteasome acts as a brake on vesicular SOCS3 packaging and EV secretion, which can be released upon its inactivation by oxidative stress. While our quantitative packaging data demonstrate augmented sorting of SOCS3 into EVs by exposure of MH-S cells to CSE and bortezomib, the effects of these stimuli on the packaging of global cargo contents of AM-derived EVs is unknown. Notably, Zarfati et al. demonstrated broad alterations in pro-inflammatory and pro-angiogenic growth factor proteins present in EVs elaborated from multiple myeloma cells following bortezomib treatment. Given the growing interest in the use of bortezomib as a therapeutic, not merely in the context of multiple myeloma (241) but also in tissue fibrosis (242-244), it is intriguing to speculate that the drug's protective effects are in part mediated by changes in vesicular communication, as has been previously suggested (203).

Although increases in vesicular SOCS3 release and proteasome inhibition during oxidative stress were strongly correlated (**Figure 2-8**), we were limited in our ability to causally link these two processes. Our attempts to overcome the stimulatory effects of ROS on SOCS3 release by overexpressing proteasome catalytic subunits were thwarted by low transfection efficiency. Additionally, treatment of MH-S cells using small molecule proteasome activator compounds was ineffective due to the non-specific nature of these drugs. Consequently, we cannot exclude the

possibility that some proportion of the augmentation of SOCS3 secretion by ROS is independent of proteasome inactivation. Given the breadth of ROS effects on cellular function, it is likely that regulation of vesicular cargo release by oxidants is mechanistically multifaceted. Nonetheless, taken together, our data do argue that proteasome inhibition represents at least one important mechanism by which oxidative stress potentiates the packaging and release of cytosolically packaged vesicular proteins.

While our original report described tonic SOCS3 secretion exclusively in annexin V^+ MVs pelleted at 17,000 x *g* (51), it is still unclear whether stimulated release by ROS and/or proteasome inhibitors involved SOCS3 packaging and release within both MVs and Exos. Of note, our NTA data indicated that the majority of CSE effects and much of bortezomib effects on stimulated EV release by MH-S cells were specific to those with a diameter of 100-300 nm, consistent with the size range reported for lEVs, including classical MVs (197). However, bortezomib did also cause a notable increase in EVs <100 nm in diameter, thus raising the possibility that SOCS3 undergoes stimulus-specific packaging into smaller MVs or Exos. Nevertheless, leveraging the well-defined sedimentation properties of EVs (82,83) we show that the stimulatory effects of CSE and bortezomib on SOCS3 secretion were entirely exclusive to a 17,000 x *g* lEV pellet but not 100,000 x *g* sEV pellet collected from MH-S cells. Therefore, we suggest that proteasome inhibition causes heightened packaging and release of SOCS3 predominantly within larger PM-derived MVs, but cannot discount the possibility that SOCS3 is subject to some amount of vesicular sorting via an endosomal pathway. Accordingly, given the potential crosstalk between secretory endocytic and autophagic systems (245), we also cannot eliminate a potential role for autophagy in elaborating an unconventional mechanism of vesicular SOCS3 release. Indeed, ROS (246-248) and proteasome inhibitors (249,250) are known to enhance autophagy, thus raising the possibility that

these stimuli might potentiate SOCS3 release by AMs by increasing fusion and secretion of autophagic/endosomal compartments.

The molecular adaptors and targeting elements that are responsible for vesicular sorting of biomolecules, particularly for cytosolic proteins packaged at the PM, represent a major gap in current knowledge (251). However, it is known that, in addition to serving as the post-translational signal responsible for targeting of substrates to the proteasome, polyubiquitination of the cargo-sorting adaptor protein ARRDC1 also enhances biogenesis of MVs at the PM (105,125,126,224). This is achieved via ARRDC1 recruitment of ESCRT machinery, which is critical for vesicle budding and release (105,220,252). Accumulation of intracellular polyubiquitinated substrates is a known consequence of proteasome inhibition (150,151). Therefore, we speculate that oxidative inactivation of the proteasome potentiates SOCS3 release from AMs due to increases in polyubiquitinated ARRDC1, thus causing enhanced cargo sorting and MV secretion from the PM. Determining the role of ARRDC1 in SOCS3 packaging, both at steady-state and under stimulatory conditions, is of substantial interest to our laboratory; unfortunately, our preliminary efforts to evaluate this possibility were hindered by the lack of reagents applicable to non-human experimental systems.

In summary, we have illuminated a previously unknown mechanism in which proteasomal control over vesicular secretion of the cytosolically localized protein SOCS3 is tuned in AMs by oxidative stimuli. We have also developed a novel assay to demonstrate that the enhanced release of vesicular SOCS3 caused by oxidative inactivation of the proteasome is at least in part due to specific increases in vesicular SOCS3 packaging. Future studies will focus on identifying the molecular chaperones and/or targeting elements sensitive to proteasome inhibition and responsible for the sorting of SOCS3 into EVs. Further, follow-up experimentation will determine the breadth

of proteasome effects on cargo content within, and on functional roles of, AM-derived EVs in the alveolar microenvironment.

Chapter 3 – ATP Citrate Lyase Links Increases in Glycolytic Flux to Diminished Release of Vesicular SOCS3 by Alveolar Macrophages

At the time of dissertation submission, this chapter is being prepared for publication:

Haggadone MD, Speth J, Hong H, Penke LR, Zhang E, Lyssiotis CA, Peters-Golden M. ATP Citrate Lyase Links Increases in Glycolytic Flux to Diminished Release of Vesicular SOCS3 by Alveolar Macrophages.

Abstract

Extracellular vesicles (EVs) are important vectors for intercellular communication. Lung-resident alveolar macrophages (AMs) tonically secrete EVs containing suppressor of cytokine signaling 3 (SOCS3), a cytosolic protein that promotes homeostasis in the distal lung via its actions in recipient neighboring epithelial cells. AMs are metabolically distinct and exhibit low levels of glycolysis at steady state. To our knowledge, whether cellular metabolism influences the packaging and release of an EV cargo molecule has never been explored in any cellular context. Here, we report that increases in glycolysis following *in vitro* exposure of AMs to the growth and activating factor granulocyte-macrophage colony-stimulating factor inhibit the release of vesicular SOCS3 by primary AMs. Glycolytically diminished SOCS3 secretion requires export of citrate from the mitochondria to the cytosol and its subsequent conversion to acetyl-CoA by ATP citrate lyase. Our data for the first time implicate perturbations in intracellular metabolites in the regulation of vesicular cargo packaging and secretion.

Introduction

Intercellular communication is central to the maintenance of tissue homeostasis. Cell-cell contact and the release of soluble factors have long been recognized as means of cellular crosstalk.

More recently, extracellular vesicles (EVs) have become increasingly appreciated for their role as vehicles for the transfer of information amongst cells (197,253). EVs are small, membrane-delimited structures that encapsulate a diverse array of molecular cargoes (e.g., lipids, nucleic acids, and proteins) and which alter phenotype and function when internalized by recipient cells (198). Historically, EVs have been classified into two major populations, exosomes (Exos) and microvesicles (MVs), distinguishable by mode of biogenesis and once thought to categorically differ in size and molecular composition. However, recent observations have revealed substantial overlap in the biochemical properties of Exos and MVs (82,83), thus complicating their discrimination.

The lung is a distinctive milieu that is continuously exposed to exogenous insults including microbes, antigens, and toxins. The protective inflammatory responses directed towards these inhaled environmental stimuli must be appropriately restrained to ensure preserved physiologic function. Achieving this delicate balance of response vs. restraint requires crosstalk between the two predominant cellular constituents of the alveoli – 1) the alveolar epithelial cells (AECs) that comprise the respiratory surface and 2) the alveolar macrophages (AMs) that are the most numerous resident immune cells. Our laboratory has recently shown that AMs secrete EVs enriched with the anti-inflammatory cytosolic protein suppressor of cytokine signaling 3 (SOCS3), which are taken up by neighboring AECs (51). This acquisition of AM-derived, SOCS3-containing EVs by AECs serves as a homeostatic mechanism for dampening pro-inflammatory Janus kinase (JAK)-signal transducer and activator of transcription 3 (STAT3) signaling responses within the lung *in vitro* and *in vivo* (51,86,87,129). Although we have shown the release of vesicular SOCS3 by AMs to be dynamically tuned by various endogenous and exogenous cues (51,85-87,254), illuminating the cellular and molecular mechanisms that control vesicular SOCS3 secretion has

remained elusive. More broadly, the cellular processes mediating the modulated packaging and release of vesicular cargo molecules of cytosolic origin are still poorly understood.

In addition to fulfilling the bioenergetic demands of the cell, metabolic processes are now recognized to control basic immune cell function. For example, metabolic rewiring is associated with functional changes that support the phenotypic characteristics of pro-inflammatory or alternatively activated macrophages, depending on the stimulus (255). AMs, however, are metabolically distinct among macrophage populations in that they exhibit remarkably low levels of glycolysis at steady state (57,59,190-194), a metabolic phenotype programmed by the lung microenvironment (192) that supports their quiescent functional status (57,59,190,192,195,196). In cancer cells, changes in cellular metabolism have been shown to influence the subtype (256-258) or number (259,260) of EVs secreted. To our knowledge, however, the ability of metabolic rewiring to dynamically alter the packaging of an EV cargo molecule has never been studied.

Granulocyte-macrophage colony-stimulating factor (GM-CSF) is a pleiotropic cytokine that promotes the survival and/or differentiation/activation of myeloid cells (261), including in the lung where it shapes AM development (9,262). Additionally, GM-CSF is known to metabolically remodel macrophages through glycolytic activation (263,264). Here, using GM-CSF as a biologically relevant *in vitro* driver of metabolic reprogramming, we show that stimulation of glycolytic activity in AMs inhibits the packaging and release of vesicular SOCS3. Increases in AM glycolytic flux were linked to diminished SOCS3 release via the activity of ATP citrate lyase (ACLY), the cytosolic enzyme responsible for converting glucose-derived citrate to acetyl-CoA (173). Our studies implicate a critical role for mitochondrial metabolites in the regulation of vesicular cargo packaging, thereby significantly advancing a mechanistic understanding of metabolic control over EV content and biology.

Methods

Isolation and in Vitro Treatment of Primary AMs for Detection of Secreted Vesicular SOCS3

As previously described (205), primary AMs were collected from the lavage fluid of pathogen-free female Wistar rats (Charles River Laboratories, Wilmington, MA, USA). Animals were maintained at the University of Michigan Unit for Laboratory Animal Medicine, and experiments were conducted with approval by the Institutional Animal Care and Use Committee. Isolated AMs (2 - 3 x 10^6 per well) were plated in serum-free RPMI 1640 culture medium (Thermo Fisher Scientific, Waltham, MA, USA) in 6-well, polystyrene plates and adhered for at least 1 h. Cells were then washed prior to treatment to remove EVs and other secreted products generated during adherence to plastic. AMs were treated continuously with recombinant GM-CSF (50 ng/mL, BioLegend, San Diego, CA, USA) or the α-ketoglutarate analog dimethyloxalylglycine (DMOG, 1 mM, Sigma-Aldrich, St. Louis, MO, USA) in serum-free medium for 20 - 24 h. For glucose dose-response experiments, AMs were treated with 50 ng/mL GM-CSF in glucose-free RPMI 1640 culture medium supplemented with the specified concentrations of D-(+)-glucose (Sigma-Aldrich). AMs were also treated exogenously with sodium citrate or sodium acetate (both 1 mM and from Sigma-Aldrich) in serum-free medium for 20 - 24 h. Additionally, the following small-molecule inhibitors were used for *in vitro* studies: 2-deoxy-D-glucose (2-DG), UK-5099, citrate transport protein (CTP) inhibitor, SB-204990, BMS-303141 (all from Sigma-Aldrich), and acyl-CoA synthetase short chain family member 2 (ACSS2) inhibitor (Selleck Chemicals, Houston, TX, USA). Inhibitors were added to AMs for 20 - 24 h during continuous treatment with GM-CSF or sodium acetate.

EV Isolation

Conditioned medium (CM) from AMs treated with GM-CSF was collected after 20 - 24 h culture and centrifuged at 500 x *g* for 5 min and 2,500 x *g* for 12 min to remove dead cells, cell debris, and apoptotic bodies. EVs were then isolated using two approaches, as previously described (254). Briefly, for rapid concentration of a total vesicular fraction, CM was centrifuged at 4,000 x *g* for 20 min in 100-kDa centrifugal filter units (MilliporeSigma, Burlington, MA, USA). The resulting >100-kDa concentrate was used for analysis of SOCS3 secretion. Alternatively, EVs were fractionated using ultracentrifugation by spinning CM at 17,000 x *g* for 160 min to pellet 17,000 x *g* EVs, from which the supernatant was then spun at 100,000 x *g* for 90 min to pellet 100,000 x *g* EVs. The resulting 17,000 x *g* and 100,000 x *g* EV fractions were used for analysis of SOCS3 and EV secretion.

Western Blot

Vesicular SOCS3 elaborated by cultured AMs was evaluated by immunoblot analysis of EV fractions consisting of either entire >100-kDa, 17,000 x *g*, or 100,000 x *g* EV samples. For immunoblotting of cell lysates, protein concentrations were determined by DC protein assay (Bio-Rad, Hercules, CA, USA), and aliquots containing 10 μg were used to detect SOCS3. All samples were separated by SDS-PAGE using 12.5% gels to probe for SOCS3. Transfer of samples to nitrocellulose membranes was performed using Trans-Blot Mini Nitrocellulose Transfer Packs (Bio-Rad). Membranes were then blocked for 1 h with 4% BSA and incubated overnight with monoclonal antibodies recognizing SOCS3 (mouse, SO1) (Abcam, Cambridge, GBR) or α-tubulin (mouse, B-5-1-2) (Sigma-Aldrich). After washing and incubation (1 h) with peroxidase-conjugated anti-mouse antibodies, the film was developed using ECL detection for lysate samples or ECL Prime detection (both from GE Healthcare, Chicago, IL, USA) for vesicular SOCS3

samples. Immunoblotting with the SOCS3 (SO1) antibody routinely identifies a single band at the predicted molecular weight of 27 kDa (51), as demonstrated in **Figure 3-1C**.

Nanoparticle Tracking Analysis (NTA)

The ZetaView Twin 405/488 (Particle Metrix GmbH, Ammersee, DEU) was used to determine the concentration of EVs secreted by AMs. Entire 17,000 x *g* or 100,000 x *g* EV fractions collected from AMs were diluted in 3 mL RPMI 1640, and 3 captures of 1 mL were collected per sample. Injection with RPMI 1640 culture medium was used to wash tubing in between samples. Data are presented as 3 independent experiments with 3 captures performed per experiment.

Isolation and in Vitro Treatment of Primary AMs for Quantitative PCR Analysis and Lactate Assay

Primary AMs were lavaged from the lungs of 6 - 8 week-old C57Bl/6 female mice (Jackson Laboratory, Bar Harbor, ME, USA) as previously described (51). AMs (0.5 - 1 x 10^6 cells per well of a 6-well tissue culture plate) were adhered overnight in RPMI 1640 supplemented with 2% FBS, washed, and then treated with GM-CSF (50 ng/mL) for 6, 12, or 24 h.

RNA Isolation and Quantitative Reverse Transcription PCR (RT-qPCR)

Total RNA was extracted from murine AMs using QIAGEN columns (QIAGEN, Hilden, DEU) per manufacturer's instructions and converted to cDNA via reverse transcription. Relative gene expression of mouse *Glut1*, *Hk2*, *Pfkp, and Idh1* was determined by ΔCt method using SYBR Green dye (Applied Biosystems, Foster City, CA) with β-actin (*Actb*) as a reference gene. The following primer sequences were used: mGlut1 Forward: CATGGTTCATTGTGGCCGAG; mGlut1 Reverse: GAAGAAGAGCACGAGGAGCA; mHk2 Forward: TCATTGTGGGTACTGGCAGT; mHk2 Reverse: TGAGCCCATGTCGATCTCTC; mPfkp

Forward: GAAGCCAAATGGGACTGTGT; mPfkp Reverse: CACGCACAGATTGGTTATGC; mIdh1 Forward: ATCATCATTGGCCGACATGC; mIdh1 Reverse: TCCTGGTTGTACATGCCCAT; mActb Forward: GACGGCCAGGTCATCACTAT; mActb Reverse: GCACTGTGTTGGCATAGAGG.

L-Lactate Assay

Primary mouse AMs were isolated and cultured as described above. Cell culture supernatants were collected after 3, 6, 12, and 24 h and centrifuged at 500 x *g* for 10 min to remove dead cells and debris. Cell-free supernatants were then deproteinized using an Abcam deproteinization kit per manufacturer's instructions. Lactic acid content was determined in the deproteinized cell culture supernatants using an L-Lactate Assay Kit (Abcam) per manufacturer's instructions.

Data Collection and Analysis

Results were from at least 3 independent experiments containing single samples per condition unless otherwise specified. When AMs were cultured with GM-CSF in the presence of various inhibitors or their vehicle controls, % SOCS3 secretion was calculated by dividing the optical density (OD) of vesicular SOCS3 released from GM-CSF-treated AMs by the OD of vesicular SOCS3 released from untreated AMs. Pooled data were expressed as mean ± SEM and analyzed using the Prism 5.0 statistical program (GraphPad Software, San Diego, CA, USA). Significance was determined using a paired student's *t*-test and was inferred at a $p < 0.05$. Asterisks (*) were used to label significant values, as specified in the figure legends.

Results

GM-CSF Inhibits the Vesicular Packaging and Release of SOCS3 by AMs

We have reported that AM secretion of SOCS3 within EVs is diminished in various inflammatory disease states and following exposure to various pro-inflammatory mediators (51,85,86). GM-CSF promotes inflammation within the lung (265-267) as well as the proliferation (268-271) and functional activation (9,272) of AMs. To test its effects on AM SOCS3 secretion, AMs were treated with GM-CSF for 20 - 24 h to allow for elaboration of EVs into CM and subsequent detection of vesicular (>100-kDa) SOCS3 by Western blot. Indeed, treatment with GM-CSF inhibited the release of AM vesicular SOCS3 (**Figure 3-1A**). Notably, this inhibitory effect was unaccompanied by any change in SOCS3 levels detected in AM lysates (**Figure 3-1B**). These data suggest that GM-CSF inhibited the secretion of SOCS3 by AMs without affecting intracellular SOCS3 content. Then, to specifically localize changes in secreted SOCS3 to EVs, we performed differential ultracentrifugation and collected two vesicular fractions: EVs pelleted at 17,000 x *g* and EVs pelleted at 100,000 x *g*. In agreement with our prior reports, we only detected tonic SOCS3 secretion in the 17,000 x *g* but not 100,000 x *g* pellet (51,254), and secretion of SOCS3 within 17,000 x *g* EVs was similarly inhibited by GM-CSF treatment of AMs (**Figure 3-1C**). However, the inhibition of SOCS3 secretion by AMs was associated with only a modest and non-significant reduction in the number of EVs detected by NTA in the 17,000 x *g* pellet (**Figure 3-1C**). GM-CSF also had no effect on the number of EVs quantified in the 100,000 x *g* pellet (**Figure 3-2**). As diminished SOCS3 secretion was unaccompanied by any substantial changes in vesiculation, we conclude that GM-CSF specifically attenuated the active sorting of SOCS3 into AM-derived 17,000 x *g* EVs (i.e., the amount of SOCS3 packaged per individual EV).

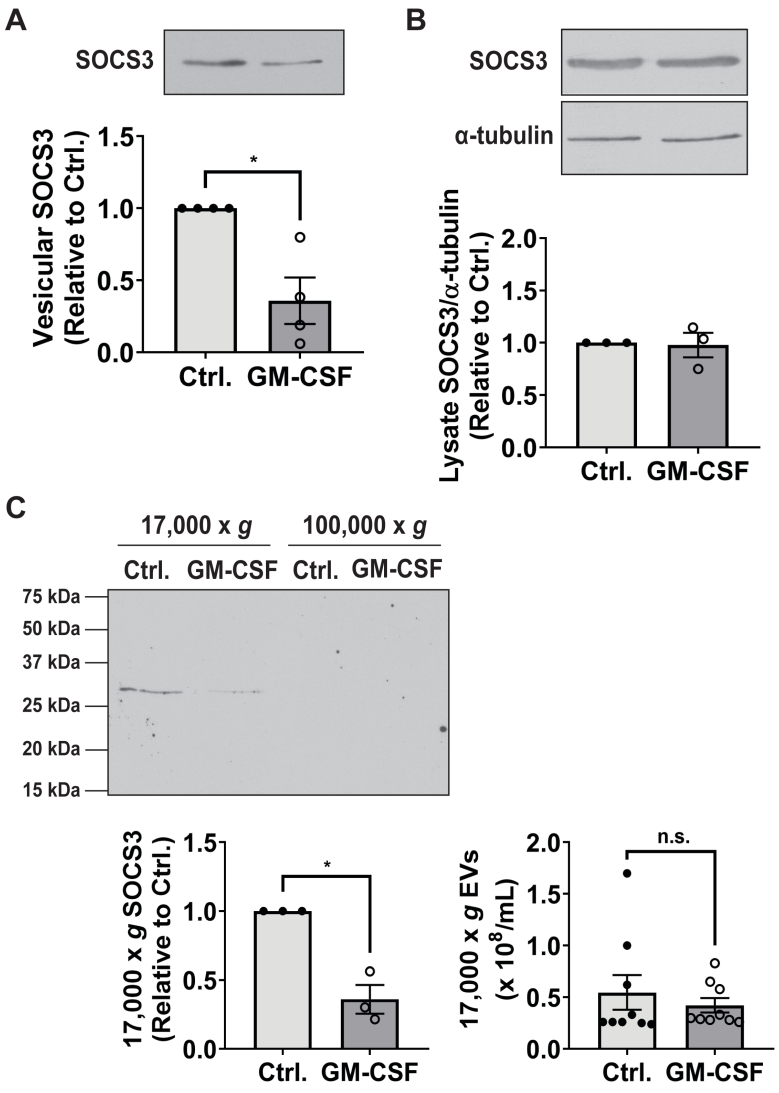

Figure 3-1: GM-CSF treatment of AMs inhibits SOCS3 packaging and release in EVs

(**A**-**C**) Adherent AMs collected by lung lavage of rats were treated with GM-CSF (50 ng/mL) for 20 - 24 h. (**A**) EVs in CM were concentrated by 100-kDa centrifugal filtration and vesicular SOCS3 secretion was determined via Western blot of the total vesicular fraction (>100-kDa) samples. (**B**) Lysates were collected and subjected to Western blot for determination of SOCS3 intracellular content, with α-tubulin as a loading control. (**C**) EVs were isolated by sequential ultracentrifugation of CM at 17,000 x *g* and 100,000 x *g*, which were then probed for SOCS3 via Western blot (*left panel, bottom*) and enumerated by NTA (*right panel, bottom*). Data (mean ± SEM) are from ≥3 independent experiments, and significance was determined using paired sample *t*-test. Ctrl. = control and n.s. = not significant. *, $p < 0.05$.

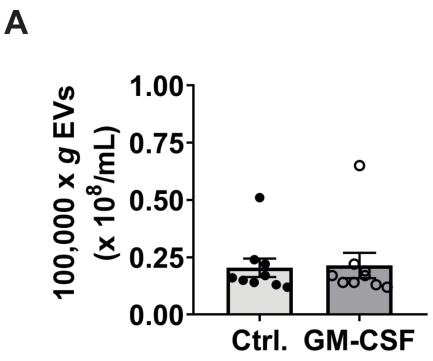

Figure 3-2: GM-CSF does not affect AM secretion of 100,000 x *g* EVs

(**A**) Adherent AMs collected by lung lavage of rats were treated with GM-CSF (50 ng/mL) for 20 - 24 h. EVs were isolated by sequential ultracentrifugation of CM at 17,000 x *g* and 100,000 x *g*, and 100,000 x *g* EVs were quantified by NTA. Data (mean ± SEM) are from 3 independent experiments. Ctrl. = control.

GM-CSF Inhibition of AM Vesicular SOCS3 Secretion is Glycolysis-Dependent

As noted previously, AMs at baseline exhibit markedly lower levels of glycolysis than do other tissue macrophage populations (57,59,190-194). Because such glycolytic restraint has been implicated in the homeostatic functions of AMs (57,59,190,192,195,196) – to which SOCS3 secretion contributes (51) – and because GM-CSF has been shown to promote glycolysis in macrophages (263,264), we hypothesized that increases in glycolysis were causally involved in the loss of vesicular SOCS3 secretion observed following treatment of AMs with GM-CSF. To evaluate the plausibility of this hypothesis, we first measured the expression of genes involved in the regulation of glucose metabolism by RT-qPCR. As shown in **Figure 3-3A**, GM-CSF enhanced the expression of the key rate-limiting glycolytic genes glucose transporter 1 (*Glut1*), hexokinase 2 (*Hk2*), and phosphofructokinase (*Pfkp*). Resulting increases in glycolytic activity were functionally confirmed by the detection of significant increases in secreted lactate caused by GM-CSF treatment of AMs (**Figure 3-3B**). We next employed a variety of approaches to determine whether the observed increases in glycolysis were implicated in the diminished release of vesicular

SOCS3. The inhibition of SOCS3 secretion by GM-CSF was dose-dependently reduced by AM culture in decreasing concentrations of glucose (**Figure 3-3C**). Additionally, culture of AMs in the presence of 2-deoxy-D-glucose (2-DG), an inhibitor of glycolysis, completely abrogated the inhibitory effect of GM-CSF on vesicular SOCS3 secretion (**Figure 3-3D**). Finally, treatment with DMOG, an analog of α-ketoglutarate that prevents degradation of the transcription factor hypoxia-inducible factor-1α and which robustly augments glycolysis in AMs (193), phenocopied GM-CSF in inhibiting the release of vesicular SOCS3 (**Figure 3-4A**) without affecting intracellular SOCS3 content (**Figure 3-4B**). Taken together, these data conclusively demonstrate that GM-CSF-induced inhibition of SOCS3 packaging and release within EVs depends on glucose utilization and glycolytic flux.

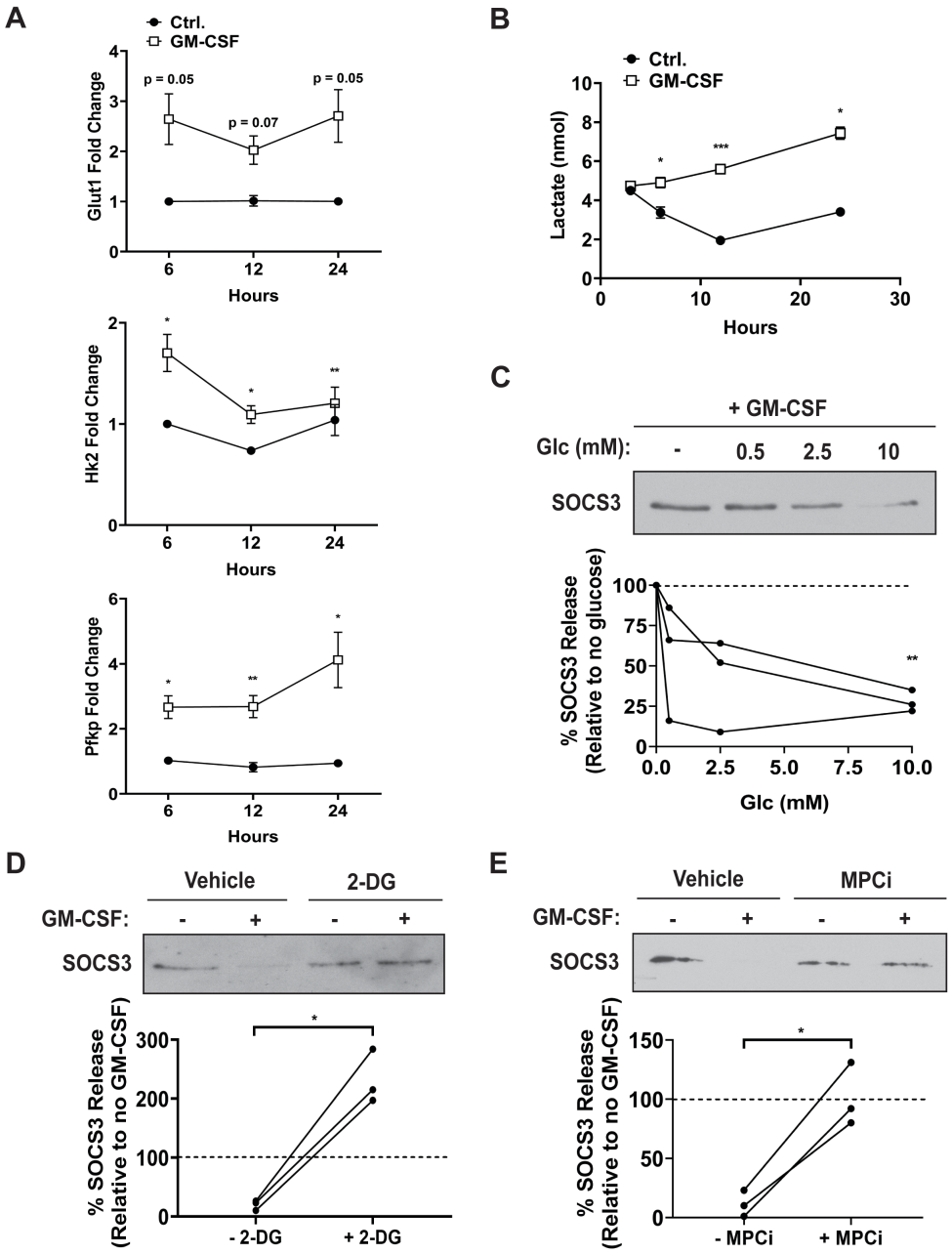

Figure 3-3: GM-CSF inhibits vesicular SOCS3 release by AMs in a glycolysis-dependent manner

(**A**-**B**) Adherent AMs collected by lung lavage of mice were treated with GM-CSF (50 ng/mL) for 3, 6, 12, or 24 h. (**A**) RNA was collected and reverse transcribed to cDNA, and relative gene expression for *Glut1*, *Hk2*, and *Pfkp* was determined by qPCR. (**B**) Cell-free supernatants from murine AMs cultured for X h as described in (**A**) were deproteinized, and extracellular lactate concentrations were measured by L-Lactate assay. (**C**-**E**) Adherent AMs collected by lung lavage of rats were treated with GM-CSF (50 ng/mL) for 20 - 24 h in varying concentrations of glucose (**C**) or in the presence or absence of 2-DG (5 mM) (**D**) or MPCi (20 μM) (**E**). EVs in CM were concentrated by 100-kDa centrifugal filtration and vesicular SOCS3 secretion was determined via Western blot of the total vesicular fraction (>100-kDa) samples. Data, expressed as mean ± SEM (**A**-**B**) or as values from individual experiments (**C**-**E**), are from 2 (**A**) or 3 (**B**-**E**) independent experiments, and significance was determined using paired sample *t*-test. Dashed line represents SOCS3 released by GM-CSF-treated AMs during culture in glucose-free medium (**C**) or by untreated AMs (i.e., no GM-CSF) during culture with inhibitor or its vehicle control (**D**-**E**). Ctrl. = control. *, **, and ***, $p < 0.05$, $p < 0.01$ and $p < 0.001$, respectively.

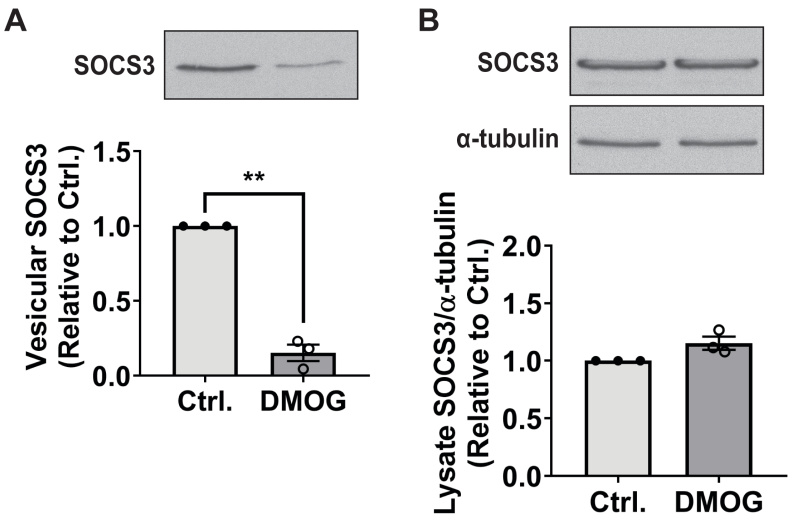

Figure 3-4: HIF-1α stabilization with DMOG inhibits vesicular SOCS3 release by AMs

(**A**-**B**) Adherent AMs collected by lung lavage of rats were treated with DMOG (1 mM) for 20 - 24 h. (**A**) EVs in CM were concentrated by 100-kDa centrifugal filtration and vesicular SOCS3 secretion was determined via Western blot of the total vesicular fraction (>100-kDa) samples. (**B**) Lysates were collected and subjected to Western blot for determination of SOCS3 intracellular content, with α-tubulin as a loading control. Data (mean ± SEM) are from 3 independent experiments, and significance was determined using paired sample *t*-test. Ctrl. = control. **, $p < 0.01$.

ACLY Mediates Glycolytic Inhibition of Vesicular SOCS3 Secretion

During aerobic metabolism, the product of glycolysis – pyruvate – undergoes transport from the cytosol into mitochondria where it is converted to acetyl-CoA to support Krebs cycle flux. To determine whether this process was required for GM-CSF's inhibitory effect on vesicular SOCS3 secretion, we evaluated the effects of UK-5099 (MPCi), a potent inhibitor of the mitochondrial pyruvate carrier (MPC). Indeed, co-treatment of AMs with MPCi negated GM-CSF's inhibitory effect on SOCS3 release by AMs (**Figure 3-3E**). Given these data, we then hypothesized that a glucose-derived Krebs cycle metabolite mediated the inhibition of AM vesicular SOCS3 release caused by GM-CSF. We first considered a potential contribution of citrate given its role in metabolic reprogramming in inflammatory myeloid cells (171,172,273,274). To evaluate this possibility, we measured the expression of isocitrate dehydrogenase 1 (*Idh1*), the enzyme responsible for converting isocitrate to oxoglutarate and

whose downregulation has been implicated in increased levels of citrate in pro-inflammatory macrophages (161). As shown in **Figure 3-5A**, treatment of AMs with GM-CSF markedly reduced *Idh1* expression. Then, to evaluate the role of mitochondrial citrate transport in the inhibition of AM secretion of SOCS3 by GM-CSF, we used a competitive inhibitor of the citrate transport protein CTP (CTPi). Indeed, culture of AMs with the CTPi reversed the GM-CSF-induced loss of vesicular SOCS3 release (**Figure 3-5B**). Also consistent with an inhibitory role for citrate on SOCS3 release, treatment of AMs with exogenous sodium citrate (1 mM) robustly inhibited vesicular SOCS3 secretion (**Figure 3-5C**). Furthermore, as GM-CSF has been previously shown to augment the expression of ACLY (275), the cytosolic enzyme responsible for converting citrate to acetyl-CoA (173), and is known to enhance the generation of acetyl-CoA in macrophages (264), we next tested whether ACLY was also involved. Indeed, ACLY inhibition with two structurally distinct inhibitors, SB-204990 (ACLYi[1]) and BMS-303141 (ACLYi[2]), overcame the attenuation of SOCS3 secretion by GM-CSF (**Figure 3-5D** and **Figure 3-6A**). Together, these data strongly suggest that the activity of ACLY links increases in glycolytic flux to diminished release of vesicular SOCS3 by way of citrate transport to the cytosol and its subsequent conversion to acetyl-CoA.

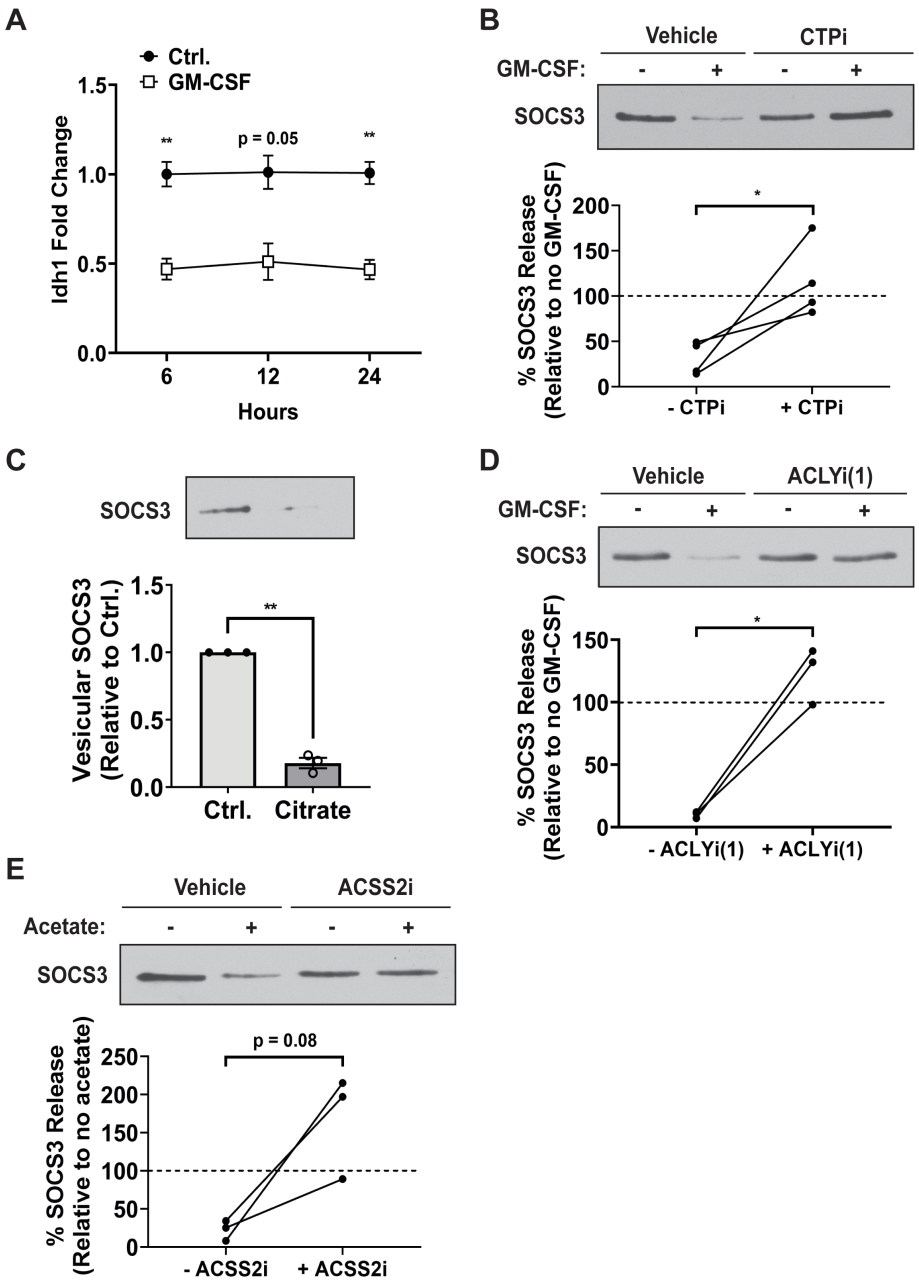

Figure 3-5: Inhibition of vesicular SOCS3 secretion by GM-CSF requires the cytosolic conversion of citrate to acetyl-CoA by ACLY

(**A**) Adherent AMs collected by lung lavage of mice were treated with GM-CSF (50 ng/mL) for 6, 12, or 24 h. RNA was collected and reverse transcribed to cDNA, and relative gene expression for *Idh1* was determined by qPCR. (**B**-**E**) Adherent AMs collected by lung lavage of rats were treated with GM-CSF (50 ng/mL) (**B** and **D**), sodium citrate (1 mM) (**C**), or sodium acetate (1 mM) (**E**) for 20 - 24 h in the presence or absence of CTPi (1 mM) (**B**), ACLYi(1) (12.5 μM) (**D**), or ACSS2i (2 μM) (**E**). EVs in CM were concentrated by 100-kDa centrifugal filtration and vesicular SOCS3 secretion was determined via Western blot of the total vesicular fraction (>100-kDa) samples. Data, expressed as (mean ± SEM) (**A** and **C**) or as values from individual experiments (**B**, **D**, and **E**), are from 2 (**A**) or ≥3 (**B**-**E**) independent experiments, and significance was determined using paired sample *t*-test. Dashed line represents SOCS3 released by untreated AMs (i.e., no GM-CSF [**B** and **D**] or sodium acetate [**E**]) during culture with inhibitor or its vehicle control. Ctrl. = control. * and **, $p < 0.05$ and $p < 0.01$, respectively.

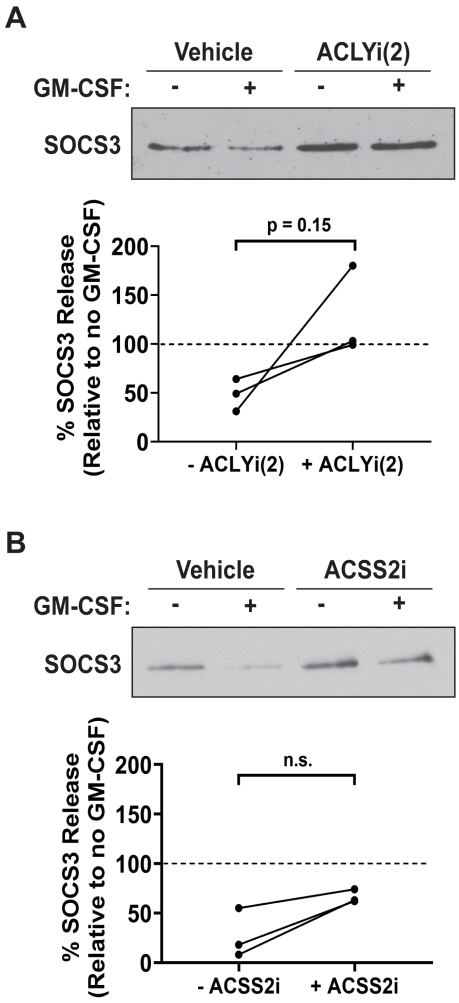

Figure 3-6: Inhibition of AM vesicular SOCS3 release by GM-CSF depends on ACLY but not ACSS2

(**A**-**B**) Adherent AMs collected by lung lavage of rats were treated with GM-CSF (50 ng/mL) for 20 - 24 h in the presence or absence of ACLYi(2) (1 μM) (**A**) or ACSS2i (2 μM) (**B**). EVs in CM were concentrated by 100-kDa centrifugal filtration and vesicular SOCS3 secretion was determined via Western blot of the total vesicular fraction (>100-kDa) samples. Data, expressed as values from individual experiments, are from 3 independent experiments, and significance was determined using paired sample *t*-test. Dashed line represents SOCS3 released by untreated AMs (i.e., no GM-CSF) during culture with inhibitor or its vehicle control. Ctrl. = control and n.s. = not significant.

Although ACLY is generally regarded as the primary enzyme responsible for generating cytosolic acetyl-CoA (173,276,277), the nucleocytosolic enzyme ACSS2, which produces acetyl-CoA from exogenous acetate, can also contribute in certain biologic scenarios (278-282). We therefore explored the possible role of this alternative route of cytosolic acetyl-CoA generation in the inhibition of secretion of SOCS3 by AMs. Treatment of AMs with sodium acetate (1 mM)

robustly inhibited SOCS3 secretion in a manner reversible by addition of an ACSS2 inhibitor (ACSS2i) (**Figure 3-5E**). However, treatment of AMs with the ACSS2i failed to substantially or significantly abrogate the inhibitory effect of GM-CSF on vesicular SOCS3 release (**Figure 3-6B**). Together, these data strongly suggest that increased acetyl-CoA production plays a critical role in mediating the diminished release of vesicular SOCS3 in response to GM-CSF. Furthermore, although acetyl-CoA can be generated from either mitochondrial-derived citrate or exogenous acetate, GM-CSF predominantly utilized citrate and the ACLY pathway to generate the acetyl-CoA responsible for inhibition of SOCS3 secretion.

Discussion

Using GM-CSF treatment as a biologically relevant *in vitro* driver of metabolic remodeling within the lung mucosal microenvironment, we demonstrate here that the resulting glycolytic flux inhibits vesicular SOCS3 release by primary AMs, a phenomenon attributable to ACLY-mediated conversion of mitochondrial-derived citrate to cytosolic acetyl-CoA. These results were also recapitulated by augmentation of glycolytic flux following AM treatment with DMOG. To our knowledge, our studies are the first to suggest that cellular metabolites control the dynamic packaging and release of a cargo molecule within EVs. Further, our findings expand on the limited body of literature exploring how lung microenvironmental perturbations alter the metabolism of resident AMs. Although we anticipate that this interplay between metabolic remodeling and EV composition extends to other cellular contexts, the importance of enhanced glycolytic flux as a determinant of these processes may be especially meaningful in the lower respiratory tract where glucose levels – measured to be 3 - 20 times lower than plasma concentrations at steady state – increase during inflammation (283-287). Additionally, given the magnitude by which increases in glycolysis diminish the release of SOCS3, our findings predict that glycolytically reprogrammed

AMs lose the ability to dampen STAT3 signaling in AECs. Therefore, we anticipate that diminished SOCS3 release by AMs underlies inflammatory dysregulation characteristic of the glycolytic alveolar milieu.

Despite the fundamental importance of metabolism for regulating cellular phenotype and function, metabolic control over the release and composition of EVs remains poorly understood. Predictably, its investigation has been restricted to the study of tumor cells where metabolic reprogramming is a hallmark of cellular transformation and an adaptive response to nutrient availability within the tumor microenvironment. For example, high levels of aerobic glycolysis have been linked to Exo secretion via phosphorylation of synaptosome-associated protein 23 by pyruvate kinase type M2 (259), thus demonstrating metabolic control over the number of secreted EVs. Furthemore, recent work from Fan et al. proposed an "exosome switch" model where deprivation of glutamine or inhibition of mechanistic target of rapamycin complex 1 caused a switch from the production of CD63-containing Exos to Rab11a-containing Exos (256). Glutamine metabolism has also been shown to uniquely drive the production of large EVs by tumor cells (257,258). These studies thus established precedent for the control of cellular metabolism over the number and subtype of EVs secreted. In contrast, we propose a novel model of metabolic regulation in which glycolytic flux dynamically inhibits the sorting of SOCS3 into AM-derived EVs. This conclusion is strongly supported by our observation that GM-CSF glycolytically inhibited the release of SOCS3 in EVs pelleted at 17,000 x *g* without significantly altering EV number (**Figure 3-1C**). Although these findings support a mechanism of diminished vesicular SOCS3 packaging, we cannot, however, eliminate the possibility of a similar "EV switch" effect where enhanced glycolysis in AMs perhaps supplants release of SOCS3-containing EVs with an alternative EV subtype. Given the lack of SOCS3 detected in a classical Exo (i.e., 100,000 x *g*)

fraction (**Figure 3-1C**) (83), it is highly unlikely that any such mechanism would be analogous to what was previously described for CD63- and Rab11a-containing Exos (256). Nonetheless, exclusion of this scenario will require a more nuanced understanding of SOCS3 sorting into EV subtypes, which we are actively investigating.

A key mechanistic conclusion from our studies is that glycolytic inhibition of vesicular SOCS3 secretion by GM-CSF requires mitochondrial pyruvate transport (**Figure 3-3E**). This finding pointed us toward a mechanism involving suppression of SOCS3 release by a mitochondrial metabolite, which we experimentally attributed to citrate and its subsequent conversion to cytosolic acetyl-CoA. Mitochondrial metabolites are recognized to assume diverse, non-metabolic signaling roles, such as in regulating chromatin modifications, DNA methylation, stem cell function, thermogenesis, tumorigenesis, and immune modulation (288). Importantly, our work reveals another arm of metabolite signaling in the control over nonclassical protein export, and we anticipate that it is relevant for the secretion of cargoes beyond SOCS3. Indeed, it will be important to determine the breadth of EV molecules whose packaging is controlled by acetyl-CoA, which is especially pertinent given its role as a central metabolic intermediate (289). Proteomic analysis of Exos derived from epithelial ovarian cancer cell lines revealed an abundance of acetylated proteins (290), suggesting positive regulation of cargo packaging by acetyl-CoA. Conversely, acetylation has been shown to inhibit the sorting of glucose-regulated protein 78 into Exos by promoting its retention in the endoplasmic reticulum (291). It is therefore likely that the effects of acetyl-CoA on EV composition are both cargo- and context-dependent, and understanding this interplay will require further investigation. Additionally, although our results implicate a causal link between enahnced glycolysis and ACLY activity in the regulation of vesicular SOCS3 secretion, it will be informative to see how alternative acetyl-CoA-generating

pathways influence cargo packaging. For example, under low-glucose, nutrient-restricted conditions or during metabolic stress, cells use exogenous acetate as a substrate for production of acetyl-CoA by ACSS2 (278-282). We demonstrated that this pathway too could diminish the release of vesicular SOCS3 (**Figure 3-5E**), but was not the predominant means of inhibition mediated by GM-CSF (**Figure 3-6B**). Furthermore, tumor cells with defective mitochondria use reductive carboxylation of glutamine to fuel acetyl-CoA production and cell growth (292,293). The extent to which these mechanisms alter vesicular cargo composition remains unknown, but they may represent attractive biologic targets for therapeutically tuning the bioactivity of EVs. Lastly, it will also be critical to determine whether metabolites other than acetyl-CoA also affect the sorting of vesicular cargoes. For example, acyl-CoA metabolites linked to major metabolic processes with known biologic functions include succinyl-CoA, propionyl-CoA, butyryl-CoA, and crotonyl-CoA (294). Future experiments will need to assess the extent to which these diverse mitochondrial metabolites control EV composition and function.

In summary, we have illuminated a previously unknown mechanism in which vesicular secretion of the cytosolically localized protein SOCS3 is tuned in AMs by glycolytic regulation of ACLY activity and the production of acetyl-CoA. Although revealed in the context of changes to the lung microenvironment, we anticipate these findings to be broadly relevant to other cellular and tissue contexts where glycolytic remodeling occurs. Future studies will be required to determine the extent to which metabolic reprogramming and metabolite flux control EV composition and bioactivity.

Chapter 4 – Discussion

Summary

Prior to the start of this thesis research, we had the goal of closing several gaps in knowledge related to the biology of extracellular vesicles (EVs). These included the cellular and molecular mechanisms of vesicular cargo release, the quantitative nature of dynamic changes in vesicular cargo packaging, and influences of the lung microenvironment on the immunoregulatory content of EVs elaborated by alveolar macrophages (AMs). Data included in this dissertation helped to bridge these gaps in knowledge and open new avenues for inquiry into the fundamental mechanistic determinants of EV cargo composition. In Chapter 2, we found that the proteasome acts as a critical brake on the packaging and release of vesicular suppressor of cytokine signaling 3 (SOCS3) by AMs. While previous work had shown that proteasome inhibitors cause substantial changes in the cargo content of EVs secreted by cancer cells (203), no study had examined the effect of a microenvironmental perturbant (e.g., reactive oxygen species, ROS) on proteasome activity and its downstream regulation of EV protein cargo secretion. Although ROS may influence cargo release via multiple mechanisms, our data suggest that proteasome inhibition is a major pathway by which it enhances the secretion of SOCS3. Additionally, the stimulated release of SOCS3 caused by ROS and proteasome inhibitors was localized exclusively to large EVs (lEVs) and involved specificity in its vesicular packaging (summarized in **Figure 4-1**).

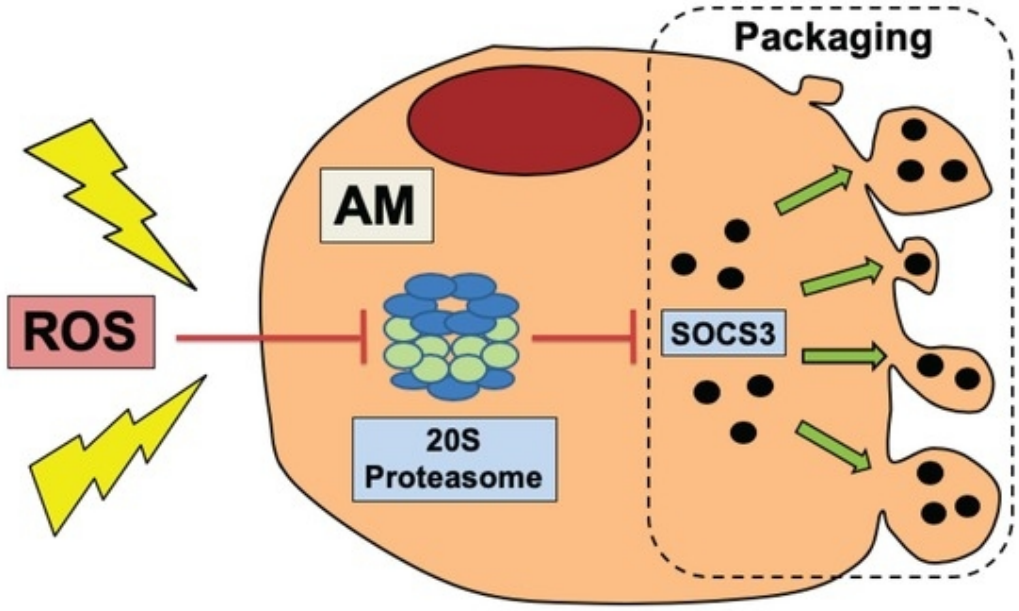

Figure 4-1: Proposed model of ROS and proteasome regulation of vesicular SOCS3 packaging and release

Research previously published from our laboratory had demonstrated that vesicular SOCS3 secretion was not a property of all macrophage populations but was particularly notable in AMs. In Chapter 3, we hypothesized that the unique metabolic phenotype exhibited by AMs was critical for the vesicular release of SOCS3. AMs residing in the lung alveolar microenvironment are exposed to low levels of glucose, and accordingly, these cells exhibit substantial glycolytic restraint. Although changes in the number of EVs secreted had been previously attributed to alterations in glycolytic activity, no study had linked the modulated release of a vesicular cargo molecule to changes in metabolism. We found that activation of glycolysis in AMs by granulocyte-macrophage colony-stimulating factor (GM-CSF) robustly inhibited the packaging and secretion of vesicular SOCS3. Additionally, our data showed that glycolytic inhibition of SOCS3 release mechanistically involves mitochondrial import of pyruvate through the mitochondrial pyruvate carrier (MPC), transport of Krebs cycle-derived citrate to the cytosol through the citrate transport protein (CTP), and the conversion of cytosolic citrate to acetyl-CoA by ATP citrate lyase (ACLY)

(summarized in **Figure 4-2**). To our knowledge, this is the first study to implicate metabolic changes and the activity of a mitochondrial metabolite in altered sorting of an EV cargo molecule.

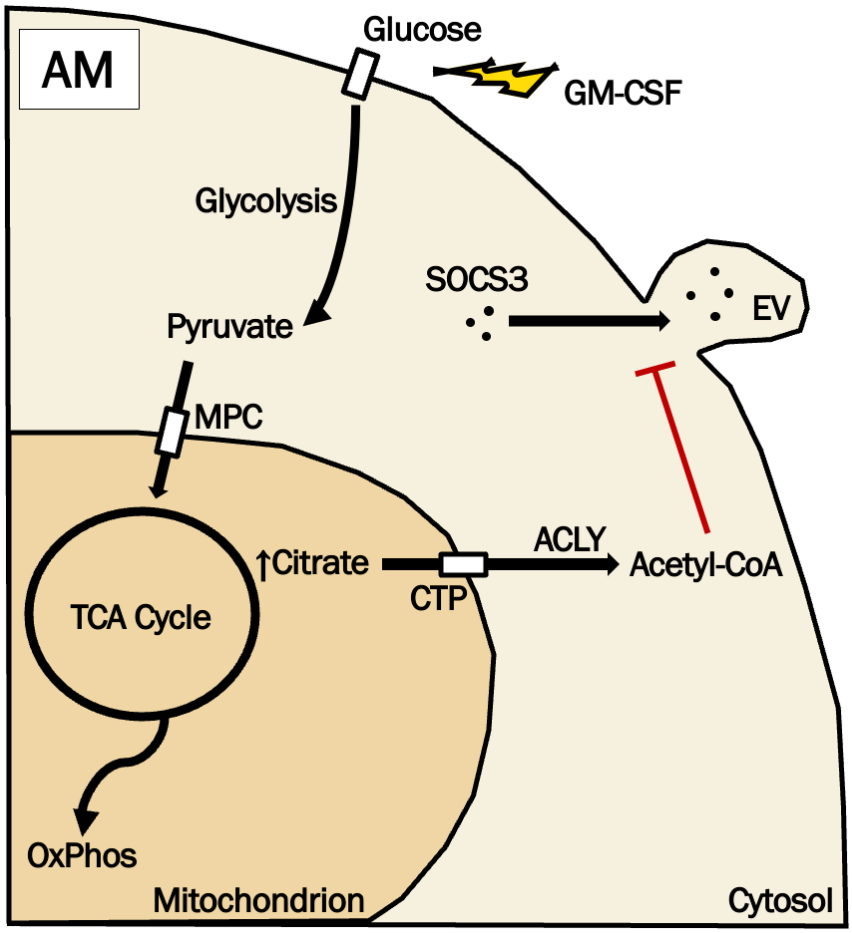

Figure 4-2: Proposed model of regulation of vesicular SOCS3 release by glycolytic flux and ACLY

Mechanisms of Vesicular SOCS3 Secretion: Unanswered Questions

As stated in the Introduction to this dissertation, one of the major gaps in knowledge surrounding the biology of EVs concerns the cellular and molecular mechanisms governing vesicular cargo sorting. This is particularly true for cytosolic proteins packaged within EVs that bud from the plasma membrane (PM), classically referred to as microvesicles (MVs). Initial

observations from our laboratory showed that SOCS3 is packaged by AMs into larger EVs pelleted at 17,000 x *g* that stain positive for annexin V (51), characteristics consistent with those described for PM-derived MVs (295). Therefore, one of the primary objectives of this dissertation research was to build upon these foundational observations by uncovering the cellular and molecular mechanisms that control SOCS3 packaging into AM-derived MVs, and thus to enhance a broader understanding of vesicular protein secretion at large.

As noted above, there are significant strengths to the research included herein. First, we have identified fundamental cellular processes (i.e., oxidative stress, proteasome inhibition, and glycolytic activation) that tune the release of vesicular SOCS3 by AMs in response to biologically and clinically relevant microenvironmental changes. Although our *in vitro* experiments were designed to model perturbations relevant to the alveolar space – where secreted SOCS3 elaborates bioactive functions in the surrounding alveolar epithelium – we expect that the mechanisms elucidated in Chapters 2 and 3 are broadly applicable to other tissues, and for other secreted vesicular cargo molecules. For example, given the dependency of cancer cells on proteasome function and metabolic adaptation for their survival and growth (296,297), we anticipate that our work will strongly inform investigation into the role of these processes for controlling proteins sorted into EVs released by transformed cells. Therefore, this research has significantly broadened the field's knowledge of the basic cellular biology influencing regulated secretion of EV cargo constituents. Another strength of the research included herein is that it comprehensively assesses the quantitative nature of protein packaging into EVs – in fact, to our knowledge, no other study has so rigorously addressed the question of specificity in cargo sorting. This concept was most robustly addressed in Chapter 2 through development of a new carboxyfluorescein succinimidyl ester-based cargo packaging assay that we anticipate will be modified/improved by other

investigators to quantitate the packaging of other intracellular protein cargoes. Thus, completion of this dissertation research substantially adds to the limited body of literature exploring the qualitative and quantitative nature of EV cargo release.

Despite these contributions, however, it is important to acknowledge the shortcomings of this work, and to expound strategies for addressing these shortcomings. The most notable research objective that remains unaddressed concerns the molecular machinery involved in vesicular SOCS3 packaging. Specifically, a major component of my thesis proposal included experiments designed to elucidate the moiety or moieties present within SOCS3 that dictate its sorting into EVs, and to determine whether a chaperone protein is needed for its vesicular inclusion. To address this, we sought to express a green fluorescent protein (GFP)-SOCS3 conjugate in AMs that would enable us to track its intracellular localization. We further envisioned the performance of site-directed mutagenesis on functional domains of potential importance for packaging into EVs, which were identified using a computational predictive model. Given the well-established role of post-translational modifications for controlling vesicular protein sorting (298), we noted several phosphorylation sites of interest. Additionally, we noted the presence of moieties that could facilitate SOCS3 packaging through interaction with candidate chaperone proteins. For example, SOCS3 contains a tyrosine-based sorting signal responsible for interaction with the μ subunit of adaptor protein complex, which has previously been identified in MVs (299). SOCS3 also has a canonical arginine-containing phospho-motif that mediates a strong interaction with 14-3-3 proteins, which have also previously been found in EVs (300). Nevertheless, our attempt to tag SOCS3 with GFP conjugated to its C-terminus resulted in the expression of a fusion protein that could not be released extracellularly, and thus, our efforts to investigate the biological importance of these moieties for vesicular secretion were thwarted. Future experiments investigating the

molecular determinants of SOCS3 sorting into EVs should use shorter tags – histidine or FLAG, for example – to minimize disruption of protein folding and function.

However, despite our inability to directly address the molecular nature of vesicular SOCS3 packaging, insights gleaned from the mechanistic studies included in Chapters 2 and 3 have enabled us to generate testable hypotheses undergoing exploration in the laboratory. For example, as discussed in Chapter 2, we are particularly interested in the potential role of arrestin domain-containing protein 1 (ARRDC1) as a SOCS3 packaging chaperone protein given its dependency on polyubiquitination for generating PM-derived MVs (105). As vesicular SOCS3 release is so heavily potentiated by oxidative and pharmacologic disruption of AM ubiquitin-proteasome homeostasis, we envision a scenario in which ARRDC1-mediated vesicular SOCS3 sorting is augmented by proteasome inhibition due to the accumulation of polyubiquitinated ARRDC1 within budding MVs. This model of enhanced SOCS3 secretion is particularly attractive given the well-established role of ARRDC1 as a chaperone/adaptor protein with activity sufficient for promoting vesicular cargo recruitment (125,126). Unfortunately, our intention to assess the biologic relevance of this mechanism was hindered by the current lack of anti-ARRDC1 antibodies suitable for non-human systems, and they must await future advances.

Additionally, observations outlined in Chapter 3 that strongly implicate an inhibitory role for ACLY and acetyl-CoA production on SOCS3 release open new avenues of inquiry into the fundamental mechanisms of vesicular cargo packaging. We postulate two scenarios that could explain how increases in acetyl-CoA might suppress the release of SOCS3 in EVs. First, given the well-described link between ACLY, acetyl-CoA production, and histone acetylation (173), it is possible that transcriptional changes in the machinery presumed to be important for EV cargo sorting are causal to the diminished release of SOCS3. Given that we measured SOCS3 secretion

after AMs were cultured for time durations sufficient to allow for altered gene expression (20+ h), we cannot eliminate this possibility. However, such a mechanism is inconsistent with our prior observations showing that SOCS3 secretion is rapidly tunable (i.e., within 15 mins after addition of various inhibitory/stimulatory signals) (51). Therefore, it is more likely that acetyl-CoA production inhibits vesicular SOCS3 release either through direct post-translational modification of SOCS3 itself or of a chaperone protein important for SOCS3 sorting. As mentioned previously, this model is consistent with the extant body of literature suggesting a broad role for post-translational modification in dictating membrane targeting of EV cargoes (298). Given that acetyl-CoA serves as a substrate for protein acetylation and as a precursor for the de novo synthesis of fatty acids involved in protein lipidation (palmitoylation and myristoylation, for example), there are several modifications that could be responsible for the inhibited release of vesicular SOCS3. We plan to test the relevance of these moieties by performing immunoprecipitation experiments involving SOCS3 pull-down coupled to immunoblotting with pan acetylation, palmitoylation, or myristoylation antibodies to identify whether SOCS3 and/or an interacting partner is chemically modified under conditions in which vesicular SOCS3 packaging is diminished. If results indicate that a SOCS3-interacting protein undergoes modification, mass spectrometry could then be used for its identification and functional investigation. Such an approach highlights the utility of leveraging the results of this dissertation for informing a more rigorous investigation into the molecular determinants of SOCS3 secretion within EVs.

Although Chapters 2 and 3 of this dissertation were presented as two distinct and seemingly unrelated stories, it is intriguing to postulate a conceptual model that could mechanistically link the influences of proteasome inhibition and acetyl-CoA accumulation on AM vesicular SOCS3 release. Accordingly, we are particularly interested to investigate the potential role of a protein

central to autophagy, microtubule-associated protein 1A/1B-light chain 3 (LC3). While LC3 is well-described to canonically regulate the growth of autophagic membranes, recognize autophagic cargoes, and control the fusion of autophagosomes with lysosomes (301-303), and thus act as a key regulator of autophagic processes, it has also very recently been ascribed a non-autophagic function in the loading of RNA and protein cargoes into EVs (127). Critically, these autophagic and non-autophagic functions require that LC3 undergoes conjugation with phosphatidylethanolamine (i.e., lipidation) to facilitate its membrane targeting (302). Interestingly, and pertinent to this dissertation research, LC3 activity is strongly regulated by both proteasomal degradation and acetylation. For example, the proteasome has been shown to degrade LC3 in a stepwise manner, first disrupting its conjugation and then degrading the protein entirely (304). Accordingly, proteasome inhibitors have been shown to increase intracellular levels of LC3 (305). Furthermore, it is known that acetylation inhibits LC3 complex formation and cargo recognition (306), and diverts LC3 localization away from the cytoplasm into the nucleus (307). Therefore, LC3 represents a potential chaperone whose regulation could explain the bidirectional tuning of vesicular SOCS3 release described herein. Specifically, we postulate that ROS/bortezomib treatment of AMs increases total levels of LC3 available for SOCS3 sorting, thus increasing its vesicular release, whereas the activation of glycolytic flux by GM-CSF inhibits SOCS3 secretion through acetylation-mediated disruption of LC3 conjugation and cargo loading. Although SOCS3 itself does not contain a LC3 interaction region, it is very plausible that vesicular sorting is a modular phenomenon, perhaps requiring that SOCS3 interact with an adaptor protein that serves as a bridge to its proximal chaperone (e.g., LC3). This is an intriguing and unifying model that awaits experimental exploration in the laboratory.

Potential Crosstalk Between the Influences of ROS and Glycolytic Remodeling on SOCS3 Secretion

A possible paradox arises from attempting to mechanistically link the findings from Chapters 2 and 3, specifically concerning the crosstalk between ROS production and glycolysis. It is well known that ROS stabilize hypoxia-inducible factor-1α (HIF-1α) and thus are capable of augmenting cellular glycolytic activity (308,309). However, glycolytically reprogrammed macrophages also generate substantial amounts of mitochondrial ROS (163). How then can we explain the potentiation of SOCS3 secretion caused by ROS (as described in Chapter 2) but the inhibition of SOCS3 secretion caused by glycolysis (as described in Chapter 3)? We speculate that the directionality of regulated SOCS3 release is the consequence of important differences in the antioxidant tone and metabolism of the primary AMs used in Chapter 3 and the immortalized AMs (MH-S) used in Chapter 2. Specifically, we hypothesize that during their residence in a microenvironment characterized by high oxygen tension, primary AMs acquire substantially greater antioxidant defenses than do MH-S cells perennially maintained in culture. This hypothesis is informed by experiments in Chapter 2 showing that primary AMs were more resistant to ROS-dependent increases in SOCS3 secretion caused by cigarette smoke (CS) extract as compared to MH-S cells. However, while primary AMs exhibit substantial glycolytic restraint at steady state, highly proliferative MH-S cells require significantly greater metabolic activity. Accordingly, we have observed that MH-S cells acidify culture medium to a much greater extent than do primary AMs (data not shown), consistent with a higher level of glycolytic activity. We therefore speculate that primary AMs are uniquely sensitive to glycolysis-induced inhibition of SOCS3 secretion but resistant to the stimulatory actions of ROS. On the other hand, we anticipate that their heightened susceptibility to oxidative stress renders MH-S cells more sensitive to the stimulatory effect of

ROS on SOCS3 secretion while their already high baseline glycolytic activity is unable to be further augmented. Why then do high levels of ROS still augment vesicular SOCS3 release by primary AMs (as shown in Chapter 2)? In this case, we hypothesize that the balance between the influences of oxidative stress and glycolytic activation tips in favor of the former, thus resulting in a net potentiation of SOCS3 secretion. Although this model rationalizes the seemingly contradictory findings described herein, testing it will require a more rigorous head-to-head comparison of the oxidative stress response within, and resting metabolism of, these two disparate sources of AMs.

Leveraging GM-CSF as a Model to Predict Glycolytic Inhibition of Vesicular SOCS3 Release

Major gaps in knowledge pertaining to AM metabolism include the microenvironmental factors that dictate glycolytic restraint at steady state and the instructive signals that promote glycolytic remodeling during inflammatory insults. Results included in this dissertation address the latter gap in knowledge by further implicating GM-CSF as an important microenvironmental factor for augmenting AM glycolysis. Furthermore, they serve to predict whether other signals present in the alveolar space might similarly inhibit vesicular SOCS3 secretion in a glycolysis-dependent manner. Although it is intuitive to expect that AM metabolism is regulated in a similar fashion to other macrophage populations, there is literature to suggest otherwise. For example, lipopolysaccharide robustly augments glycolysis in conventional bone marrow-derived macrophages but has no effect on the metabolic phenotype of AMs (193). Therefore, any such prediction must necessarily leverage the limited body of literature examining glycolytic remodeling in AMs. Importantly, data included in Chapter 3 and in prior publications (193,194) implicate a critical role for HIF-1α in potentiating AM glycolysis. Given our work showing inhibition of AM vesicular SOCS3 secretion caused by pharmacologic stabilization of HIF-1α, we

expect that microenvironmental factors promoting HIF-1α activity should have the same effect on SOCS3 release as does GM-CSF. Critically, GM-CSF signals through mammalian target of rapamycin (mTOR), a key protein involved in growth factor signaling that is known to upregulate HIF-1α expression in AMs (269). Although we did not directly test the reliance of GM-CSF on HIF-1α for suppressing SOCS3 release, we anticipate that it assumes a key role. Accordingly, we are also keen to investigate whether other mTOR-activating growth factors present in the alveolar microenvironment – Wnt, insulin-like growth factor-1 (IGF-1), and tumor necrosis factor α (TNFα), for example – might also suppress vesicular SOCS3 secretion through upregulation of HIF-1α. For example, Wnt was recently shown to promote glycolysis-dependent inflammatory functions in AMs through HIF-1α-upregulation (310). IGF-1 production is also prominent during various types of lung inflammation (311) including pulmonary fibrosis during which AMs undergo glycolytic remodeling (195). The same is also true for TNFα (312). Additionally, given the prominence of hypoxia – a key signal promoting HIF-1α stabilization (313) – during various forms of chronic lung disease (314), we anticipate that it, too, could inhibit AM vesicular SOCS3 secretion in a glycolysis-dependent manner. Finally, CS is another microenvironmental factor of clinical relevance that is known to activate HIF-1α (315) and thus could glycolytically inhibit vesicular SOCS3 release by AMs. As discussed below, this might mechanistically explain the loss of SOCS3 secretion observed in cigarette smokers (51). Ultimately, direct experimentation is needed to determine whether these HIF-1α-promoting factors inhibit vesicular SOCS3 release and the extent to which they contribute to diminished SOCS3 secretion observed during chronic lung inflammation *in vivo*.

Tuning of Vesicular SOCS3 Secretion as a Therapeutic Strategy

One of the key questions that arises from observations included in this dissertation is whether the mechanisms uncovered in Chapters 2 and 3 might be exploited for therapeutic benefit. To reiterate, SOCS3 is not merely a random cargo constituent of EVs; rather, its local release is also the basis for a physiologically important homeostatic communication network established between AMs and the alveolar epithelium. Accordingly, prior observations from our laboratory showing that SOCS3 secretion is lost during a variety of chronic lung inflammatory diseases – such as cigarette smoking (51), allergic asthma (85), and lung cancer (86) – have clear biological and clinical implications. Furthermore, we have experimentally demonstrated that diminished SOCS3 release contributes to the pathophysiology of these conditions (85,86). Therefore, a major objective of our laboratory's research is to identify therapeutic strategies for restoring SOCS3 secretion *in vivo* to dampen dysregulated inflammatory signaling within the alveolar epithelium. To achieve this end, we have considered and tested the utility of administering artificial liposomes encapsulating recombinant SOCS3 protein, which have proved efficacious *in vitro* and *in vivo* for restraining allergic inflammation (85) and suppressing tumorigenesis (86). However, to date, we have not been able to devise a strategy targeting the restoration of endogenous SOCS3 secretion by AMs, as illuminating the mechanisms causal to loss of its release *in vivo* has remained elusive.

As shown in Chapter 2, the proteasome inhibitor bortezomib is a robust potentiator of vesicular SOCS3 packaging and thus could be considered for its potential therapeutic utility in the context of diminished SOCS3 secretion. It is already approved by the Food and Drug Administration for treating multiple myeloma and mantle cell lymphoma, and has been previously shown to alter the bioactivity of EVs released by multiple myeloma cells (203). Therefore, it is theoretically an attractive candidate drug for augmenting endogenous secretion of SOCS3 by AMs.

However, a major limitation inherent to pharmacologically modifying the molecular content of biologic EVs – particularly in this context – concerns the specificity of a drug's effect on the secretion of a single cargo molecule. For example, bortezomib was shown to elicit substantial changes to the overall proteome of EVs secreted by multiple myeloma cells (203). While we demonstrated in Chapter 2 that bortezomib does exert some specificity in potentiating SOCS3 release relative to all intracellular protein cargoes, SOCS3 is likely not the only bioactive constituent to undergo alterations in its vesicular packaging. Therefore, it is possible that eliciting changes in the proteome of AM-derived EVs that are not entirely specific may offset the intended protective effect of potentiating vesicular SOCS3 content. Accordingly, preliminary experiments completed during my PhD demonstrated that EVs collected from bortezomib-treated AMs in fact augmented Janus kinase-signal transducer and activator of transcription 3 (JAK-STAT3) signaling when delivered to interleukin-6-treated alveolar epithelial cells (AECs), even despite containing more SOCS3 protein (data not shown). These results indicate that even though vesicular SOCS3 content is increased by bortezomib, the drug's net effect is a potentiation of inflammatory activity in AM-derived EVs. Therefore, we argue that the most efficacious way to restore endogenous SOCS3 secretion in the lung is to exploit the specific mechanism causing its diminished release *in vivo* as opposed to employing drugs that augment packaging in an untargeted manner.

As a result, we are currently dedicating our efforts to testing whether the metabolism-related mechanism outlined in Chapter 3 may underly the AM-intrinsic defect in SOCS3 secretion observed during cigarette smoking, allergic asthma, and lung cancer. Of note, GM-CSF is produced during exposure to CS, and its neutralization dampens smoke-induced inflammation (316). Accordingly, AMs taken from human smokers have been shown to exhibit higher rates of basal glycolysis (317). GM-CSF production is also prominent during allergic asthma, and it drives

inflammation (266). The same is true for many solid tumors, which are well-described to secrete GM-CSF (318). Therefore, we postulate that the diminished release of vesicular SOCS3 observed during all three of these chronic lung inflammatory conditions is the result of one unifying mechanism: glycolytic flux in AMs causing the accumulation of citrate and its cytosolic conversion to acetyl-CoA by ACLY. Although experimentation is ongoing, we have two interesting pieces of preliminary data to suggest the relevance of this pathway. First, using an ovalbumin-induced model of allergic asthma, we have observed that AMs taken from the allergic inflammatory milieu exhibit higher levels of glycolysis than do AMs taken from the lungs of control mice, as measured by the uptake of a fluorescent glucose analog (data not shown). Furthermore, we have evidence showing that the SOCS3 secretion defect exhibited by AMs taken from mice bearing lung tumors is reversed by overnight culture with the inhibitor of glycolysis 2-deoxy-D-glucose (data not shown). These two lines of evidence have motivated further investigation into the influence of glycolytic flux and a potential role for ACLY and acetyl-CoA on the loss of SOCS3 secretion *in vivo*. We plan to collect AMs from smoke-exposed, asthmatic, and tumor-bearing mice to test whether culture with an ACLY inhibitor reverses their inability to release SOCS3 *ex vivo*. If so, we are enthusiastic to investigate the utility of employing an ACLY inhibitor *in vivo* for restoring endogenous SOCS3 secretion. However, as detailed above, it is plausible that changes in acetyl-CoA levels influence the packaging of several cargoes beyond SOCS3. Therefore, it will be imperative to demonstrate that ACLY inhibitors restore SOCS3 release while also retaining the vesicular bioactivity needed to suppress inflammatory JAK-STAT3 signaling in recipient AECs.

Final Thoughts

There are obvious strengths and weaknesses inherent to having focused the entirety of our efforts on studying the secretion of a single EV cargo molecule. On the one hand, investigating the mechanisms of vesicular SOCS3 release afforded us the opportunity to address a major gap in knowledge in the field concerning the cellular determinants of vesicular cargo sorting. Many studies published on changes in EV composition lack mechanistic detail, yet here we have leveraged our interest in SOCS3 secretion to comprehensively illuminate cellular processes controlling its release in EVs. Centering our attention on SOCS3 also afforded us the opportunity to address the fundamental and yet nebulous concept of vesicular cargo packaging: the hypothesis that altered cargo secretion involves – at least to some extent – active changes in the amount of a molecule packaged per individual EV. Our unbiased approach to doing so was imperfect: it was only semi-quantitative, and analyses were performed on bulk EV populations (i.e., either >100-kDa fractions or sub-fractions collected by ultracentrifugation) as opposed to single EVs. As improvements are made to platforms enabling single-vesicle analyses, the quantitative nature of cargo packaging can be further investigated on a more granular scale. Nevertheless, our work provides needed proof of concept for a fundamental hypothesis demanding further investigation.

As alluded to in this Discussion, however, a major drawback to having uniquely assessed SOCS3 secretion is that we still do not know how broadly oxidative stress, the proteasome, and metabolic remodeling regulate EV cargo composition. Are their influences specific to vesicular SOCS3 release, or do they tune the sorting and secretion of additional EV proteins? Not only is this question important for understanding the fundamental nature of vesicular cargo sorting, but it is also critical for predicting the bioactivity and therapeutic potential of EVs *in vivo*. In the absence of proteomics experiments designed to measure the breadth of changes in EV composition, we can

only provide speculation informed by the extant body of literature. As such, our current working model is that SOCS3 packaging is a modular phenomenon with secretion linked to the release of cargoes that share the same "packaging module," a complex of vesicular constituents that interact, either directly or indirectly, with a deterministic sorting chaperone. This hypothesis accommodates our data suggesting that changes in vesicular secretion are, at least to some extent, specific to SOCS3 while also aligning with data produced by other groups describing relatively broad alterations in vesicular protein content caused by an external stimulus (203). Clearly, the notion that a molecular constituent is specifically and actively sorted into a budding EV remains poorly understood and understudied. Although this dissertation fell short of fully unraveling such a conundrum, it does still serve to generate provocative and exciting hypotheses for other investigators to explore with greater depth and rigor.

After all, the adventures that fail to reach their intended finish line are nevertheless the most instructive and meaningful.

References

1. Guo, M., Du, Y., Gokey, J. J., Ray, S., Bell, S. M., Adam, M., Sudha, P., Perl, A. K., Deshmukh, H., Potter, S. S., Whitsett, J. A., and Xu, Y. (2019) Single cell RNA analysis identifies cellular heterogeneity and adaptive responses of the lung at birth. *Nat Commun* **10**, 37

2. Travaglini, K. J., Nabhan, A. N., Penland, L., Sinha, R., Gillich, A., Sit, R. V., Chang, S., Conley, S. D., Mori, Y., Seita, J., Berry, G. J., Shrager, J. B., Metzger, R. J., Kuo, C. S., Neff, N., Weissman, I. L., Quake, S. R., and Krasnow, M. A. (2020) A molecular cell atlas of the human lung from single-cell RNA sequencing. *Nature* **587**, 619-625

3. Vieira Braga, F. A., Kar, G., Berg, M., Carpaij, O. A., Polanski, K., Simon, L. M., Brouwer, S., Gomes, T., Hesse, L., Jiang, J., Fasouli, E. S., Efremova, M., Vento-Tormo, R., Talavera-Lopez, C., Jonker, M. R., Affleck, K., Palit, S., Strzelecka, P. M., Firth, H. V., Mahbubani, K. T., Cvejic, A., Meyer, K. B., Saeb-Parsy, K., Luinge, M., Brandsma, C. A., Timens, W., Angelidis, I., Strunz, M., Koppelman, G. H., van Oosterhout, A. J., Schiller, H. B., Theis, F. J., van den Berge, M., Nawijn, M. C., and Teichmann, S. A. (2019) A cellular census of human lungs identifies novel cell states in health and in asthma. *Nat Med* **25**, 1153-1163

4. Barkauskas, C. E., Cronce, M. J., Rackley, C. R., Bowie, E. J., Keene, D. R., Stripp, B. R., Randell, S. H., Noble, P. W., and Hogan, B. L. (2013) Type 2 alveolar cells are stem cells in adult lung. *J Clin Invest* **123**, 3025-3036

5. T'Jonck, W., Guilliams, M., and Bonnardel, J. (2018) Niche signals and transcription factors involved in tissue-resident macrophage development. *Cell Immunol* **330**, 43-53

6. Ginhoux, F., and Jung, S. (2014) Monocytes and macrophages: developmental pathways and tissue homeostasis. *Nat Rev Immunol* **14**, 392-404

7. Ginhoux, F., and Guilliams, M. (2016) Tissue-Resident Macrophage Ontogeny and Homeostasis. *Immunity* **44**, 439-449

8. Schneider, C., Nobs, S. P., Kurrer, M., Rehrauer, H., Thiele, C., and Kopf, M. (2014) Induction of the nuclear receptor PPAR-gamma by the cytokine GM-CSF is critical for the differentiation of fetal monocytes into alveolar macrophages. *Nat Immunol* **15**, 1026-1037

9. Shibata, Y., Berclaz, P. Y., Chroneos, Z. C., Yoshida, M., Whitsett, J. A., and Trapnell, B. C. (2001) GM-CSF regulates alveolar macrophage differentiation and innate immunity in the lung through PU.1. *Immunity* **15**, 557-567

10. Yu, X., Buttgereit, A., Lelios, I., Utz, S. G., Cansever, D., Becher, B., and Greter, M. (2017) The Cytokine TGF-beta Promotes the Development and Homeostasis of Alveolar Macrophages. *Immunity* **47**, 903-912 e904

11. Nakamura, A., Ebina-Shibuya, R., Itoh-Nakadai, A., Muto, A., Shima, H., Saigusa, D., Aoki, J., Ebina, M., Nukiwa, T., and Igarashi, K. (2013) Transcription repressor Bach2 is required for pulmonary surfactant homeostasis and alveolar macrophage function. *J Exp Med* **210**, 2191-2204

12. Cain, D. W., O'Koren, E. G., Kan, M. J., Womble, M., Sempowski, G. D., Hopper, K., Gunn, M. D., and Kelsoe, G. (2013) Identification of a tissue-specific, C/EBPbeta-dependent pathway of differentiation for murine peritoneal macrophages. *J Immunol* **191**, 4665-4675

13. MacDonald, K. P., Palmer, J. S., Cronau, S., Seppanen, E., Olver, S., Raffelt, N. C., Kuns, R., Pettit, A. R., Clouston, A., Wainwright, B., Branstetter, D., Smith, J., Paxton, R. J., Cerretti, D. P., Bonham, L., Hill, G. R., and Hume, D. A. (2010) An antibody against the colony-stimulating factor 1 receptor depletes the resident subset of monocytes and tissue- and tumor-associated macrophages but does not inhibit inflammation. *Blood* **116**, 3955-3963

14. Hashimoto, D., Chow, A., Noizat, C., Teo, P., Beasley, M. B., Leboeuf, M., Becker, C. D., See, P., Price, J., Lucas, D., Greter, M., Mortha, A., Boyer, S. W., Forsberg, E. C., Tanaka, M., van Rooijen, N., Garcia-Sastre, A., Stanley, E. R., Ginhoux, F., Frenette, P. S., and Merad, M. (2013) Tissue-resident macrophages self-maintain locally throughout adult life with minimal contribution from circulating monocytes. *Immunity* **38**, 792-804

15. Yona, S., Kim, K. W., Wolf, Y., Mildner, A., Varol, D., Breker, M., Strauss-Ayali, D., Viukov, S., Guilliams, M., Misharin, A., Hume, D. A., Perlman, H., Malissen, B., Zelzer, E., and Jung, S. (2013) Fate mapping reveals origins and dynamics of monocytes and tissue macrophages under homeostasis. *Immunity* **38**, 79-91

16. Guilliams, M., De Kleer, I., Henri, S., Post, S., Vanhoutte, L., De Prijck, S., Deswarte, K., Malissen, B., Hammad, H., and Lambrecht, B. N. (2013) Alveolar macrophages develop from fetal monocytes that differentiate into long-lived cells in the first week of life via GM-CSF. *J Exp Med* **210**, 1977-1992

17. Murphy, J., Summer, R., Wilson, A. A., Kotton, D. N., and Fine, A. (2008) The prolonged life-span of alveolar macrophages. *Am J Respir Cell Mol Biol* **38**, 380-385

18. Nayak, D. K., Zhou, F., Xu, M., Huang, J., Tsuji, M., Hachem, R., and Mohanakumar, T. (2016) Long-Term Persistence of Donor Alveolar Macrophages in Human Lung Transplant Recipients That Influences Donor-Specific Immune Responses. *Am J Transplant* **16**, 2300-2311

19. Eguiluz-Gracia, I., Schultz, H. H., Sikkeland, L. I., Danilova, E., Holm, A. M., Pronk, C. J., Agace, W. W., Iversen, M., Andersen, C., Jahnsen, F. L., and Baekkevold, E. S. (2016) Long-term persistence of human donor alveolar macrophages in lung transplant recipients. *Thorax* **71**, 1006-1011

20. Ghoneim, H. E., Thomas, P. G., and McCullers, J. A. (2013) Depletion of alveolar macrophages during influenza infection facilitates bacterial superinfections. *J Immunol* **191**, 1250-1259

21. Janssen, W. J., Barthel, L., Muldrow, A., Oberley-Deegan, R. E., Kearns, M. T., Jakubzick, C., and Henson, P. M. (2011) Fas determines differential fates of resident and recruited macrophages during resolution of acute lung injury. *Am J Respir Crit Care Med* **184**, 547-560

22. Machiels, B., Dourcy, M., Xiao, X., Javaux, J., Mesnil, C., Sabatel, C., Desmecht, D., Lallemand, F., Martinive, P., Hammad, H., Guilliams, M., Dewals, B., Vanderplasschen, A., Lambrecht, B. N., Bureau, F., and Gillet, L. (2017) A gammaherpesvirus provides protection against allergic asthma by inducing the replacement of resident alveolar macrophages with regulatory monocytes. *Nat Immunol* **18**, 1310-1320

23. Maus, U. A., Janzen, S., Wall, G., Srivastava, M., Blackwell, T. S., Christman, J. W., Seeger, W., Welte, T., and Lohmeyer, J. (2006) Resident alveolar macrophages are replaced by recruited monocytes in response to endotoxin-induced lung inflammation. *Am J Respir Cell Mol Biol* **35**, 227-235

24. Guilliams, M., and Scott, C. L. (2017) Does niche competition determine the origin of tissue-resident macrophages? *Nat Rev Immunol* **17**, 451-460

25. Gibbings, S. L., Thomas, S. M., Atif, S. M., McCubbrey, A. L., Desch, A. N., Danhorn, T., Leach, S. M., Bratton, D. L., Henson, P. M., Janssen, W. J., and Jakubzick, C. V. (2017) Three Unique Interstitial Macrophages in the Murine Lung at Steady State. *Am J Respir Cell Mol Biol* **57**, 66-76

26. Gautier, E. L., Shay, T., Miller, J., Greter, M., Jakubzick, C., Ivanov, S., Helft, J., Chow, A., Elpek, K. G., Gordonov, S., Mazloom, A. R., Ma'ayan, A., Chua, W. J., Hansen, T. H., Turley, S. J., Merad, M., Randolph, G. J., and Immunological Genome, C. (2012) Gene-expression profiles and transcriptional regulatory pathways that underlie the identity and diversity of mouse tissue macrophages. *Nat Immunol* **13**, 1118-1128

27. Misharin, A. V., Morales-Nebreda, L., Mutlu, G. M., Budinger, G. R., and Perlman, H. (2013) Flow cytometric analysis of macrophages and dendritic cell subsets in the mouse lung. *Am J Respir Cell Mol Biol* **49**, 503-510

28. Sabatel, C., Radermecker, C., Fievez, L., Paulissen, G., Chakarov, S., Fernandes, C., Olivier, S., Toussaint, M., Pirottin, D., Xiao, X., Quatresooz, P., Sirard, J. C., Cataldo, D., Gillet, L., Bouabe, H., Desmet, C. J., Ginhoux, F., Marichal, T., and Bureau, F. (2017)

Exposure to Bacterial CpG DNA Protects from Airway Allergic Inflammation by Expanding Regulatory Lung Interstitial Macrophages. *Immunity* **46**, 457-473

29. Tan, S. Y., and Krasnow, M. A. (2016) Developmental origin of lung macrophage diversity. *Development* **143**, 1318-1327

30. Chakarov, S., Lim, H. Y., Tan, L., Lim, S. Y., See, P., Lum, J., Zhang, X. M., Foo, S., Nakamizo, S., Duan, K., Kong, W. T., Gentek, R., Balachander, A., Carbajo, D., Bleriot, C., Malleret, B., Tam, J. K. C., Baig, S., Shabeer, M., Toh, S. E. S., Schlitzer, A., Larbi, A., Marichal, T., Malissen, B., Chen, J., Poidinger, M., Kabashima, K., Bajenoff, M., Ng, L. G., Angeli, V., and Ginhoux, F. (2019) Two distinct interstitial macrophage populations coexist across tissues in specific subtissular niches. *Science* **363**, eaau0964

31. Bittmann, I., Dose, T., Baretton, G. B., Muller, C., Schwaiblmair, M., Kur, F., and Lohrs, U. (2001) Cellular chimerism of the lung after transplantation. An interphase cytogenetic study. *Am J Clin Pathol* **115**, 525-533

32. Izquierdo, H. M., Brandi, P., Gomez, M. J., Conde-Garrosa, R., Priego, E., Enamorado, M., Martinez-Cano, S., Sanchez, I., Conejero, L., Jimenez-Carretero, D., Martin-Puig, S., Guilliams, M., and Sancho, D. (2018) Von Hippel-Lindau Protein Is Required for Optimal Alveolar Macrophage Terminal Differentiation, Self-Renewal, and Function. *Cell Rep* **24**, 1738-1746

33. Dranoff, G., Crawford, A. D., Sadelain, M., Ream, B., Rashid, A., Bronson, R. T., Dickersin, G. R., Bachurski, C. J., Mark, E. L., Whitsett, J. A., and et al. (1994) Involvement of granulocyte-macrophage colony-stimulating factor in pulmonary homeostasis. *Science* **264**, 713-716

34. Thepen, T., Van Rooijen, N., and Kraal, G. (1989) Alveolar macrophage elimination in vivo is associated with an increase in pulmonary immune response in mice. *J Exp Med* **170**, 499-509

35. Gautier, E. L., Chow, A., Spanbroek, R., Marcelin, G., Greter, M., Jakubzick, C., Bogunovic, M., Leboeuf, M., van Rooijen, N., Habenicht, A. J., Merad, M., and Randolph, G. J. (2012) Systemic analysis of PPARgamma in mouse macrophage populations reveals marked diversity in expression with critical roles in resolution of inflammation and airway immunity. *J Immunol* **189**, 2614-2624

36. Morris, D. G., Huang, X., Kaminski, N., Wang, Y., Shapiro, S. D., Dolganov, G., Glick, A., and Sheppard, D. (2003) Loss of integrin alpha(v)beta6-mediated TGF-beta activation causes Mmp12-dependent emphysema. *Nature* **422**, 169-173

37. Toews, G. B., Vial, W. C., Dunn, M. M., Guzzetta, P., Nunez, G., Stastny, P., and Lipscomb, M. F. (1984) The accessory cell function of human alveolar macrophages in specific T cell proliferation. *J Immunol* **132**, 181-186

38. Lyons, C. R., Ball, E. J., Toews, G. B., Weissler, J. C., Stastny, P., and Lipscomb, M. F. (1986) Inability of human alveolar macrophages to stimulate resting T cells correlates with decreased antigen-specific T cell-macrophage binding. *J Immunol* **137**, 1173-1180

39. Lipscomb, M. F., Lyons, C. R., Nunez, G., Ball, E. J., Stastny, P., Vial, W., Lem, V., Weissler, J., and Miller, L. M. (1986) Human alveolar macrophages: HLA-DR-positive macrophages that are poor stimulators of a primary mixed leukocyte reaction. *J Immunol* **136**, 497-504

40. Blumenthal, R. L., Campbell, D. E., Hwang, P., DeKruyff, R. H., Frankel, L. R., and Umetsu, D. T. (2001) Human alveolar macrophages induce functional inactivation in antigen-specific CD4 T cells. *J Allergy Clin Immunol* **107**, 258-264

41. Roth, M. D., and Golub, S. H. (1993) Human pulmonary macrophages utilize prostaglandins and transforming growth factor beta 1 to suppress lymphocyte activation. *J Leukoc Biol* **53**, 366-371

42. Coleman, M. M., Ruane, D., Moran, B., Dunne, P. J., Keane, J., and Mills, K. H. (2013) Alveolar macrophages contribute to respiratory tolerance by inducing FoxP3 expression in naive T cells. *Am J Respir Cell Mol Biol* **48**, 773-780

43. Huynh, M. L., Fadok, V. A., and Henson, P. M. (2002) Phosphatidylserine-dependent ingestion of apoptotic cells promotes TGF-beta1 secretion and the resolution of inflammation. *J Clin Invest* **109**, 41-50

44. Hoffmann, P. R., Kench, J. A., Vondracek, A., Kruk, E., Daleke, D. L., Jordan, M., Marrack, P., Henson, P. M., and Fadok, V. A. (2005) Interaction between phosphatidylserine and the phosphatidylserine receptor inhibits immune responses in vivo. *J Immunol* **174**, 1393-1404

45. Fadok, V. A., Bratton, D. L., Konowal, A., Freed, P. W., Westcott, J. Y., and Henson, P. M. (1998) Macrophages that have ingested apoptotic cells in vitro inhibit proinflammatory cytokine production through autocrine/paracrine mechanisms involving TGF-beta, PGE2, and PAF. *J Clin Invest* **101**, 890-898

46. Snelgrove, R. J., Goulding, J., Didierlaurent, A. M., Lyonga, D., Vekaria, S., Edwards, L., Gwyer, E., Sedgwick, J. D., Barclay, A. N., and Hussell, T. (2008) A critical function for CD200 in lung immune homeostasis and the severity of influenza infection. *Nat Immunol* **9**, 1074-1083

47. Bonfield, T. L., Konstan, M. W., Burfeind, P., Panuska, J. R., Hilliard, J. B., and Berger, M. (1995) Normal bronchial epithelial cells constitutively produce the anti-inflammatory cytokine interleukin-10, which is downregulated in cystic fibrosis. *Am J Respir Cell Mol Biol* **13**, 257-261

48. Haczku, A. (2008) Protective role of the lung collectins surfactant protein A and surfactant protein D in airway inflammation. *J Allergy Clin Immunol* **122**, 861-879

49. Steele, C., Marrero, L., Swain, S., Harmsen, A. G., Zheng, M., Brown, G. D., Gordon, S., Shellito, J. E., and Kolls, J. K. (2003) Alveolar macrophage-mediated killing of Pneumocystis carinii f. sp. muris involves molecular recognition by the Dectin-1 beta-glucan receptor. *J Exp Med* **198**, 1677-1688

50. Han, C. Z., Juncadella, I. J., Kinchen, J. M., Buckley, M. W., Klibanov, A. L., Dryden, K., Onengut-Gumuscu, S., Erdbrugger, U., Turner, S. D., Shim, Y. M., Tung, K. S., and Ravichandran, K. S. (2016) Macrophages redirect phagocytosis by non-professional phagocytes and influence inflammation. *Nature* **539**, 570-574

51. Bourdonnay, E., Zaslona, Z., Penke, L. R., Speth, J. M., Schneider, D. J., Przybranowski, S., Swanson, J. A., Mancuso, P., Freeman, C. M., Curtis, J. L., and Peters-Golden, M. (2015) Transcellular delivery of vesicular SOCS proteins from macrophages to epithelial cells blunts inflammatory signaling. *J Exp Med* **212**, 729-742

52. Westphalen, K., Gusarova, G. A., Islam, M. N., Subramanian, M., Cohen, T. S., Prince, A. S., and Bhattacharya, J. (2014) Sessile alveolar macrophages communicate with alveolar epithelium to modulate immunity. *Nature* **506**, 503-506

53. Byrne, A. J., Mathie, S. A., Gregory, L. G., and Lloyd, C. M. (2015) Pulmonary macrophages: key players in the innate defence of the airways. *Thorax* **70**, 1189-1196

54. Aegerter, H., Kulikauskaite, J., Crotta, S., Patel, H., Kelly, G., Hessel, E. M., Mack, M., Beinke, S., and Wack, A. (2020) Influenza-induced monocyte-derived alveolar macrophages confer prolonged antibacterial protection. *Nat Immunol* **21**, 145-157

55. Misharin, A. V., Morales-Nebreda, L., Reyfman, P. A., Cuda, C. M., Walter, J. M., McQuattie-Pimentel, A. C., Chen, C. I., Anekalla, K. R., Joshi, N., Williams, K. J. N., Abdala-Valencia, H., Yacoub, T. J., Chi, M., Chiu, S., Gonzalez-Gonzalez, F. J., Gates, K., Lam, A. P., Nicholson, T. T., Homan, P. J., Soberanes, S., Dominguez, S., Morgan, V. K., Saber, R., Shaffer, A., Hinchcliff, M., Marshall, S. A., Bharat, A., Berdnikovs, S., Bhorade, S. M., Bartom, E. T., Morimoto, R. I., Balch, W. E., Sznajder, J. I., Chandel, N. S., Mutlu, G. M., Jain, M., Gottardi, C. J., Singer, B. D., Ridge, K. M., Bagheri, N., Shilatifard, A., Budinger, G. R. S., and Perlman, H. (2017) Monocyte-derived alveolar macrophages drive lung fibrosis and persist in the lung over the life span. *J Exp Med* **214**, 2387-2404

56. Zaslona, Z., Przybranowski, S., Wilke, C., van Rooijen, N., Teitz-Tennenbaum, S., Osterholzer, J. J., Wilkinson, J. E., Moore, B. B., and Peters-Golden, M. (2014) Resident alveolar macrophages suppress, whereas recruited monocytes promote, allergic lung inflammation in murine models of asthma. *J Immunol* **193**, 4245-4253

57. Mould, K. J., Barthel, L., Mohning, M. P., Thomas, S. M., McCubbrey, A. L., Danhorn, T., Leach, S. M., Fingerlin, T. E., O'Connor, B. P., Reisz, J. A., D'Alessandro, A., Bratton, D. L., Jakubzick, C. V., and Janssen, W. J. (2017) Cell Origin Dictates Programming of Resident versus Recruited Macrophages during Acute Lung Injury. *Am J Respir Cell Mol Biol* **57**, 294-306

58. Kamei, A., Gao, G., Neale, G., Loh, L. N., Vogel, P., Thomas, P. G., Tuomanen, E. I., and Murray, P. J. (2016) Exogenous remodeling of lung resident macrophages protects against infectious consequences of bone marrow-suppressive chemotherapy. *Proc Natl Acad Sci U S A* **113**, E6153-E6161

59. Yao, Y., Jeyanathan, M., Haddadi, S., Barra, N. G., Vaseghi-Shanjani, M., Damjanovic, D., Lai, R., Afkhami, S., Chen, Y., Dvorkin-Gheva, A., Robbins, C. S., Schertzer, J. D., and Xing, Z. (2018) Induction of Autonomous Memory Alveolar Macrophages Requires T Cell Help and Is Critical to Trained Immunity. *Cell* **175**, 1634-1650 e1617

60. Wilks, A. F., Harpur, A. G., Kurban, R. R., Ralph, S. J., Zurcher, G., and Ziemiecki, A. (1991) Two novel protein-tyrosine kinases, each with a second phosphotransferase-related catalytic domain, define a new class of protein kinase. *Mol Cell Biol* **11**, 2057-2065

61. Wilks, A. F. (1989) Two putative protein-tyrosine kinases identified by application of the polymerase chain reaction. *Proc Natl Acad Sci U S A* **86**, 1603-1607

62. Velazquez, L., Fellous, M., Stark, G. R., and Pellegrini, S. (1992) A protein tyrosine kinase in the interferon alpha/beta signaling pathway. *Cell* **70**, 313-322

63. Firmbach-Kraft, I., Byers, M., Shows, T., Dalla-Favera, R., and Krolewski, J. J. (1990) tyk2, prototype of a novel class of non-receptor tyrosine kinase genes. *Oncogene* **5**, 1329-1336

64. Kawamura, M., McVicar, D. W., Johnston, J. A., Blake, T. B., Chen, Y. Q., Lal, B. K., Lloyd, A. R., Kelvin, D. J., Staples, J. E., Ortaldo, J. R., and et al. (1994) Molecular cloning of L-JAK, a Janus family protein-tyrosine kinase expressed in natural killer cells and activated leukocytes. *Proc Natl Acad Sci U S A* **91**, 6374-6378

65. Feng, J., Witthuhn, B. A., Matsuda, T., Kohlhuber, F., Kerr, I. M., and Ihle, J. N. (1997) Activation of Jak2 catalytic activity requires phosphorylation of Y1007 in the kinase activation loop. *Mol Cell Biol* **17**, 2497-2501

66. Argetsinger, L. S., Campbell, G. S., Yang, X., Witthuhn, B. A., Silvennoinen, O., Ihle, J. N., and Carter-Su, C. (1993) Identification of JAK2 as a growth hormone receptor-associated tyrosine kinase. *Cell* **74**, 237-244

67. Shuai, K., Schindler, C., Prezioso, V. R., and Darnell, J. E., Jr. (1992) Activation of transcription by IFN-gamma: tyrosine phosphorylation of a 91-kD DNA binding protein. *Science* **258**, 1808-1812

68. Schindler, C., Shuai, K., Prezioso, V. R., and Darnell, J. E., Jr. (1992) Interferon-dependent tyrosine phosphorylation of a latent cytoplasmic transcription factor. *Science* **257**, 809-813

69. Yoshimura, A., Ohkubo, T., Kiguchi, T., Jenkins, N. A., Gilbert, D. J., Copeland, N. G., Hara, T., and Miyajima, A. (1995) A novel cytokine-inducible gene CIS encodes an SH2-containing protein that binds to tyrosine-phosphorylated interleukin 3 and erythropoietin receptors. *EMBO J* **14**, 2816-2826

70. Endo, T. A., Masuhara, M., Yokouchi, M., Suzuki, R., Sakamoto, H., Mitsui, K., Matsumoto, A., Tanimura, S., Ohtsubo, M., Misawa, H., Miyazaki, T., Leonor, N., Taniguchi, T., Fujita, T., Kanakura, Y., Komiya, S., and Yoshimura, A. (1997) A new protein containing an SH2 domain that inhibits JAK kinases. *Nature* **387**, 921-924

71. Standke, G. J., Meier, V. S., and Groner, B. (1994) Mammary gland factor activated by prolactin on mammary epithelial cells and acute-phase response factor activated by interleukin-6 in liver cells share DNA binding and transactivation potential. *Mol Endocrinol* **8**, 469-477

72. Zhong, Z., Wen, Z., and Darnell, J. E., Jr. (1994) Stat3: a STAT family member activated by tyrosine phosphorylation in response to epidermal growth factor and interleukin-6. *Science* **264**, 95-98

73. Ruff-Jamison, S., Zhong, Z., Wen, Z., Chen, K., Darnell, J. E., Jr., and Cohen, S. (1994) Epidermal growth factor and lipopolysaccharide activate Stat3 transcription factor in mouse liver. *J Biol Chem* **269**, 21933-21935

74. Tian, S. S., Lamb, P., Seidel, H. M., Stein, R. B., and Rosen, J. (1994) Rapid activation of the STAT3 transcription factor by granulocyte colony-stimulating factor. *Blood* **84**, 1760-1764

75. Gavino, A. C., Nahmod, K., Bharadwaj, U., Makedonas, G., and Tweardy, D. J. (2016) STAT3 inhibition prevents lung inflammation, remodeling, and accumulation of Th2 and Th17 cells in a murine asthma model. *Allergy* **71**, 1684-1692

76. Zhao, J., Yu, H., Liu, Y., Gibson, S. A., Yan, Z., Xu, X., Gaggar, A., Li, P. K., Li, C., Wei, S., Benveniste, E. N., and Qin, H. (2016) Protective effect of suppressing STAT3 activity in LPS-induced acute lung injury. *Am J Physiol Lung Cell Mol Physiol* **311**, L868-L880

77. Pechkovsky, D. V., Prele, C. M., Wong, J., Hogaboam, C. M., McAnulty, R. J., Laurent, G. J., Zhang, S. S., Selman, M., Mutsaers, S. E., and Knight, D. A. (2012) STAT3-mediated signaling dysregulates lung fibroblast-myofibroblast activation and differentiation in UIP/IPF. *Am J Pathol* **180**, 1398-1412

78. Zou, S., Tong, Q., Liu, B., Huang, W., Tian, Y., and Fu, X. (2020) Targeting STAT3 in Cancer Immunotherapy. *Mol Cancer* **19**, 145

79. White, G. E., Cotterill, A., Addley, M. R., Soilleux, E. J., and Greaves, D. R. (2011) Suppressor of cytokine signalling protein SOCS3 expression is increased at sites of acute and chronic inflammation. *J Mol Histol* **42**, 137-151

80. Akram, K. M., Lomas, N. J., Forsyth, N. R., and Spiteri, M. A. (2014) Alveolar epithelial cells in idiopathic pulmonary fibrosis display upregulation of TRAIL, DR4 and DR5 expression with simultaneous preferential over-expression of pro-apoptotic marker p53. *Int J Clin Exp Pathol* **7**, 552-564

81. van Niel, G., D'Angelo, G., and Raposo, G. (2018) Shedding light on the cell biology of extracellular vesicles. *Nat Rev Mol Cell Biol* **19**, 213-228

82. Kowal, J., Arras, G., Colombo, M., Jouve, M., Morath, J. P., Primdal-Bengtson, B., Dingli, F., Loew, D., Tkach, M., and Thery, C. (2016) Proteomic comparison defines novel markers to characterize heterogeneous populations of extracellular vesicle subtypes. *Proc Natl Acad Sci U S A* **113**, E968-977

83. Jeppesen, D. K., Fenix, A. M., Franklin, J. L., Higginbotham, J. N., Zhang, Q., Zimmerman, L. J., Liebler, D. C., Ping, J., Liu, Q., Evans, R., Fissell, W. H., Patton, J. G., Rome, L. H., Burnette, D. T., and Coffey, R. J. (2019) Reassessment of Exosome Composition. *Cell* **177**, 428-445 e418

84. Tkach, M., Kowal, J., Zucchetti, A. E., Enserink, L., Jouve, M., Lankar, D., Saitakis, M., Martin-Jaular, L., and Thery, C. (2017) Qualitative differences in T-cell activation by dendritic cell-derived extracellular vesicle subtypes. *EMBO J* **36**, 3012-3028

85. Draijer, C., Speth, J. M., Penke, L. R. K., Zaslona, Z., Bazzill, J. D., Lugogo, N., Huang, Y. J., Moon, J. J., and Peters-Golden, M. (2020) Resident alveolar macrophage-derived vesicular SOCS3 dampens allergic airway inflammation. *FASEB J* **34**, 4718-4731

86. Speth, J. M., Penke, L. R., Bazzill, J. D., Park, K. S., de Rubio, R. G., Schneider, D. J., Ouchi, H., Moon, J. J., Keshamouni, V. G., Zemans, R. L., Lama, V. N., Arenberg, D. A., and Peters-Golden, M. (2019) Alveolar macrophage secretion of vesicular SOCS3 represents a platform for lung cancer therapeutics. *JCI Insight* **4**, e131340

87. Speth, J. M., Bourdonnay, E., Penke, L. R., Mancuso, P., Moore, B. B., Weinberg, J. B., and Peters-Golden, M. (2016) Alveolar Epithelial Cell-Derived Prostaglandin E2 Serves as a Request Signal for Macrophage Secretion of Suppressor of Cytokine Signaling 3 during Innate Inflammation. *J Immunol* **196**, 5112-5120

88. Moon, H. G., Cao, Y., Yang, J., Lee, J. H., Choi, H. S., and Jin, Y. (2015) Lung epithelial cell-derived extracellular vesicles activate macrophage-mediated inflammatory responses via ROCK1 pathway. *Cell Death Dis* **6**, e2016

89. Lee, H., Zhang, D., Zhu, Z., Dela Cruz, C. S., and Jin, Y. (2016) Epithelial cell-derived microvesicles activate macrophages and promote inflammation via microvesicle-containing microRNAs. *Sci Rep* **6**, 35250

90. Kulshreshtha, A., Ahmad, T., Agrawal, A., and Ghosh, B. (2013) Proinflammatory role of epithelial cell-derived exosomes in allergic airway inflammation. *J Allergy Clin Immunol* **131**, 1194-1203, 1203 e1191-1114

91. Chahar, H. S., Corsello, T., Kudlicki, A. S., Komaravelli, N., and Casola, A. (2018) Respiratory Syncytial Virus Infection Changes Cargo Composition of Exosome Released from Airway Epithelial Cells. *Sci Rep* **8**, 387

92. Lee, H., Zhang, D., Wu, J., Otterbein, L. E., and Jin, Y. (2017) Lung Epithelial Cell-Derived Microvesicles Regulate Macrophage Migration via MicroRNA-17/221-Induced Integrin beta1 Recycling. *J Immunol* **199**, 1453-1464

93. Szul, T., Bratcher, P. E., Fraser, K. B., Kong, M., Tirouvanziam, R., Ingersoll, S., Sztul, E., Rangarajan, S., Blalock, J. E., Xu, X., and Gaggar, A. (2016) Toll-Like Receptor 4 Engagement Mediates Prolyl Endopeptidase Release from Airway Epithelia via Exosomes. *Am J Respir Cell Mol Biol* **54**, 359-369

94. Bastarache, J. A., Fremont, R. D., Kropski, J. A., Bossert, F. R., and Ware, L. B. (2009) Procoagulant alveolar microparticles in the lungs of patients with acute respiratory distress syndrome. *Am J Physiol Lung Cell Mol Physiol* **297**, L1035-1041

95. Cordazzo, C., Petrini, S., Neri, T., Lombardi, S., Carmazzi, Y., Pedrinelli, R., Paggiaro, P., and Celi, A. (2014) Rapid shedding of proinflammatory microparticles by human mononuclear cells exposed to cigarette smoke is dependent on Ca2+ mobilization. *Inflamm Res* **63**, 539-547

96. Soni, S., Wilson, M. R., O'Dea, K. P., Yoshida, M., Katbeh, U., Woods, S. J., and Takata, M. (2016) Alveolar macrophage-derived microvesicles mediate acute lung injury. *Thorax* **71**, 1020-1029

97. Henne, W. M., Stenmark, H., and Emr, S. D. (2013) Molecular mechanisms of the membrane sculpting ESCRT pathway. *Cold Spring Harb Perspect Biol* **5**

98. Colombo, M., Moita, C., van Niel, G., Kowal, J., Vigneron, J., Benaroch, P., Manel, N., Moita, L. F., Thery, C., and Raposo, G. (2013) Analysis of ESCRT functions in exosome biogenesis, composition and secretion highlights the heterogeneity of extracellular vesicles. *J Cell Sci* **126**, 5553-5565

99. Escola, J. M., Kleijmeer, M. J., Stoorvogel, W., Griffith, J. M., Yoshie, O., and Geuze, H. J. (1998) Selective enrichment of tetraspan proteins on the internal vesicles of multivesicular endosomes and on exosomes secreted by human B-lymphocytes. *J Biol Chem* **273**, 20121-20127

100. Chairoungdua, A., Smith, D. L., Pochard, P., Hull, M., and Caplan, M. J. (2010) Exosome release of beta-catenin: a novel mechanism that antagonizes Wnt signaling. *J Cell Biol* **190**, 1079-1091

101. Nazarenko, I., Rana, S., Baumann, A., McAlear, J., Hellwig, A., Trendelenburg, M., Lochnit, G., Preissner, K. T., and Zoller, M. (2010) Cell surface tetraspanin Tspan8 contributes to molecular pathways of exosome-induced endothelial cell activation. *Cancer Res* **70**, 1668-1678

102. Hurwitz, S. N., Conlon, M. M., Rider, M. A., Brownstein, N. C., and Meckes, D. G., Jr. (2016) Nanoparticle analysis sheds budding insights into genetic drivers of extracellular vesicle biogenesis. *J Extracell Vesicles* **5**, 31295

103. Trajkovic, K., Hsu, C., Chiantia, S., Rajendran, L., Wenzel, D., Wieland, F., Schwille, P., Brugger, B., and Simons, M. (2008) Ceramide triggers budding of exosome vesicles into multivesicular endosomes. *Science* **319**, 1244-1247

104. Matusek, T., Wendler, F., Poles, S., Pizette, S., D'Angelo, G., Furthauer, M., and Therond, P. P. (2014) The ESCRT machinery regulates the secretion and long-range activity of Hedgehog. *Nature* **516**, 99-103

105. Nabhan, J. F., Hu, R., Oh, R. S., Cohen, S. N., and Lu, Q. (2012) Formation and release of arrestin domain-containing protein 1-mediated microvesicles (ARMMs) at plasma membrane by recruitment of TSG101 protein. *Proc Natl Acad Sci U S A* **109**, 4146-4151

106. Schlienger, S., Campbell, S., and Claing, A. (2014) ARF1 regulates the Rho/MLC pathway to control EGF-dependent breast cancer cell invasion. *Mol Biol Cell* **25**, 17-29

107. Muralidharan-Chari, V., Clancy, J., Plou, C., Romao, M., Chavrier, P., Raposo, G., and D'Souza-Schorey, C. (2009) ARF6-regulated shedding of tumor cell-derived plasma membrane microvesicles. *Curr Biol* **19**, 1875-1885

108. Li, B., Antonyak, M. A., Zhang, J., and Cerione, R. A. (2012) RhoA triggers a specific signaling pathway that generates transforming microvesicles in cancer cells. *Oncogene* **31**, 4740-4749

109. Bianco, F., Perrotta, C., Novellino, L., Francolini, M., Riganti, L., Menna, E., Saglietti, L., Schuchman, E. H., Furlan, R., Clementi, E., Matteoli, M., and Verderio, C. (2009) Acid sphingomyelinase activity triggers microparticle release from glial cells. *EMBO J* **28**, 1043-1054

110. Awojoodu, A. O., Keegan, P. M., Lane, A. R., Zhang, Y., Lynch, K. R., Platt, M. O., and Botchwey, E. A. (2014) Acid sphingomyelinase is activated in sickle cell erythrocytes and contributes to inflammatory microparticle generation in SCD. *Blood* **124**, 1941-1950

111. Moreno-Gonzalo, O., Fernandez-Delgado, I., and Sanchez-Madrid, F. (2018) Post-translational add-ons mark the path in exosomal protein sorting. *Cell Mol Life Sci* **75**, 1-19

112. Smith, V. L., Jackson, L., and Schorey, J. S. (2015) Ubiquitination as a Mechanism To Transport Soluble Mycobacterial and Eukaryotic Proteins to Exosomes. *J Immunol* **195**, 2722-2730

113. Cheng, Y., and Schorey, J. S. (2016) Targeting soluble proteins to exosomes using a ubiquitin tag. *Biotechnol Bioeng* **113**, 1315-1324

114. Luhtala, N., Aslanian, A., Yates, J. R., 3rd, and Hunter, T. (2017) Secreted Glioblastoma Nanovesicles Contain Intracellular Signaling Proteins and Active Ras Incorporated in a Farnesylation-dependent Manner. *J Biol Chem* **292**, 611-628

115. McKenzie, A. J., Hoshino, D., Hong, N. H., Cha, D. J., Franklin, J. L., Coffey, R. J., Patton, J. G., and Weaver, A. M. (2016) KRAS-MEK Signaling Controls Ago2 Sorting into Exosomes. *Cell Rep* **15**, 978-987

116. van Niel, G., Charrin, S., Simoes, S., Romao, M., Rochin, L., Saftig, P., Marks, M. S., Rubinstein, E., and Raposo, G. (2011) The tetraspanin CD63 regulates ESCRT-independent and -dependent endosomal sorting during melanogenesis. *Dev Cell* **21**, 708-721

117. Villarroya-Beltri, C., Gutierrez-Vazquez, C., Sanchez-Cabo, F., Perez-Hernandez, D., Vazquez, J., Martin-Cofreces, N., Martinez-Herrera, D. J., Pascual-Montano, A., Mittelbrunn, M., and Sanchez-Madrid, F. (2013) Sumoylated hnRNPA2B1 controls the sorting of miRNAs into exosomes through binding to specific motifs. *Nat Commun* **4**, 2980

118. Santangelo, L., Giurato, G., Cicchini, C., Montaldo, C., Mancone, C., Tarallo, R., Battistelli, C., Alonzi, T., Weisz, A., and Tripodi, M. (2016) The RNA-Binding Protein SYNCRIP Is a Component of the Hepatocyte Exosomal Machinery Controlling MicroRNA Sorting. *Cell Rep* **17**, 799-808

119. Hobor, F., Dallmann, A., Ball, N. J., Cicchini, C., Battistelli, C., Ogrodowicz, R. W., Christodoulou, E., Martin, S. R., Castello, A., Tripodi, M., Taylor, I. A., and Ramos, A. (2018) A cryptic RNA-binding domain mediates Syncrip recognition and exosomal partitioning of miRNA targets. *Nat Commun* **9**, 831

120. Batagov, A. O., and Kurochkin, I. V. (2013) Exosomes secreted by human cells transport largely mRNA fragments that are enriched in the 3'-untranslated regions. *Biol Direct* **8**, 12

121. Bolukbasi, M. F., Mizrak, A., Ozdener, G. B., Madlener, S., Strobel, T., Erkan, E. P., Fan, J. B., Breakefield, X. O., and Saydam, O. (2012) miR-1289 and "Zipcode"-like Sequence Enrich mRNAs in Microvesicles. *Mol Ther Nucleic Acids* **1**, e10

122. Fang, Y., Wu, N., Gan, X., Yan, W., Morrell, J. C., and Gould, S. J. (2007) Higher-order oligomerization targets plasma membrane proteins and HIV gag to exosomes. *PLoS Biol* **5**, e158

123. Shen, B., Wu, N., Yang, J. M., and Gould, S. J. (2011) Protein targeting to exosomes/microvesicles by plasma membrane anchors. *J Biol Chem* **286**, 14383-14395

124. Shen, B., Fang, Y., Wu, N., and Gould, S. J. (2011) Biogenesis of the posterior pole is mediated by the exosome/microvesicle protein-sorting pathway. *J Biol Chem* **286**, 44162-44176

125. Wang, Q., and Lu, Q. (2017) Plasma membrane-derived extracellular microvesicles mediate non-canonical intercellular NOTCH signaling. *Nat Commun* **8**, 709

126. Mackenzie, K., Foot, N. J., Anand, S., Dalton, H. E., Chaudhary, N., Collins, B. M., Mathivanan, S., and Kumar, S. (2016) Regulation of the divalent metal ion transporter via membrane budding. *Cell Discov* **2**, 16011

127. Leidal, A. M., Huang, H. H., Marsh, T., Solvik, T., Zhang, D., Ye, J., Kai, F., Goldsmith, J., Liu, J. Y., Huang, Y. H., Monkkonen, T., Vlahakis, A., Huang, E. J., Goodarzi, H., Yu, L., Wiita, A. P., and Debnath, J. (2020) The LC3-conjugation machinery specifies the loading of RNA-binding proteins into extracellular vesicles. *Nat Cell Biol* **22**, 187-199

128. Mulcahy, L. A., Pink, R. C., and Carter, D. R. (2014) Routes and mechanisms of extracellular vesicle uptake. *J Extracell Vesicles* **3**

129. Schneider, D. J., Speth, J. M., Penke, L. R., Wettlaufer, S. H., Swanson, J. A., and Peters-Golden, M. (2017) Mechanisms and modulation of microvesicle uptake in a model of alveolar cell communication. *J Biol Chem* **292**, 20897-20910

130. Barres, C., Blanc, L., Bette-Bobillo, P., Andre, S., Mamoun, R., Gabius, H. J., and Vidal, M. (2010) Galectin-5 is bound onto the surface of rat reticulocyte exosomes and modulates vesicle uptake by macrophages. *Blood* **115**, 696-705

131. Feng, D., Zhao, W. L., Ye, Y. Y., Bai, X. C., Liu, R. Q., Chang, L. F., Zhou, Q., and Sui, S. F. (2010) Cellular internalization of exosomes occurs through phagocytosis. *Traffic* **11**, 675-687

132. Fitzner, D., Schnaars, M., van Rossum, D., Krishnamoorthy, G., Dibaj, P., Bakhti, M., Regen, T., Hanisch, U. K., and Simons, M. (2011) Selective transfer of exosomes from oligodendrocytes to microglia by macropinocytosis. *J Cell Sci* **124**, 447-458

133. Parolini, I., Federici, C., Raggi, C., Lugini, L., Palleschi, S., De Milito, A., Coscia, C., Iessi, E., Logozzi, M., Molinari, A., Colone, M., Tatti, M., Sargiacomo, M., and Fais, S. (2009) Microenvironmental pH is a key factor for exosome traffic in tumor cells. *J Biol Chem* **284**, 34211-34222

134. Montecalvo, A., Larregina, A. T., Shufesky, W. J., Stolz, D. B., Sullivan, M. L., Karlsson, J. M., Baty, C. J., Gibson, G. A., Erdos, G., Wang, Z., Milosevic, J., Tkacheva, O. A., Divito, S. J., Jordan, R., Lyons-Weiler, J., Watkins, S. C., and Morelli, A. E. (2012) Mechanism of transfer of functional microRNAs between mouse dendritic cells via exosomes. *Blood* **119**, 756-766

135. Tian, T., Wang, Y., Wang, H., Zhu, Z., and Xiao, Z. (2010) Visualizing of the cellular uptake and intracellular trafficking of exosomes by live-cell microscopy. *J Cell Biochem* **111**, 488-496

136. Sahay, G., Querbes, W., Alabi, C., Eltoukhy, A., Sarkar, S., Zurenko, C., Karagiannis, E., Love, K., Chen, D., Zoncu, R., Buganim, Y., Schroeder, A., Langer, R., and Anderson, D. G. (2013) Efficiency of siRNA delivery by lipid nanoparticles is limited by endocytic recycling. *Nat Biotechnol* **31**, 653-658

137. Gilleron, J., Querbes, W., Zeigerer, A., Borodovsky, A., Marsico, G., Schubert, U., Manygoats, K., Seifert, S., Andree, C., Stoter, M., Epstein-Barash, H., Zhang, L., Koteliansky, V., Fitzgerald, K., Fava, E., Bickle, M., Kalaidzidis, Y., Akinc, A., Maier, M., and Zerial, M. (2013) Image-based analysis of lipid nanoparticle-mediated siRNA delivery, intracellular trafficking and endosomal escape. *Nat Biotechnol* **31**, 638-646

138. Hung, M. E., and Leonard, J. N. (2016) A platform for actively loading cargo RNA to elucidate limiting steps in EV-mediated delivery. *J Extracell Vesicles* **5**, 31027

139. Heusermann, W., Hean, J., Trojer, D., Steib, E., von Bueren, S., Graff-Meyer, A., Genoud, C., Martin, K., Pizzato, N., Voshol, J., Morrissey, D. V., Andaloussi, S. E., Wood, M. J., and Meisner-Kober, N. C. (2016) Exosomes surf on filopodia to enter cells at endocytic hot spots, traffic within endosomes, and are targeted to the ER. *J Cell Biol* **213**, 173-184

140. Holmstrom, K. M., and Finkel, T. (2014) Cellular mechanisms and physiological consequences of redox-dependent signalling. *Nat Rev Mol Cell Biol* **15**, 411-421

141. Lambeth, J. D. (2004) NOX enzymes and the biology of reactive oxygen. *Nat Rev Immunol* **4**, 181-189

142. Zorov, D. B., Juhaszova, M., and Sollott, S. J. (2014) Mitochondrial reactive oxygen species (ROS) and ROS-induced ROS release. *Physiol Rev* **94**, 909-950

143. Bard, J. A. M., Goodall, E. A., Greene, E. R., Jonsson, E., Dong, K. C., and Martin, A. (2018) Structure and Function of the 26S Proteasome. *Annu Rev Biochem* **87**, 697-724

144. Rechsteiner, M., and Hill, C. P. (2005) Mobilizing the proteolytic machine: cell biological roles of proteasome activators and inhibitors. *Trends Cell Biol* **15**, 27-33

145. Lee, B. H., Lee, M. J., Park, S., Oh, D. C., Elsasser, S., Chen, P. C., Gartner, C., Dimova, N., Hanna, J., Gygi, S. P., Wilson, S. M., King, R. W., and Finley, D. (2010) Enhancement of proteasome activity by a small-molecule inhibitor of USP14. *Nature* **467**, 179-184

146. Shringarpure, R., Grune, T., Mehlhase, J., and Davies, K. J. (2003) Ubiquitin conjugation is not required for the degradation of oxidized proteins by proteasome. *J Biol Chem* **278**, 311-318

147. Davies, K. J. (2001) Degradation of oxidized proteins by the 20S proteasome. *Biochimie* **83**, 301-310

148. Wang, X., Yen, J., Kaiser, P., and Huang, L. (2010) Regulation of the 26S proteasome complex during oxidative stress. *Sci Signal* **3**, ra88

149. Shang, F., and Taylor, A. (1995) Oxidative stress and recovery from oxidative stress are associated with altered ubiquitin conjugating and proteolytic activities in bovine lens epithelial cells. *Biochem J* **307 (Pt 1)**, 297-303

150. Ishii, T., Sakurai, T., Usami, H., and Uchida, K. (2005) Oxidative modification of proteasome: identification of an oxidation-sensitive subunit in 26 S proteasome. *Biochemistry* **44**, 13893-13901

151. Bulteau, A. L., Lundberg, K. C., Humphries, K. M., Sadek, H. A., Szweda, P. A., Friguet, B., and Szweda, L. I. (2001) Oxidative modification and inactivation of the proteasome during coronary occlusion/reperfusion. *J Biol Chem* **276**, 30057-30063

152. Reinheckel, T., Sitte, N., Ullrich, O., Kuckelkorn, U., Davies, K. J., and Grune, T. (1998) Comparative resistance of the 20S and 26S proteasome to oxidative stress. *Biochem J* **335 (Pt 3)**, 637-642

153. Shang, F., Gong, X., and Taylor, A. (1997) Activity of ubiquitin-dependent pathway in response to oxidative stress. Ubiquitin-activating enzyme is transiently up-regulated. *J Biol Chem* **272**, 23086-23093

154. Kaur, J., and Debnath, J. (2015) Autophagy at the crossroads of catabolism and anabolism. *Nat Rev Mol Cell Biol* **16**, 461-472

155. Scherz-Shouval, R., and Elazar, Z. (2011) Regulation of autophagy by ROS: physiology and pathology. *Trends Biochem Sci* **36**, 30-38

156. Xiao, B., Goh, J. Y., Xiao, L., Xian, H., Lim, K. L., and Liou, Y. C. (2017) Reactive oxygen species trigger Parkin/PINK1 pathway-dependent mitophagy by inducing mitochondrial recruitment of Parkin. *J Biol Chem* **292**, 16697-16708

157. Kiffin, R., Christian, C., Knecht, E., and Cuervo, A. M. (2004) Activation of chaperone-mediated autophagy during oxidative stress. *Mol Biol Cell* **15**, 4829-4840

158. Hard, G. C. (1970) Some biochemical aspects of the immune macrophage. *Br J Exp Pathol* **51**, 97-105

159. Freemerman, A. J., Johnson, A. R., Sacks, G. N., Milner, J. J., Kirk, E. L., Troester, M. A., Macintyre, A. N., Goraksha-Hicks, P., Rathmell, J. C., and Makowski, L. (2014) Metabolic reprogramming of macrophages: glucose transporter 1 (GLUT1)-mediated glucose metabolism drives a proinflammatory phenotype. *J Biol Chem* **289**, 7884-7896

160. Tannahill, G. M., Curtis, A. M., Adamik, J., Palsson-McDermott, E. M., McGettrick, A. F., Goel, G., Frezza, C., Bernard, N. J., Kelly, B., Foley, N. H., Zheng, L., Gardet, A., Tong, Z., Jany, S. S., Corr, S. C., Haneklaus, M., Caffrey, B. E., Pierce, K., Walmsley, S., Beasley, F. C., Cummins, E., Nizet, V., Whyte, M., Taylor, C. T., Lin, H., Masters, S. L., Gottlieb, E., Kelly, V. P., Clish, C., Auron, P. E., Xavier, R. J., and O'Neill, L. A. (2013) Succinate is an inflammatory signal that induces IL-1beta through HIF-1alpha. *Nature* **496**, 238-242

161. Jha, A. K., Huang, S. C., Sergushichev, A., Lampropoulou, V., Ivanova, Y., Loginicheva, E., Chmielewski, K., Stewart, K. M., Ashall, J., Everts, B., Pearce, E. J., Driggers, E. M., and Artyomov, M. N. (2015) Network integration of parallel metabolic and transcriptional data reveals metabolic modules that regulate macrophage polarization. *Immunity* **42**, 419-430

162. Cramer, T., Yamanishi, Y., Clausen, B. E., Forster, I., Pawlinski, R., Mackman, N., Haase, V. H., Jaenisch, R., Corr, M., Nizet, V., Firestein, G. S., Gerber, H. P., Ferrara, N., and Johnson, R. S. (2003) HIF-1alpha is essential for myeloid cell-mediated inflammation. *Cell* **112**, 645-657

163. Mills, E. L., Kelly, B., Logan, A., Costa, A. S. H., Varma, M., Bryant, C. E., Tourlomousis, P., Dabritz, J. H. M., Gottlieb, E., Latorre, I., Corr, S. C., McManus, G., Ryan, D., Jacobs, H. T., Szibor, M., Xavier, R. J., Braun, T., Frezza, C., Murphy, M. P., and O'Neill, L. A. (2016) Succinate Dehydrogenase Supports Metabolic Repurposing of Mitochondria to Drive Inflammatory Macrophages. *Cell* **167**, 457-470 e413

164. van Uden, P., Kenneth, N. S., and Rocha, S. (2008) Regulation of hypoxia-inducible factor-1alpha by NF-kappaB. *Biochem J* **412**, 477-484

165. Cheng, S. C., Quintin, J., Cramer, R. A., Shepardson, K. M., Saeed, S., Kumar, V., Giamarellos-Bourboulis, E. J., Martens, J. H., Rao, N. A., Aghajanirefah, A., Manjeri, G. R., Li, Y., Ifrim, D. C., Arts, R. J., van der Veer, B. M., Deen, P. M., Logie, C., O'Neill, L. A., Willems, P., van de Veerdonk, F. L., van der Meer, J. W., Ng, A., Joosten, L. A., Wijmenga, C., Stunnenberg, H. G., Xavier, R. J., and Netea, M. G. (2014) mTOR- and HIF-1alpha-mediated aerobic glycolysis as metabolic basis for trained immunity. *Science* **345**, 1250684

166. Michl, J., Ohlbaum, D. J., and Silverstein, S. C. (1976) 2-Deoxyglucose selectively inhibits Fc and complement receptor-mediated phagocytosis in mouse peritoneal macrophages II.

Dissociation of the inhibitory effects of 2-deoxyglucose on phagocytosis and ATP generation. *J Exp Med* **144**, 1484-1493

167. Van den Bossche, J., O'Neill, L. A., and Menon, D. (2017) Macrophage Immunometabolism: Where Are We (Going)? *Trends Immunol* **38**, 395-406

168. Munder, M., Eichmann, K., and Modolell, M. (1998) Alternative metabolic states in murine macrophages reflected by the nitric oxide synthase/arginase balance: competitive regulation by CD4+ T cells correlates with Th1/Th2 phenotype. *J Immunol* **160**, 5347-5354

169. Carneiro, F. R. G., Lepelley, A., Seeley, J. J., Hayden, M. S., and Ghosh, S. (2018) An Essential Role for ECSIT in Mitochondrial Complex I Assembly and Mitophagy in Macrophages. *Cell Rep* **22**, 2654-2666

170. West, A. P., Brodsky, I. E., Rahner, C., Woo, D. K., Erdjument-Bromage, H., Tempst, P., Walsh, M. C., Choi, Y., Shadel, G. S., and Ghosh, S. (2011) TLR signalling augments macrophage bactericidal activity through mitochondrial ROS. *Nature* **472**, 476-480

171. Infantino, V., Iacobazzi, V., Menga, A., Avantaggiati, M. L., and Palmieri, F. (2014) A key role of the mitochondrial citrate carrier (SLC25A1) in TNFalpha- and IFNgamma-triggered inflammation. *Biochim Biophys Acta* **1839**, 1217-1225

172. Infantino, V., Iacobazzi, V., Palmieri, F., and Menga, A. (2013) ATP-citrate lyase is essential for macrophage inflammatory response. *Biochem Biophys Res Commun* **440**, 105-111

173. Wellen, K. E., Hatzivassiliou, G., Sachdeva, U. M., Bui, T. V., Cross, J. R., and Thompson, C. B. (2009) ATP-citrate lyase links cellular metabolism to histone acetylation. *Science* **324**, 1076-1080

174. Martin, D. B., and Vagelos, P. R. (1962) The mechanism of tricarboxylic acid cycle regulation of fatty acid synthesis. *J Biol Chem* **237**, 1787-1792

175. Strelko, C. L., Lu, W., Dufort, F. J., Seyfried, T. N., Chiles, T. C., Rabinowitz, J. D., and Roberts, M. F. (2011) Itaconic acid is a mammalian metabolite induced during macrophage activation. *J Am Chem Soc* **133**, 16386-16389

176. Michelucci, A., Cordes, T., Ghelfi, J., Pailot, A., Reiling, N., Goldmann, O., Binz, T., Wegner, A., Tallam, A., Rausell, A., Buttini, M., Linster, C. L., Medina, E., Balling, R., and Hiller, K. (2013) Immune-responsive gene 1 protein links metabolism to immunity by catalyzing itaconic acid production. *Proc Natl Acad Sci U S A* **110**, 7820-7825

177. Naujoks, J., Tabeling, C., Dill, B. D., Hoffmann, C., Brown, A. S., Kunze, M., Kempa, S., Peter, A., Mollenkopf, H. J., Dorhoi, A., Kershaw, O., Gruber, A. D., Sander, L. E., Witzenrath, M., Herold, S., Nerlich, A., Hocke, A. C., van Driel, I., Suttorp, N., Bedoui, S., Hilbi, H., Trost, M., and Opitz, B. (2016) IFNs Modify the Proteome of Legionella-

Containing Vacuoles and Restrict Infection Via IRG1-Derived Itaconic Acid. *PLoS Pathog* **12**, e1005408

178. McFadden, B. A., and Purohit, S. (1977) Itaconate, an isocitrate lyase-directed inhibitor in Pseudomonas indigofera. *J Bacteriol* **131**, 136-144

179. Lampropoulou, V., Sergushichev, A., Bambouskova, M., Nair, S., Vincent, E. E., Loginicheva, E., Cervantes-Barragan, L., Ma, X., Huang, S. C., Griss, T., Weinheimer, C. J., Khader, S., Randolph, G. J., Pearce, E. J., Jones, R. G., Diwan, A., Diamond, M. S., and Artyomov, M. N. (2016) Itaconate Links Inhibition of Succinate Dehydrogenase with Macrophage Metabolic Remodeling and Regulation of Inflammation. *Cell Metab* **24**, 158-166

180. Mills, E. L., Ryan, D. G., Prag, H. A., Dikovskaya, D., Menon, D., Zaslona, Z., Jedrychowski, M. P., Costa, A. S. H., Higgins, M., Hams, E., Szpyt, J., Runtsch, M. C., King, M. S., McGouran, J. F., Fischer, R., Kessler, B. M., McGettrick, A. F., Hughes, M. M., Carroll, R. G., Booty, L. M., Knatko, E. V., Meakin, P. J., Ashford, M. L. J., Modis, L. K., Brunori, G., Sevin, D. C., Fallon, P. G., Caldwell, S. T., Kunji, E. R. S., Chouchani, E. T., Frezza, C., Dinkova-Kostova, A. T., Hartley, R. C., Murphy, M. P., and O'Neill, L. A. (2018) Itaconate is an anti-inflammatory metabolite that activates Nrf2 via alkylation of KEAP1. *Nature* **556**, 113-117

181. Xie, Z., Dai, J., Dai, L., Tan, M., Cheng, Z., Wu, Y., Boeke, J. D., and Zhao, Y. (2012) Lysine succinylation and lysine malonylation in histones. *Mol Cell Proteomics* **11**, 100-107

182. Park, J., Chen, Y., Tishkoff, D. X., Peng, C., Tan, M., Dai, L., Xie, Z., Zhang, Y., Zwaans, B. M., Skinner, M. E., Lombard, D. B., and Zhao, Y. (2013) SIRT5-mediated lysine desuccinylation impacts diverse metabolic pathways. *Mol Cell* **50**, 919-930

183. Wang, F., Wang, K., Xu, W., Zhao, S., Ye, D., Wang, Y., Xu, Y., Zhou, L., Chu, Y., Zhang, C., Qin, X., Yang, P., and Yu, H. (2017) SIRT5 Desuccinylates and Activates Pyruvate Kinase M2 to Block Macrophage IL-1beta Production and to Prevent DSS-Induced Colitis in Mice. *Cell Rep* **19**, 2331-2344

184. Littlewood-Evans, A., Sarret, S., Apfel, V., Loesle, P., Dawson, J., Zhang, J., Muller, A., Tigani, B., Kneuer, R., Patel, S., Valeaux, S., Gommermann, N., Rubic-Schneider, T., Junt, T., and Carballido, J. M. (2016) GPR91 senses extracellular succinate released from inflammatory macrophages and exacerbates rheumatoid arthritis. *J Exp Med* **213**, 1655-1662

185. Van den Bossche, J., Baardman, J., and de Winther, M. P. (2015) Metabolic Characterization of Polarized M1 and M2 Bone Marrow-derived Macrophages Using Real-time Extracellular Flux Analysis. *J Vis Exp* 53424

186. Wang, F., Zhang, S., Vuckovic, I., Jeon, R., Lerman, A., Folmes, C. D., Dzeja, P. P., and Herrmann, J. (2018) Glycolytic Stimulation Is Not a Requirement for M2 Macrophage Differentiation. *Cell Metab* **28**, 463-475 e464

187. Odegaard, J. I., Ricardo-Gonzalez, R. R., Goforth, M. H., Morel, C. R., Subramanian, V., Mukundan, L., Red Eagle, A., Vats, D., Brombacher, F., Ferrante, A. W., and Chawla, A. (2007) Macrophage-specific PPARgamma controls alternative activation and improves insulin resistance. *Nature* **447**, 1116-1120

188. Vats, D., Mukundan, L., Odegaard, J. I., Zhang, L., Smith, K. L., Morel, C. R., Wagner, R. A., Greaves, D. R., Murray, P. J., and Chawla, A. (2006) Oxidative metabolism and PGC-1beta attenuate macrophage-mediated inflammation. *Cell Metab* **4**, 13-24

189. Liu, P. S., Wang, H., Li, X., Chao, T., Teav, T., Christen, S., Di Conza, G., Cheng, W. C., Chou, C. H., Vavakova, M., Muret, C., Debackere, K., Mazzone, M., Huang, H. D., Fendt, S. M., Ivanisevic, J., and Ho, P. C. (2017) alpha-ketoglutarate orchestrates macrophage activation through metabolic and epigenetic reprogramming. *Nat Immunol* **18**, 985-994

190. Huang, L., Nazarova, E. V., Tan, S., Liu, Y., and Russell, D. G. (2018) Growth of Mycobacterium tuberculosis in vivo segregates with host macrophage metabolism and ontogeny. *J Exp Med* **215**, 1135-1152

191. Lavrich, K. S., Speen, A. M., Ghio, A. J., Bromberg, P. A., Samet, J. M., and Alexis, N. E. (2018) Macrophages from the upper and lower human respiratory tract are metabolically distinct. *Am J Physiol Lung Cell Mol Physiol* **315**, L752-L764

192. Svedberg, F. R., Brown, S. L., Krauss, M. Z., Campbell, L., Sharpe, C., Clausen, M., Howell, G. J., Clark, H., Madsen, J., Evans, C. M., Sutherland, T. E., Ivens, A. C., Thornton, D. J., Grencis, R. K., Hussell, T., Cunoosamy, D. M., Cook, P. C., and MacDonald, A. S. (2019) The lung environment controls alveolar macrophage metabolism and responsiveness in type 2 inflammation. *Nat Immunol* **20**, 571-580

193. Woods, P. S., Kimmig, L. M., Meliton, A. Y., Sun, K. A., Tian, Y., O'Leary, E. M., Gokalp, G. A., Hamanaka, R. B., and Mutlu, G. M. (2020) Tissue-Resident Alveolar Macrophages Do Not Rely on Glycolysis for LPS-induced Inflammation. *Am J Respir Cell Mol Biol* **62**, 243-255

194. Zhang, W., Li, Q., Li, D., Li, J., Aki, D., and Liu, Y. C. (2018) The E3 ligase VHL controls alveolar macrophage function via metabolic-epigenetic regulation. *J Exp Med* **215**, 3180-3193

195. Xie, N., Cui, H., Ge, J., Banerjee, S., Guo, S., Dubey, S., Abraham, E., Liu, R. M., and Liu, G. (2017) Metabolic characterization and RNA profiling reveal glycolytic dependence of profibrotic phenotype of alveolar macrophages in lung fibrosis. *Am J Physiol Lung Cell Mol Physiol* **313**, L834-L844

196. Gleeson, L. E., Sheedy, F. J., Palsson-McDermott, E. M., Triglia, D., O'Leary, S. M., O'Sullivan, M. P., O'Neill, L. A., and Keane, J. (2016) Cutting Edge: Mycobacterium tuberculosis Induces Aerobic Glycolysis in Human Alveolar Macrophages That Is Required for Control of Intracellular Bacillary Replication. *J Immunol* **196**, 2444-2449

197. Raposo, G., and Stoorvogel, W. (2013) Extracellular vesicles: exosomes, microvesicles, and friends. *J Cell Biol* **200**, 373-383

198. Pitt, J. M., Kroemer, G., and Zitvogel, L. (2016) Extracellular vesicles: masters of intercellular communication and potential clinical interventions. *J Clin Invest* **126**, 1139-1143

199. Kosmidou, I., Vassilakopoulos, T., Xagorari, A., Zakynthinos, S., Papapetropoulos, A., and Roussos, C. (2002) Production of interleukin-6 by skeletal myotubes: role of reactive oxygen species. *Am J Respir Cell Mol Biol* **26**, 587-593

200. Yoon, S., Woo, S. U., Kang, J. H., Kim, K., Kwon, M. H., Park, S., Shin, H. J., Gwak, H. S., and Chwae, Y. J. (2010) STAT3 transcriptional factor activated by reactive oxygen species induces IL6 in starvation-induced autophagy of cancer cells. *Autophagy* **6**, 1125-1138

201. Paramore, A., and Frantz, S. (2003) Bortezomib. *Nat Rev Drug Discov* **2**, 611-612

202. Huang, Z., Wu, Y., Zhou, X., Xu, J., Zhu, W., Shu, Y., and Liu, P. (2014) Efficacy of therapy with bortezomib in solid tumors: a review based on 32 clinical trials. *Future Oncol* **10**, 1795-1807

203. Zarfati, M., Avivi, I., Brenner, B., Katz, T., and Aharon, A. (2019) Extracellular vesicles of multiple myeloma cells utilize the proteasome inhibitor mechanism to moderate endothelial angiogenesis. *Angiogenesis* **22**, 185-196

204. Phipps, J. C., Aronoff, D. M., Curtis, J. L., Goel, D., O'Brien, E., and Mancuso, P. (2010) Cigarette smoke exposure impairs pulmonary bacterial clearance and alveolar macrophage complement-mediated phagocytosis of Streptococcus pneumoniae. *Infect Immun* **78**, 1214-1220

205. Peters-Golden, M., and Thebert, P. (1987) Inhibition by methylprednisolone of zymosan-induced leukotriene synthesis in alveolar macrophages. *Am Rev Respir Dis* **135**, 1020-1026

206. Doyle, L. M., and Wang, M. Z. (2019) Overview of Extracellular Vesicles, Their Origin, Composition, Purpose, and Methods for Exosome Isolation and Analysis. *Cells* **8**, 727

207. Scott, A., Lugg, S. T., Aldridge, K., Lewis, K. E., Bowden, A., Mahida, R. Y., Grudzinska, F. S., Dosanjh, D., Parekh, D., Foronjy, R., Sapey, E., Naidu, B., and Thickett, D. R. (2018) Pro-inflammatory effects of e-cigarette vapour condensate on human alveolar macrophages. *Thorax* **73**, 1161-1169

208. Wang, H., and Joseph, J. A. (1999) Quantifying cellular oxidative stress by dichlorofluorescein assay using microplate reader. *Free Radic Biol Med* **27**, 612-616

209. Pryor, W. A., Prier, D. G., and Church, D. F. (1983) Electron-spin resonance study of mainstream and sidestream cigarette smoke: nature of the free radicals in gas-phase smoke and in cigarette tar. *Environ Health Perspect* **47**, 345-355

210. Pryor, W. A., Terauchi, K., and Davis, W. H., Jr. (1976) Electron spin resonance (ESR) study of cigarette smoke by use of spin trapping techniques. *Environ Health Perspect* **16**, 161-176

211. Valavanidis, A., and Haralambous, E. (2001) A comparative study by electron paramagnetic resonance of free radical species in the mainstream and sidestream smoke of cigarettes with conventional acetate filters and 'bio-filters'. *Redox Rep* **6**, 161-171

212. van der Toorn, M., Rezayat, D., Kauffman, H. F., Bakker, S. J., Gans, R. O., Koeter, G. H., Choi, A. M., van Oosterhout, A. J., and Slebos, D. J. (2009) Lipid-soluble components in cigarette smoke induce mitochondrial production of reactive oxygen species in lung epithelial cells. *Am J Physiol Lung Cell Mol Physiol* **297**, L109-114

213. Malinska, D., Szymanski, J., Patalas-Krawczyk, P., Michalska, B., Wojtala, A., Prill, M., Partyka, M., Drabik, K., Walczak, J., Sewer, A., Johne, S., Luettich, K., Peitsch, M. C., Hoeng, J., Duszynski, J., Szczepanowska, J., van der Toorn, M., and Wieckowski, M. R. (2018) Assessment of mitochondrial function following short- and long-term exposure of human bronchial epithelial cells to total particulate matter from a candidate modified-risk tobacco product and reference cigarettes. *Food Chem Toxicol* **115**, 1-12

214. Shih, R. H., Cheng, S. E., Hsiao, L. D., Kou, Y. R., and Yang, C. M. (2011) Cigarette smoke extract upregulates heme oxygenase-1 via PKC/NADPH oxidase/ROS/PDGFR/PI3K/Akt pathway in mouse brain endothelial cells. *J Neuroinflammation* **8**, 104

215. Starke, R. M., Thompson, J. W., Ali, M. S., Pascale, C. L., Martinez Lege, A., Ding, D., Chalouhi, N., Hasan, D. M., Jabbour, P., Owens, G. K., Toborek, M., Hare, J. M., and Dumont, A. S. (2018) Cigarette Smoke Initiates Oxidative Stress-Induced Cellular Phenotypic Modulation Leading to Cerebral Aneurysm Pathogenesis. *Arterioscler Thromb Vasc Biol* **38**, 610-621

216. Asano, H., Horinouchi, T., Mai, Y., Sawada, O., Fujii, S., Nishiya, T., Minami, M., Katayama, T., Iwanaga, T., Terada, K., and Miwa, S. (2012) Nicotine- and tar-free cigarette smoke induces cell damage through reactive oxygen species newly generated by PKC-dependent activation of NADPH oxidase. *J Pharmacol Sci* **118**, 275-287

217. Jaimes, E. A., DeMaster, E. G., Tian, R. X., and Raij, L. (2004) Stable compounds of cigarette smoke induce endothelial superoxide anion production via NADPH oxidase activation. *Arterioscler Thromb Vasc Biol* **24**, 1031-1036

218. Li, C. J., Liu, Y., Chen, Y., Yu, D., Williams, K. J., and Liu, M. L. (2013) Novel proteolytic microvesicles released from human macrophages after exposure to tobacco smoke. *Am J Pathol* **182**, 1552-1562

219. Li, M., Yu, D., Williams, K. J., and Liu, M. L. (2010) Tobacco smoke induces the generation of procoagulant microvesicles from human monocytes/macrophages. *Arterioscler Thromb Vasc Biol* **30**, 1818-1824

220. Jackson, C. E., Scruggs, B. S., Schaffer, J. E., and Hanson, P. I. (2017) Effects of Inhibiting VPS4 Support a General Role for ESCRTs in Extracellular Vesicle Biogenesis. *Biophys J* **113**, 1342-1352

221. Hedlund, M., Nagaeva, O., Kargl, D., Baranov, V., and Mincheva-Nilsson, L. (2011) Thermal- and oxidative stress causes enhanced release of NKG2D ligand-bearing immunosuppressive exosomes in leukemia/lymphoma T and B cells. *PLoS One* **6**, e16899

222. Harmati, M., Gyukity-Sebestyen, E., Dobra, G., Janovak, L., Dekany, I., Saydam, O., Hunyadi-Gulyas, E., Nagy, I., Farkas, A., Pankotai, T., Ujfaludi, Z., Horvath, P., Piccinini, F., Kovacs, M., Biro, T., and Buzas, K. (2019) Small extracellular vesicles convey the stress-induced adaptive responses of melanoma cells. *Sci Rep* **9**, 15329

223. Saeed-Zidane, M., Linden, L., Salilew-Wondim, D., Held, E., Neuhoff, C., Tholen, E., Hoelker, M., Schellander, K., and Tesfaye, D. (2017) Cellular and exosome mediated molecular defense mechanism in bovine granulosa cells exposed to oxidative stress. *PLoS One* **12**, e0187569

224. Wang, Q., Yu, J., Kadungure, T., Beyene, J., Zhang, H., and Lu, Q. (2018) ARMMs as a versatile platform for intracellular delivery of macromolecules. *Nat Commun* **9**, 960

225. Zhang, X., Zhou, J., Fernandes, A. F., Sparrow, J. R., Pereira, P., Taylor, A., and Shang, F. (2008) The proteasome: a target of oxidative damage in cultured human retina pigment epithelial cells. *Invest Ophthalmol Vis Sci* **49**, 3622-3630

226. Yu, C., Wang, X., Huszagh, A. S., Viner, R., Novitsky, E., Rychnovsky, S. D., and Huang, L. (2019) Probing H2O2-mediated Structural Dynamics of the Human 26S Proteasome Using Quantitative Cross-linking Mass Spectrometry (QXL-MS). *Mol Cell Proteomics* **18**, 954-967

227. Kisselev, A. F., Callard, A., and Goldberg, A. L. (2006) Importance of the different proteolytic sites of the proteasome and the efficacy of inhibitors varies with the protein substrate. *J Biol Chem* **281**, 8582-8590

228. Soni, S., O'Dea, K. P., Tan, Y. Y., Cho, K., Abe, E., Romano, R., Cui, J., Ma, D., Sarathchandra, P., Wilson, M. R., and Takata, M. (2019) ATP redirects cytokine trafficking and promotes novel membrane TNF signaling via microvesicles. *FASEB J* **33**, 6442-6455

229. Eldh, M., Ekstrom, K., Valadi, H., Sjostrand, M., Olsson, B., Jernas, M., and Lotvall, J. (2010) Exosomes communicate protective messages during oxidative stress; possible role of exosomal shuttle RNA. *PLoS One* **5**, e15353

230. Xiao, J., Pan, Y., Li, X. H., Yang, X. Y., Feng, Y. L., Tan, H. H., Jiang, L., Feng, J., and Yu, X. Y. (2016) Cardiac progenitor cell-derived exosomes prevent cardiomyocytes apoptosis through exosomal miR-21 by targeting PDCD4. *Cell Death Dis* **7**, e2277

231. Grindheim, A. K., Hollas, H., Raddum, A. M., Saraste, J., and Vedeler, A. (2016) Reactive oxygen species exert opposite effects on Tyr23 phosphorylation of the nuclear and cortical pools of annexin A2. *J Cell Sci* **129**, 314-328

232. Kennedy-Feitosa, E., Pinto, R. F., Pires, K. M., Monteiro, A. P., Machado, M. N., Santos, J. C., Ribeiro, M. L., Zin, W. A., Canetti, C. A., Romana-Souza, B., Porto, L. C., and Valenca, S. S. (2014) The influence of 5-lipoxygenase on cigarette smoke-induced emphysema in mice. *Biochim Biophys Acta* **1840**, 199-208

233. Kayyali, U. S., Budhiraja, R., Pennella, C. M., Cooray, S., Lanzillo, J. J., Chalkley, R., and Hassoun, P. M. (2003) Upregulation of xanthine oxidase by tobacco smoke condensate in pulmonary endothelial cells. *Toxicol Appl Pharmacol* **188**, 59-68

234. Kim, B. S., Serebreni, L., Hamdan, O., Wang, L., Parniani, A., Sussan, T., Scott Stephens, R., Boyer, L., Damarla, M., Hassoun, P. M., and Damico, R. (2013) Xanthine oxidoreductase is a critical mediator of cigarette smoke-induced endothelial cell DNA damage and apoptosis. *Free Radic Biol Med* **60**, 336-346

235. Jorgensen, E., Stinson, A., Shan, L., Yang, J., Gietl, D., and Albino, A. P. (2008) Cigarette smoke induces endoplasmic reticulum stress and the unfolded protein response in normal and malignant human lung cells. *BMC Cancer* **8**, 229

236. Tagawa, Y., Hiramatsu, N., Kasai, A., Hayakawa, K., Okamura, M., Yao, J., and Kitamura, M. (2008) Induction of apoptosis by cigarette smoke via ROS-dependent endoplasmic reticulum stress and CCAAT/enhancer-binding protein-homologous protein (CHOP). *Free Radic Biol Med* **45**, 50-59

237. Tucher, C., Bode, K., Schiller, P., Classen, L., Birr, C., Souto-Carneiro, M. M., Blank, N., Lorenz, H. M., and Schiller, M. (2018) Extracellular Vesicle Subtypes Released From Activated or Apoptotic T-Lymphocytes Carry a Specific and Stimulus-Dependent Protein Cargo. *Front Immunol* **9**, 534

238. Dieude, M., Bell, C., Turgeon, J., Beillevaire, D., Pomerleau, L., Yang, B., Hamelin, K., Qi, S., Pallet, N., Beland, C., Dhahri, W., Cailhier, J. F., Rousseau, M., Duchez, A. C., Levesque, T., Lau, A., Rondeau, C., Gingras, D., Muruve, D., Rivard, A., Cardinal, H., Perreault, C., Desjardins, M., Boilard, E., Thibault, P., and Hebert, M. J. (2015) The 20S proteasome core, active within apoptotic exosome-like vesicles, induces autoantibody production and accelerates rejection. *Sci Transl Med* **7**, 318ra200

239. Lai, R. C., Tan, S. S., Teh, B. J., Sze, S. K., Arslan, F., de Kleijn, D. P., Choo, A., and Lim, S. K. (2012) Proteolytic Potential of the MSC Exosome Proteome: Implications for an Exosome-Mediated Delivery of Therapeutic Proteasome. *Int J Proteomics* **2012**, 971907

240. Bochmann, I., Ebstein, F., Lehmann, A., Wohlschlaeger, J., Sixt, S. U., Kloetzel, P. M., and Dahlmann, B. (2014) T lymphocytes export proteasomes by way of microparticles: a possible mechanism for generation of extracellular proteasomes. *J Cell Mol Med* **18**, 59-68

241. Hideshima, T., Richardson, P., Chauhan, D., Palombella, V. J., Elliott, P. J., Adams, J., and Anderson, K. C. (2001) The proteasome inhibitor PS-341 inhibits growth, induces apoptosis, and overcomes drug resistance in human multiple myeloma cells. *Cancer Res* **61**, 3071-3076

242. Mutlu, G. M., Budinger, G. R., Wu, M., Lam, A. P., Zirk, A., Rivera, S., Urich, D., Chiarella, S. E., Go, L. H., Ghosh, A. K., Selman, M., Pardo, A., Varga, J., Kamp, D. W., Chandel, N. S., Sznajder, J. I., and Jain, M. (2012) Proteasomal inhibition after injury prevents fibrosis by modulating TGF-beta(1) signalling. *Thorax* **67**, 139-146

243. Zeniya, M., Mori, T., Yui, N., Nomura, N., Mandai, S., Isobe, K., Chiga, M., Sohara, E., Rai, T., and Uchida, S. (2017) The proteasome inhibitor bortezomib attenuates renal fibrosis in mice via the suppression of TGF-beta1. *Sci Rep* **7**, 13086

244. Koca, S. S., Ozgen, M., Dagli, F., Tuzcu, M., Ozercan, I. H., Sahin, K., and Isik, A. (2012) Proteasome inhibition prevents development of experimental dermal fibrosis. *Inflammation* **35**, 810-817

245. Murrow, L., Malhotra, R., and Debnath, J. (2015) ATG12-ATG3 interacts with Alix to promote basal autophagic flux and late endosome function. *Nat Cell Biol* **17**, 300-310

246. Chen, Y., Azad, M. B., and Gibson, S. B. (2009) Superoxide is the major reactive oxygen species regulating autophagy. *Cell Death Differ* **16**, 1040-1052

247. Scherz-Shouval, R., Shvets, E., Fass, E., Shorer, H., Gil, L., and Elazar, Z. (2019) Reactive oxygen species are essential for autophagy and specifically regulate the activity of Atg4. *EMBO J* **38**, e101812

248. Chen, Y., McMillan-Ward, E., Kong, J., Israels, S. J., and Gibson, S. B. (2007) Mitochondrial electron-transport-chain inhibitors of complexes I and II induce autophagic cell death mediated by reactive oxygen species. *J Cell Sci* **120**, 4155-4166

249. Selimovic, D., Porzig, B. B., El-Khattouti, A., Badura, H. E., Ahmad, M., Ghanjati, F., Santourlidis, S., Haikel, Y., and Hassan, M. (2013) Bortezomib/proteasome inhibitor triggers both apoptosis and autophagy-dependent pathways in melanoma cells. *Cell Signal* **25**, 308-318

250. Chang, I., and Wang, C. Y. (2016) Inhibition of HDAC6 Protein Enhances Bortezomib-induced Apoptosis in Head and Neck Squamous Cell Carcinoma (HNSCC) by Reducing Autophagy. *J Biol Chem* **291**, 18199-18209

251. Haggadone, M. D., and Peters-Golden, M. (2018) Microenvironmental Influences on Extracellular Vesicle-Mediated Communication in the Lung. *Trends Mol Med* **24**, 963-975

252. Choudhuri, K., Llodra, J., Roth, E. W., Tsai, J., Gordo, S., Wucherpfennig, K. W., Kam, L. C., Stokes, D. L., and Dustin, M. L. (2014) Polarized release of T-cell-receptor-enriched microvesicles at the immunological synapse. *Nature* **507**, 118-123

253. Thery, C., Zitvogel, L., and Amigorena, S. (2002) Exosomes: composition, biogenesis and function. *Nat Rev Immunol* **2**, 569-579

254. Haggadone, M. D., Mancuso, P., and Peters-Golden, M. (2020) Oxidative Inactivation of the Proteasome Augments Alveolar Macrophage Secretion of Vesicular SOCS3. *Cells* **9**, 1589

255. Ryan, D. G., and O'Neill, L. A. J. (2020) Krebs Cycle Reborn in Macrophage Immunometabolism. *Annu Rev Immunol* **38**, 289-313

256. Fan, S. J., Kroeger, B., Marie, P. P., Bridges, E. M., Mason, J. D., McCormick, K., Zois, C. E., Sheldon, H., Khalid Alham, N., Johnson, E., Ellis, M., Stefana, M. I., Mendes, C. C., Wainwright, S. M., Cunningham, C., Hamdy, F. C., Morris, J. F., Harris, A. L., Wilson, C., and Goberdhan, D. C. (2020) Glutamine deprivation alters the origin and function of cancer cell exosomes. *EMBO J* **39**, e103009

257. Santana, S. M., Antonyak, M. A., Cerione, R. A., and Kirby, B. J. (2014) Cancerous epithelial cell lines shed extracellular vesicles with a bimodal size distribution that is sensitive to glutamine inhibition. *Phys Biol* **11**, 065001

258. Dorai, T., Shah, A., Summers, F., Mathew, R., Huang, J., Hsieh, T. C., and Wu, J. M. (2018) NRH:quinone oxidoreductase 2 (NQO2) and glutaminase (GLS) both play a role in large extracellular vesicles (LEV) formation in preclinical LNCaP-C4-2B prostate cancer model of progressive metastasis. *Prostate* **78**, 1181-1195

259. Wei, Y., Wang, D., Jin, F., Bian, Z., Li, L., Liang, H., Li, M., Shi, L., Pan, C., Zhu, D., Chen, X., Hu, G., Liu, Y., Zhang, C. Y., and Zen, K. (2017) Pyruvate kinase type M2 promotes tumour cell exosome release via phosphorylating synaptosome-associated protein 23. *Nat Commun* **8**, 14041

260. Song, Y. H., Warncke, C., Choi, S. J., Choi, S., Chiou, A. E., Ling, L., Liu, H. Y., Daniel, S., Antonyak, M. A., Cerione, R. A., and Fischbach, C. (2017) Breast cancer-derived extracellular vesicles stimulate myofibroblast differentiation and pro-angiogenic behavior of adipose stem cells. *Matrix Biol* **60-61**, 190-205

261. Hamilton, J. A. (2008) Colony-stimulating factors in inflammation and autoimmunity. *Nat Rev Immunol* **8**, 533-544

262. Kitamura, T., Tanaka, N., Watanabe, J., Uchida, Kanegasaki, S., Yamada, Y., and Nakata, K. (1999) Idiopathic pulmonary alveolar proteinosis as an autoimmune disease with neutralizing antibody against granulocyte/macrophage colony-stimulating factor. *J Exp Med* **190**, 875-880

263. Liu, X., Boyer, M. A., Holmgren, A. M., and Shin, S. (2020) Legionella-Infected Macrophages Engage the Alveolar Epithelium to Metabolically Reprogram Myeloid Cells and Promote Antibacterial Inflammation. *Cell Host Microbe* **28**, 683-698 e686

264. Na, Y. R., Gu, G. J., Jung, D., Kim, Y. W., Na, J., Woo, J. S., Cho, J. Y., Youn, H., and Seok, S. H. (2016) GM-CSF Induces Inflammatory Macrophages by Regulating Glycolysis and Lipid Metabolism. *J Immunol* **197**, 4101-4109

265. Sheih, A., Parks, W. C., and Ziegler, S. F. (2017) GM-CSF produced by the airway epithelium is required for sensitization to cockroach allergen. *Mucosal Immunol* **10**, 705-715

266. Nobs, S. P., Kayhan, M., and Kopf, M. (2019) GM-CSF intrinsically controls eosinophil accumulation in the setting of allergic airway inflammation. *J Allergy Clin Immunol* **143**, 1513-1524 e1512

267. Su, Y. C., Rolph, M. S., Hansbro, N. G., Mackay, C. R., and Sewell, W. A. (2008) Granulocyte-macrophage colony-stimulating factor is required for bronchial eosinophilia in a murine model of allergic airway inflammation. *J Immunol* **180**, 2600-2607

268. Draijer, C., Penke, L. R. K., and Peters-Golden, M. (2019) Distinctive Effects of GM-CSF and M-CSF on Proliferation and Polarization of Two Major Pulmonary Macrophage Populations. *J Immunol* **202**, 2700-2709

269. Deng, W., Yang, J., Lin, X., Shin, J., Gao, J., and Zhong, X. P. (2017) Essential Role of mTORC1 in Self-Renewal of Murine Alveolar Macrophages. *J Immunol* **198**, 492-504

270. Chen, B. D., Mueller, M., and Chou, T. H. (1988) Role of granulocyte/macrophage colony-stimulating factor in the regulation of murine alveolar macrophage proliferation and differentiation. *J Immunol* **141**, 139-144

271. Akagawa, K. S., Kamoshita, K., and Tokunaga, T. (1988) Effects of granulocyte-macrophage colony-stimulating factor and colony-stimulating factor-1 on the proliferation and differentiation of murine alveolar macrophages. *J Immunol* **141**, 3383-3390

272. Berclaz, P. Y., Shibata, Y., Whitsett, J. A., and Trapnell, B. C. (2002) GM-CSF, via PU.1, regulates alveolar macrophage Fcgamma R-mediated phagocytosis and the IL-18/IFN-

gamma -mediated molecular connection between innate and adaptive immunity in the lung. *Blood* **100**, 4193-4200

273. Infantino, V., Convertini, P., Cucci, L., Panaro, M. A., Di Noia, M. A., Calvello, R., Palmieri, F., and Iacobazzi, V. (2011) The mitochondrial citrate carrier: a new player in inflammation. *Biochem J* **438**, 433-436

274. Everts, B., Amiel, E., Huang, S. C., Smith, A. M., Chang, C. H., Lam, W. Y., Redmann, V., Freitas, T. C., Blagih, J., van der Windt, G. J., Artyomov, M. N., Jones, R. G., Pearce, E. L., and Pearce, E. J. (2014) TLR-driven early glycolytic reprogramming via the kinases TBK1-IKKvarepsilon supports the anabolic demands of dendritic cell activation. *Nat Immunol* **15**, 323-332

275. Na, Y. R., Hong, J. H., Lee, M. Y., Jung, J. H., Jung, D., Kim, Y. W., Son, D., Choi, M., Kim, K. P., and Seok, S. H., 2nd. (2015) Proteomic Analysis Reveals Distinct Metabolic Differences Between Granulocyte-Macrophage Colony Stimulating Factor (GM-CSF) and Macrophage Colony Stimulating Factor (M-CSF) Grown Macrophages Derived from Murine Bone Marrow Cells. *Mol Cell Proteomics* **14**, 2722-2732

276. Hatzivassiliou, G., Zhao, F., Bauer, D. E., Andreadis, C., Shaw, A. N., Dhanak, D., Hingorani, S. R., Tuveson, D. A., and Thompson, C. B. (2005) ATP citrate lyase inhibition can suppress tumor cell growth. *Cancer Cell* **8**, 311-321

277. Bauer, D. E., Hatzivassiliou, G., Zhao, F., Andreadis, C., and Thompson, C. B. (2005) ATP citrate lyase is an important component of cell growth and transformation. *Oncogene* **24**, 6314-6322

278. Vysochan, A., Sengupta, A., Weljie, A. M., Alwine, J. C., and Yu, Y. (2017) ACSS2-mediated acetyl-CoA synthesis from acetate is necessary for human cytomegalovirus infection. *Proc Natl Acad Sci U S A* **114**, E1528-E1535

279. Comerford, S. A., Huang, Z., Du, X., Wang, Y., Cai, L., Witkiewicz, A. K., Walters, H., Tantawy, M. N., Fu, A., Manning, H. C., Horton, J. D., Hammer, R. E., McKnight, S. L., and Tu, B. P. (2014) Acetate dependence of tumors. *Cell* **159**, 1591-1602

280. Li, X., Yu, W., Qian, X., Xia, Y., Zheng, Y., Lee, J. H., Li, W., Lyu, J., Rao, G., Zhang, X., Qian, C. N., Rozen, S. G., Jiang, T., and Lu, Z. (2017) Nucleus-Translocated ACSS2 Promotes Gene Transcription for Lysosomal Biogenesis and Autophagy. *Mol Cell* **66**, 684-697 e689

281. Schug, Z. T., Peck, B., Jones, D. T., Zhang, Q., Grosskurth, S., Alam, I. S., Goodwin, L. M., Smethurst, E., Mason, S., Blyth, K., McGarry, L., James, D., Shanks, E., Kalna, G., Saunders, R. E., Jiang, M., Howell, M., Lassailly, F., Thin, M. Z., Spencer-Dene, B., Stamp, G., van den Broek, N. J., Mackay, G., Bulusu, V., Kamphorst, J. J., Tardito, S., Strachan, D., Harris, A. L., Aboagye, E. O., Critchlow, S. E., Wakelam, M. J., Schulze, A.,

and Gottlieb, E. (2015) Acetyl-CoA synthetase 2 promotes acetate utilization and maintains cancer cell growth under metabolic stress. *Cancer Cell* **27**, 57-71

282. Mashimo, T., Pichumani, K., Vemireddy, V., Hatanpaa, K. J., Singh, D. K., Sirasanagandla, S., Nannepaga, S., Piccirillo, S. G., Kovacs, Z., Foong, C., Huang, Z., Barnett, S., Mickey, B. E., DeBerardinis, R. J., Tu, B. P., Maher, E. A., and Bachoo, R. M. (2014) Acetate is a bioenergetic substrate for human glioblastoma and brain metastases. *Cell* **159**, 1603-1614

283. Garnett, J. P., Baker, E. H., and Baines, D. L. (2012) Sweet talk: insights into the nature and importance of glucose transport in lung epithelium. *Eur Respir J* **40**, 1269-1276

284. Baker, E. H., and Baines, D. L. (2018) Airway Glucose Homeostasis: A New Target in the Prevention and Treatment of Pulmonary Infection. *Chest* **153**, 507-514

285. Baker, E. H., Clark, N., Brennan, A. L., Fisher, D. A., Gyi, K. M., Hodson, M. E., Philips, B. J., Baines, D. L., and Wood, D. M. (2007) Hyperglycemia and cystic fibrosis alter respiratory fluid glucose concentrations estimated by breath condensate analysis. *J Appl Physiol (1985)* **102**, 1969-1975

286. Saumon, G., Martet, G., and Loiseau, P. (1996) Glucose transport and equilibrium across alveolar-airway barrier of rat. *Am J Physiol* **270**, L183-190

287. Barker, P. M., Boyd, C. A., Ramsden, C. A., Strang, L. B., and Walters, D. V. (1989) Pulmonary glucose transport in the fetal sheep. *J Physiol* **409**, 15-27

288. Martinez-Reyes, I., and Chandel, N. S. (2020) Mitochondrial TCA cycle metabolites control physiology and disease. *Nat Commun* **11**, 102

289. Pietrocola, F., Galluzzi, L., Bravo-San Pedro, J. M., Madeo, F., and Kroemer, G. (2015) Acetyl coenzyme A: a central metabolite and second messenger. *Cell Metab* **21**, 805-821

290. Sinha, A., Ignatchenko, V., Ignatchenko, A., Mejia-Guerrero, S., and Kislinger, T. (2014) In-depth proteomic analyses of ovarian cancer cell line exosomes reveals differential enrichment of functional categories compared to the NCI 60 proteome. *Biochem Biophys Res Commun* **445**, 694-701

291. Li, Z., Zhuang, M., Zhang, L., Zheng, X., Yang, P., and Li, Z. (2016) Acetylation modification regulates GRP78 secretion in colon cancer cells. *Sci Rep* **6**, 30406

292. Mullen, A. R., Wheaton, W. W., Jin, E. S., Chen, P. H., Sullivan, L. B., Cheng, T., Yang, Y., Linehan, W. M., Chandel, N. S., and DeBerardinis, R. J. (2011) Reductive carboxylation supports growth in tumour cells with defective mitochondria. *Nature* **481**, 385-388

293. Gaude, E., Schmidt, C., Gammage, P. A., Dugourd, A., Blacker, T., Chew, S. P., Saez-Rodriguez, J., O'Neill, J. S., Szabadkai, G., Minczuk, M., and Frezza, C. (2018) NADH Shuttling Couples Cytosolic Reductive Carboxylation of Glutamine with Glycolysis in Cells with Mitochondrial Dysfunction. *Mol Cell* **69**, 581-593 e587

294. Trefely, S., Lovell, C. D., Snyder, N. W., and Wellen, K. E. (2020) Compartmentalised acyl-CoA metabolism and roles in chromatin regulation. *Mol Metab* **38**, 100941

295. Hugel, B., Martinez, M. C., Kunzelmann, C., and Freyssinet, J. M. (2005) Membrane microparticles: two sides of the coin. *Physiology (Bethesda)* **20**, 22-27

296. Manasanch, E. E., and Orlowski, R. Z. (2017) Proteasome inhibitors in cancer therapy. *Nat Rev Clin Oncol* **14**, 417-433

297. Boroughs, L. K., and DeBerardinis, R. J. (2015) Metabolic pathways promoting cancer cell survival and growth. *Nat Cell Biol* **17**, 351-359

298. Carnino, J. M., Ni, K., and Jin, Y. (2020) Post-translational Modification Regulates Formation and Cargo-Loading of Extracellular Vesicles. *Front Immunol* **11**, 948

299. Salazar, G., Craige, B., Styers, M. L., Newell-Litwa, K. A., Doucette, M. M., Wainer, B. H., Falcon-Perez, J. M., Dell'Angelica, E. C., Peden, A. A., Werner, E., and Faundez, V. (2006) BLOC-1 complex deficiency alters the targeting of adaptor protein complex-3 cargoes. *Mol Biol Cell* **17**, 4014-4026

300. Wang, X., Shen, H., Zhangyuan, G., Huang, R., Zhang, W., He, Q., Jin, K., Zhuo, H., Zhang, Z., Wang, J., Sun, B., and Lu, X. (2018) 14-3-3zeta delivered by hepatocellular carcinoma-derived exosomes impaired anti-tumor function of tumor-infiltrating T lymphocytes. *Cell Death Dis* **9**, 159

301. Nakatogawa, H., Ichimura, Y., and Ohsumi, Y. (2007) Atg8, a ubiquitin-like protein required for autophagosome formation, mediates membrane tethering and hemifusion. *Cell* **130**, 165-178

302. Ichimura, Y., Kirisako, T., Takao, T., Satomi, Y., Shimonishi, Y., Ishihara, N., Mizushima, N., Tanida, I., Kominami, E., Ohsumi, M., Noda, T., and Ohsumi, Y. (2000) A ubiquitin-like system mediates protein lipidation. *Nature* **408**, 488-492

303. Pankiv, S., Alemu, E. A., Brech, A., Bruun, J. A., Lamark, T., Overvatn, A., Bjorkoy, G., and Johansen, T. (2010) FYCO1 is a Rab7 effector that binds to LC3 and PI3P to mediate microtubule plus end-directed vesicle transport. *J Cell Biol* **188**, 253-269

304. Gao, Z., Gammoh, N., Wong, P. M., Erdjument-Bromage, H., Tempst, P., and Jiang, X. (2010) Processing of autophagic protein LC3 by the 20S proteasome. *Autophagy* **6**, 126-137

305. Li, C., Wang, X., Li, X., Qiu, K., Jiao, F., Liu, Y., Kong, Q., Liu, Y., and Wu, Y. (2019) Proteasome Inhibition Activates Autophagy-Lysosome Pathway Associated With TFEB Dephosphorylation and Nuclear Translocation. *Front Cell Dev Biol* **7**, 170

306. Song, T., Su, H., Yin, W., Wang, L., and Huang, R. (2019) Acetylation modulates LC3 stability and cargo recognition. *FEBS Lett* **593**, 414-422

307. Huang, R., Xu, Y., Wan, W., Shou, X., Qian, J., You, Z., Liu, B., Chang, C., Zhou, T., Lippincott-Schwartz, J., and Liu, W. (2015) Deacetylation of nuclear LC3 drives autophagy initiation under starvation. *Mol Cell* **57**, 456-466

308. Shi, D. Y., Xie, F. Z., Zhai, C., Stern, J. S., Liu, Y., and Liu, S. L. (2009) The role of cellular oxidative stress in regulating glycolysis energy metabolism in hepatoma cells. *Mol Cancer* **8**, 32

309. Jung, S. N., Yang, W. K., Kim, J., Kim, H. S., Kim, E. J., Yun, H., Park, H., Kim, S. S., Choe, W., Kang, I., and Ha, J. (2008) Reactive oxygen species stabilize hypoxia-inducible factor-1 alpha protein and stimulate transcriptional activity via AMP-activated protein kinase in DU145 human prostate cancer cells. *Carcinogenesis* **29**, 713-721

310. Zhu, B., Wu, Y., Huang, S., Zhang, R., Son, Y. M., Li, C., Cheon, I. S., Gao, X., Wang, M., Chen, Y., Zhou, X., Nguyen, Q., Phan, A. T., Behl, S., Taketo, M. M., Mack, M., Shapiro, V. S., Zeng, H., Ebihara, H., Mullon, J. J., Edell, E. S., Reisenauer, J. S., Demirel, N., Kern, R. M., Chakraborty, R., Cui, W., Kaplan, M. H., Zhou, X., Goldrath, A. W., and Sun, J. (2021) Uncoupling of macrophage inflammation from self-renewal modulates host recovery from respiratory viral infection. *Immunity* **54**, 1200-1218 e1209

311. Wang, Z., Li, W., Guo, Q., Wang, Y., Ma, L., and Zhang, X. (2018) Insulin-Like Growth Factor-1 Signaling in Lung Development and Inflammatory Lung Diseases. *Biomed Res Int* **2018**, 6057589

312. Piguet, P. F., Collart, M. A., Grau, G. E., Kapanci, Y., and Vassalli, P. (1989) Tumor necrosis factor/cachectin plays a key role in bleomycin-induced pneumopathy and fibrosis. *J Exp Med* **170**, 655-663

313. Jeong, J. W., Bae, M. K., Ahn, M. Y., Kim, S. H., Sohn, T. K., Bae, M. H., Yoo, M. A., Song, E. J., Lee, K. J., and Kim, K. W. (2002) Regulation and destabilization of HIF-1alpha by ARD1-mediated acetylation. *Cell* **111**, 709-720

314. Tuder, R. M., Yun, J. H., Bhunia, A., and Fijalkowska, I. (2007) Hypoxia and chronic lung disease. *J Mol Med (Berl)* **85**, 1317-1324

315. Daijo, H., Hoshino, Y., Kai, S., Suzuki, K., Nishi, K., Matsuo, Y., Harada, H., and Hirota, K. (2016) Cigarette smoke reversibly activates hypoxia-inducible factor 1 in a reactive oxygen species-dependent manner. *Sci Rep* **6**, 34424

316. Vlahos, R., Bozinovski, S., Chan, S. P., Ivanov, S., Linden, A., Hamilton, J. A., and Anderson, G. P. (2010) Neutralizing granulocyte/macrophage colony-stimulating factor inhibits cigarette smoke-induced lung inflammation. *Am J Respir Crit Care Med* **182**, 34-40

317. O'Beirne, S. L., Kikkers, S. A., Oromendia, C., Salit, J., Rostmai, M. R., Ballman, K. V., Kaner, R. J., Crystal, R. G., and Cloonan, S. M. (2020) Alveolar Macrophage Immunometabolism and Lung Function Impairment in Smoking and Chronic Obstructive Pulmonary Disease. *Am J Respir Crit Care Med* **201**, 735-739

318. Bronte, V., Chappell, D. B., Apolloni, E., Cabrelle, A., Wang, M., Hwu, P., and Restifo, N. P. (1999) Unopposed production of granulocyte-macrophage colony-stimulating factor by tumors inhibits CD8+ T cell responses by dysregulating antigen-presenting cell maturation. *J Immunol* **162**, 5728-5737